Abstracts, Division of Biological Chemistry, 190th National Meeting of the American Chemical Society, September 8–13, 1985

P. Schimmel, Chairman; J. Peisach, Secretary
R. G. Matthews and G. Kenyon, Program Cochairmen

MONDAY MORNING—SYMPOSIUM IN HONOR OF GARVAN MEDALIST MARTHA LUDWIG—I. KLOTZ, SYMPOSIUM CHAIRMAN

1. Carboxypeptidase A. New Results on Binding of Ligands. *W. N. Lipscomb.* Department of Chemistry, Harvard University, Cambridge, MA 02138.

No abstract available.

2. FMN–Protein Interactions in Flavodoxins. *M. L. Ludwig*, K. D. Watenpaugh, and K. A. Pattridge. Biophysics Research Division, The University of Michigan, Ann Arbor, MI 48104, and Upjohn Company, Kalamazoo, MI 49001.

Flavodoxins, the FMN-containing electron carriers present in a variety of microorganisms, have lower oxidation–reduction potentials than other members of the flavoprotein family. Crystal structure analyses of these proteins, with FMN in the oxidized, semiquinone, and reduced forms, have been carried out in an attempt to understand how the interaction with proteins modulates the oxidation–reduction potential of flavins. Initial studies with flavodoxin from *Clostridium* MP have suggested that the oxidized/semiquinone potential depends on formation of a hydrogen bond between the polypeptide backbone and the NH(5) of the flavin semiquinone, while the semiquinone/reduced potential may depend on constraints on the bending and motion of the reduced isoalloxazine ring. These proposals have been explored by structural comparisons with other species of flavodoxins, especially the protein from *Anacystis nidulans*, which has a higher potential for the oxidized/semiquinone equilibrium than most other flavodoxins.

3. Long-Range Electron Transfer at Fixed and Known Distance and Orientation. *B. M. Hoffman.* Departments of Chemistry and Biochemistry, Molecular Biology, and Cell Biology, Northwestern University, Evanston, IL 60201.

Transfer of an electron from one site to another is one of the fundamental processes in chemistry and biochemistry. We have used zinc-substituted hemoproteins to study long-range electron transfer between redox centers at fixed and known distances. The photoexcited zinc triplet state in one subunit of [Zn,Fe] hybrid hemoglobins transfers an electron a distance of 25 Å to its partner aquoferriheme at a range $k_t = 100\ s^{-1}$. The temperature dependence is comparable to that given in the classic biological study of nonadiabatic electron tunneling from cytochrome to chlorophyll in *Chromatium vinosum*. For the complex between zinc-substituted yeast cytochrome *c* peroxidase and native yeast cytochrome *c*, electron transfer occurs with a rate, $k_t = 138\ s^{-1}$, that is remarkably larger than that in the complex between the yeast enzyme and horse cytochrome *c*, $k_t = 17\ s^{-1}$, demonstrating the fine degree of species specificity involved in physiological electron transfer.

4. Multinuclear Magnetic Resonance Investigations of Intermediates in an Enzyme-Catalyzed Reaction: Phosphoglucomutase. *John L. Markley*, Gyung Ihm Rhyu, and William J. Ray, Jr. Department of Biochemistry, University of Wisconsin—Madison, Madison, WI 53706, and Department of Chemistry and Department of Biological Sciences, Purdue University, West Lafayette, IN 47907.

NMR spectroscopy offers an attractive method for investigating enzyme mechanisms because of its ability to provide chemical information about individual atoms in a protein–ligand complex. The experimental possibilities are expanded greatly by utilizing the wide range of heteronuclear NMR methods now available. Two prerequisites for NMR spectral studies of intermediates are (1) trapping or stabilization of mechanistically relevant species and (2) detection of NMR signals that report on interesting parts of the complex. These preconditions have been met to some extent in our studies of phosphoglucomutase, an enzyme that catalyzes the conversion of glucose 1-phosphate to glucose 6-phosphate. The normal active form of the enzyme has a phosphoserine at position 116 and bound Mg^{2+}. We have utilized several strategies, including substituting metal ions (Li^+, Cd^{2+}, and others) and nonreacting substrate analogues (deoxyglucose phosphates), to model enzyme-bound intermediates. We have studied the species so isolated by ^1H, ^7Li, ^{31}P, and ^{113}Cd NMR spectroscopy. Several mechanistic details have emerged concerning the properties of the phosphoserine and histidine residues in various intermediates and a metal–ligand exchange reaction that accompanies substrate binding.

MONDAY AFTERNOON—SYMPOSIUM ON ENZYMES, COFACTORS, AND PROSTHETIC GROUPS—R. G. MATTHEWS, SYMPOSIUM CHAIRMAN

5. Molecular Basis of Bacterial Resistance to Mercurials. *C. Walsh.* Departments of Chemistry and Biology, Massachusetts Institute of Technology, Cambridge, MA 02139.

Bacterial resistance to mercurials is mediated by the genes of the mer operon, usually found on transposable elements. Two unusual enzymes are involved in mercurial metabolism: (1) organomercury lyase, cleaving RHgX to RH and Hg(II), an enzyme cleaving an organometallic bond reductively, and (2) mercuric ion reductase, a disulfide-containing flavoprotein, catalyzing the NADPH-dependent reduction of Hg(II) to Hg, a unique reduction of inorganic mercuric ions. Mechanistic studies on these enzymes will be reported.

6. Evolution of Synthetic Analogues to the Fe/Mo/S Aggregate in Nitrogenase and the Nitrogenase Cofactor. *D.*

0006-2960/85/0424-3355$01.50/0

Coucouvanis and M. G. Kanatzidis. Department of Chemistry, University of Michigan, Ann Arbor, MI 48109.

The available structural (EXAFS) and spectroscopic (ESR, Mössbauer, etc.) data on the Fe/Mo aggregate in nitrogenase and the nitrogenase cofactor define roughly the minimum characteristics required for acceptable synthetic analogues. Our studies, which originated with the synthesis of elementary Fe/Mo oligomers as potential building blocks for larger aggregates, now have evolved to the synthesis of Fe/Mo/S aggregates with atomic ratios resembling the one in nitrogenase. The syntheses and properties of clusters that contain the Fe_6S_6Mo and $Fe_6S_6Mo_2$ cores will be discussed and compared to those of the Fe/Mo center in nitrogenase.

7. Recent Studies on Rhodopsins. *K. Nakanishi.* Department of Chemistry, Columbia University, New York, NY 10027.

Various structurally modified retinal analogues or retinals carrying isotopes have been incorporated into bovine rhodopsin, bacteriorhodopsin, sensory rhodopsin, etc. In addition, bacteriorhodopsin with labeled amino acid residues has been prepared. An outline of recent spectroscopic and bioorganic studies with these rhodopsin analogues will be given.

8. Studies on Cobalamin-Dependent Methionine Synthase. Verna Frasca, Keith Matthews, Barbara Stephenson, and *Rowena G. Matthews.* Department of Biological Chemistry, The University of Michigan, Ann Arbor, MI 48109.

The cobalamin-dependent methionine synthase enzymes from bacterial and mammalian sources show very similar catalytic properties, including requirement for activation by a reducing system and adenosylmethionine during turnover and lability of enzyme activity under aerobic conditions. Purified methionine synthase from both *Escherichia coli* and pig liver is inactivated during turnover in solutions equilibrated with nitrous oxide (N_2O). In each case, the enzyme is irreversibly inactivated. Inactivation of the bacterial enzyme results in partial dissociation of the cobalamin prosthetic group, but the released cobalamin does not appear to be altered structurally. The remaining bound cobalamin retains the spectral properties of the uninhibited holoenzyme. Our results are consistent with a model in which the enzyme induces homolytic cleavage of the N–O bond in N_2O with resultant inactivation of the apoprotein by attack of hydroxyl radical or its equivalent. We have also examined the physiological reducing system required for activation of methionine synthase from pig liver. In the presence of oxygen scavenging systems, a wide variety of thiols can activate the enzyme. In crude homogenates, cysteine and cysteamine are effective activators, probably because they are substrates for oxygenases in the extracts.

MONDAY AFTERNOON—POSTER SESSION—G. KENYON, CHAIRMAN

9. Variation of Isotope Effects with Solution Viscosity To Distinguish Internal and External Commitments. *Charles B. Grissom* and W. W. Cleland. Department of Biochemistry, University of Wisconsin—Madison, Madison, WI 53706.

Kirsch [Brouwer, A. C., & Kirsch, J. F. (1982) *Biochemistry 21*, 1302] has used the variation of V/K values with relative viscosity to determine the external commitments (stickiness factors) for enzymatic reactions. We have adapted this procedure to the variation in isotope effects with viscosity. A 2.35-fold increase in relative solution microviscosity by the addition of sucrose causes a reduction in the observed ^{13}C kinetic isotope effect with chicken liver TPN malic enzyme from 1.0316 ± 0.0001 to 1.0293 ± 0.0007 at pH 6. This is caused by a decrease in the rate of dissociation of malate from the enzyme relative to catalysis (i.e., increased stickiness of malate). Since the total commitment to hydride transfer for the forward direction and the intrinsic isotope effects on hydride transfer and decarboxylation are known [Grissom, C. B., & Cleland, W. W. (1985) *Biochemistry 24*, 944], it is possible to dissect the total forward commitment to hydride transfer into its internal (partition ratios of intermediates not affected by reaction conditions) and external components (partition ratios involving substrate dissociation). For malic enzyme, 88% is internal and 12% is external, consistent with the pH independence of observed deuterium isotope effects.

10. Use of Nitrogen-15 Isotope Effects To Study the Chemical Mechanism of Alanine Dehydrogenase. *Paul M. Weiss* and W. W. Cleland. Department of Biochemistry, University of Wisconsin, Madison, WI 53706.

Alanine dehydrogenase from *Bacillus subtilis* catalyzes the deamination of L-alanine or L-serine to ammonia and pyruvate or β-hydroxypyruvate, with the reduction of NAD. We have measured ^{15}N isotope effects on the reverse reaction by comparing the ^{15}N content in initial and residual ammonia after partial reaction, using the natural abundance of ^{15}N as the label and an isotope ratio mass spectrometer to make the measurements. The values at pH 6.8 were 1.0093 ± 0.0005 with pyruvate and 0.9995 ± 0.0003 with β-hydroxypyruvate. At pH 7.1 the values with pyruvate were 1.0104 ± 0.0005 (NADH) and 1.0081 ± 0.0005 (NADD), while with β-hydroxypyruvate the value was 1.004 ± 0.001 with both NADH and NADD. These values and the calculated deuterium isotope effect of 1.74 will be used to estimate partition ratios for intermediates in the reaction.

11. Kinetics of 1-Thio- and 1-Aminopropanediols as Substrates for Glycerokinase. *W. B. Knight* and W. W. Cleland. Department of Biochemistry, University of Wisconsin, Madison, WI 53706.

We have studied the reactions of amino and thio analogues of glycerol as substrates and inhibitors of glycerokinase (GK). At pH 8.3 GK catalyzed the phosphorylation of the 3-OH of (*S*)-thiopropanediol with $V \times 0.036$ and $K_m \times 2200$ and the 1-thiol group of the *R* isomer with $V \times 3 \times 10^{-6}$ relative to glycerol. (*RS*)-Glycerothiophosphate reacted with MgADP with $V \times 0.0035$ relative to glycerol-1-P. The V/K profile for GK with glycerol showed a group with $pK = 9.1$ that must be protonated, while V was pH independent. The pH profiles of the thiol analogues were similar, indicating that the pH dependence is the result of an enzyme group involved in binding the substrate. The amino group of the *S* isomer of (*RS*)-aminopropanediol was phosphorylated ($V \times 0.0035$, $K_m \times 11$ relative to glycerol) >10-fold faster than the 3-OH of the *R* isomer. It is clear from these results that (1) the hydroxyl group at C-2 determines the orientation of the substrate in the active site, (2) the enzyme phosphorylates 3-amino or 3-thiol analogues of glycerol with greatly reduced rates, and (3) replacement of the hydroxyl group at C-1 with an amino or thiol group lowers both affinity and the rate of phosphorylation at C-3.

12. Kinetic Studies of Trifunctional Enzyme: A Novel Application of Isotope Effects. *Jacalyn Green*, Robert E. MacKenzie, and Rowena G. Matthews. Department of Biological Chemistry, The University of Michigan, Ann Arbor,

MI 48109, and Department of Biochemistry, McGill University, Montreal, Quebec, Canada.

Folates exist intracellularly with polyglutamate tails containing five to eight residues. The polyglutamate tail may be used to provide binding energy to facilitate catalysis. Trifunctional enzyme (TFE) interconverts tetrahydrofolate cofactors to provide one-carbon units for purine biosynthesis. Although inhibition studies of the $NADP^+$-linked methylenetetrahydrofolate dehydrogenase activity of TFE have shown a 2.5-fold difference in binding energy for folyl mono- and pentaglutamate inhibitors, kinetic studies reveal no difference in V_{max} or in the K_m for either substrate with mono- and pentaglutamate substrates. Routine steady-state kinetic methods do not yield the K_d for the second substrate in an ordered bi-bi reaction. Klinman and Matthews [(1985) *J. Am. Chem. Soc. 107*, 1058–1060] have shown that $K_{mB} = K_{dB}({}^DV - 1)/({}^DV/K - 1)$. We have measured the kinetic isotope effects on V and V/K in an attempt to use this relationship to determine K_{dB} for the dehydrogenase activity of TFE. The K_d values for both mono- and pentaglutamate substrates will be estimated by this method.

13. Determination of Carbon Isotope Effects and Substrate Preference for Acetolactate Synthase by Isotope Ratio Mass Spectroscopy. *Lynn M. Abell*, Marion H. O'Leary, and John V. Schloss. Department of Chemistry, University of Wisconsin, Madison, WI 53706, and Central Research and Development Department, Experimental Station E328, E. I. du Pont de Nemours and Company, Wilmington, DE 19898.

Acetolactate synthase (ALS) is the first enzyme of branched-chain amino acid biosynthesis. Besides the known reactions for ALS, condensation of two pyruvates to form acetolactate/CO_2 and condensation of pyruvate with α-ketobutyrate (αkb) to form α-aceto-α-hydroxybutyrate/CO_2, we have found that ALS from *Salmonella typhimurium* (isozyme II) also catalyzes condensation of αkb with αkb. Saturation of either homologous condensation reaction is directly proportional to pyruvate or αkb at low concentration, despite two molecules of either being involved in the reaction. Determination of the kinetic carbon isotope effects gave 1.006 ± 0.002 and 1.008 ± 0.002 for homologous condensation of pyruvate and αkb, respectively. These small isotope effects explain the saturation kinetics (the first substrate is "sticky"). Use of equal molar mixtures of pyruvate and αkb, in which pyruvate's carboxyl is enriched in ^{13}C, allowed us to determine the preference of either substrate for the first substrate position (carboxyl loss) vs. the second position (carboxyl retention). Analyses of enzyme-derived CO_2 suggested a preference for pyruvate in the first site (pyruvate/αkb = 19) and a corresponding preference for αkb in the second.

14. Reaction Intermediates of the Acetolactate Synthase Reaction: Effect of Sulfometuron Methyl. *Larry M. Ciskanik* and John V. Schloss. Central Research and Development Department, Experimental Station E328, E. I. du Pont de Nemours and Company, Wilmington, DE 19898.

Chemical quench experiments have been carried out with acetolactate synthase (ALS) and [^{14}C]pyruvate (C-1, C-2, and C-3 labeled) or [^{14}C]thiamin pyrophosphate (TPP) in an attempt to trap and identify reaction intermediates. Enzymic reaction mixtures were quenched in steady state (100 ms) with 0.1 N acetic acid in methanol and then analyzed by chromatography on DEAE-650M Fractogel TSK. In the presence of 5 mM pyruvate, 0.0041 mol of hydroxyethyl-TPP/mol of enzymic protomer (69000g) was recovered, which increased to 0.011 mol/mol when pyruvate was increased to 50 mM (saturating). The identity of this intermediate is based on its cochromatography with authentic hydroxyethyl-TPP (HETPP) and on the fact that it contained label from C-2 or C-3 [^{14}C]pyruvate or [^{14}C]TPP, but not from C-1 [^{14}C]pyruvate, and its presence was dependent on TPP being bound to ALS. When the enzyme was preincubated with 1 mM sulfometuron methyl prior to conducting the chemical quench, the level of HETPP obtained was 0.016 mol/mol. Thus, although the level of sulfometuron methyl employed virtually eliminated the net enzymic reaction, it actually increased the level of the HETPP intermediate on the enzyme. These results are consistent with the conclusions drawn from steady-state kinetic experiments.

15. Secondary Isotope Effects and Transition-State Structures for Acetylcholinesterase-Catalyzed Hydrolysis of Anilides and Esters. *Scott A. Acheson*, Paul N. Barlow, and Daniel M. Quinn. Chemistry Department, University of Iowa, Iowa City, IA 52242.

Kinetic α- and β-deuterium secondary isotope effects (KSIE's) have been used as probes of transition-state structures for acetylcholinesterase (AChE) catalyzed hydrolysis of *o*-nitroformanilide (ONFA), *o*-nitrochloroacetanilide (ONCA), *o*-nitroacetanilide (ONAC), and *p*-methoxyphenyl formate (PMPF). KSIE's for acylation (${}^DV/K$) and for deacylation (${}^DV$) are listed below. ${}^DV/K$'s are more inverse for less reactive substrates, consistent with increasing exposure with decreasing reactivity of transition states that involve nucleophilic AChE–substrate interactions. Rate-determining deformylation is accompanied by a modest α-KSIE. These results indicate a high degree of reactivity-dependent transition-state-structure variability and are interpreted in terms of virtual transition states for AChE catalysis.

substrate	10^6V (M s^{-1})	$10^3V/K$ (s^{-1})	${}^DV$	${}^DV/K$
ONFA	0.218 ± 0.002	0.12		0.886 ± 0.004
ONAC	9.73 ± 0.23	0.48		0.982 ± 0.005
ONCA	5.10 ± 0.08	6.4		1.025 ± 0.017
PMPF	149 ± 2	102	0.934 ± 0.016	0.99 ± 0.01

16. Interfacial Michaelis–Menten Kinetics for Lipoprotein Lipase Catalysis. *Rebecca A. Burdette* and Daniel M. Quinn. Chemistry Department, University of Iowa, Iowa City, IA 52242.

Physiological lipoprotein lipase (LpL) catalysis is heterogeneous biocatalysis since the reaction occurs at lipid–water interfaces. Accordingly, V_{max}^{app} and K_m^{app} obtained from bulk assays of LpL activity bear no simple relationship to microscopic steps of the LpL mechanism. We have developed a model substrate that consists of fatty acyl *p*-nitrophenyl esters that are contained in Triton X-100 micelles. LpL-catalyzed hydrolysis of fatty acyl *p*-nitrophenyl esters can be followed continuously at 400 nm with a UV–visible spectrophotometer. Above the cmc of the mixed micelles, the time courses for complete LpL-catalyzed hydrolysis of the esters are described by the integrated form of the Michaelis–Menten equation. Least-squares analysis of time-course data thus produces the interfacial kinetic parameters V_{max}^* and K_m^* from each kinetic run. The computational and experimental methodology used to determine the interfacial kinetic parameters will be presented. Application of our methods to characterization of intrinsic LpL fatty acyl specificity and fatty acid product inhibition will be described, and evidence for an interfacial

acyl enzyme mechanism will be presented.

17. Complex Reaction Dynamics and Virtual Transition States for the Acylation Step of Acetylcholinesterase Catalysis. *Paul N. Barlow*, Scott A. Acheson, and Daniel M. Quinn. Chemistry Department, University of Iowa, Iowa City, IA 52242.

Dependences of V/K (monitors rate-determining acylation) for the acetylcholinesterase (AChE) catalyzed hydrolysis of *o*-nitroacetanilide (ONAC) and *o*-nitroformanilide (ONFA) on pL (L = H, D) give low pK_a's and small solvent isotope effects ($^{D_2O}V/K$). For ONAC, pK_a's are 5.63 ± 0.03 (H_2O) and 6.44 ± 0.04 (D_2O), ΔpK_a = 0.81 ± 0.07, and $^{D_2O}V/K$ = 1.55 ± 0.03. For ONFA, pK_a's are 5.62 ± 0.04 (H_2O) and 6.23 ± 0.03 (D_2O), ΔpK_a = 0.61 ± 0.07, and $^{D_2O}V/K$ = 1.41 ± 0.03. Proton inventory plots of partial solvent isotope effect vs. atom fraction of deuterium in mixed H_2O–D_2O buffers are bowing upward in shape and are interpreted in terms of virtual acylation transition states that contain contributions from solvent isotope insensitive and solvent isotope sensitive serial microscopic steps. Nonlinear least-squares analysis of the proton inventories allows calculation (for ONAC and ONFA, respectively) of commitments to proton transfer catalysis of 1.36 ± 0.30 and 2.02 ± 0.59, intrinsic solvent isotope effects of 2.5 ± 0.2 and 2.3 ± 0.3, and intrinsic pK_a's of 6.00 ± 0.09 and 6.10 ± 0.12. These results will be discussed in terms of models for AChE acylation dynamics that involve partial rate determination by product release or induced fit [Rosenberry, T. L. (1975) *Proc. Natl. Acad. Sci. U.S.A. 72*, 3834–3838].

18. Carbamates as Active-Site-Directed Inhibitors of Cholesterol Esterase. *Lynn Hosie*, Jeff L. Bebensee, Larry D. Sutton, and Daniel M. Quinn. Chemistry Department, University of Iowa, Iowa City, IA 52242.

The following carbamates have been synthesized and tested as inhibitors of cholesterol esterase (CEase).

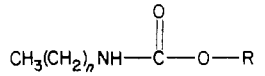

I, n = 3, R = *p*-nitrophenyl
II, n = 7, R = *p*-nitrophenyl
III, n = 3, R = cholesteryl
IV, n = 7, R = cholesteryl

The water-soluble compound I is a potent time-dependent inhibitor of bovine pancreatic CEase-catalyzed hydrolysis of *p*-nitrophenyl butyrate (PNPB); inhibition is complete in 200 s in the presence of 2 μM I. Compound II contained in phosphatidylcholine–taurocholate (PC–TC) mixed micelles gives first-order though incomplete inhibition of porcine pancreatic CEase catalyzed hydrolysis of PNPB. The cholesteryl analogue IV contained in PC–TC micelles also gives first-order and incomplete inhibition of porcine pancreatic CEase. TLC of a hexane extract of the reaction mixture indicates that inhibition is accompanied by release of cholesterol. These results are interpreted in terms of inhibition via carbamylation of an active-site residue (probably serine) of CEase.

19. Hexose-6-phosphate Dehydrogenase: Kinetic Mechanism. *Ira J. Ropson* and Dennis A. Powers. Department of Biology, The Johns Hopkins University, Baltimore, MD 21218.

Hexose-6-phosphate dehydrogenase (H6pdh) was purified to homogeneity from the liver microsomal fraction of the marsh minnow *Fundulus heteroclitus*. H6pdh catalyzes a reaction similar to that of glucose-6-phosphate dehydrogenase, but with unusually high variability for substrate and coenzyme. Glucose-6-P, galactose-6-P, 2-deoxyglucose-6-P, and glucose are all good substrates when NADP, 3-acetylpyridine–NADP, or 6-deamino-NADP is used as the coenzyme. However, when NAD is used, the only reactive substrate is glucose. Preliminary studies of the reaction NADP + glucose-6-P → NADPH + 6-phosphogluconate favor a random Bi-Bi reaction mechanism: $K_m^{NADP} \cong 1.5$ μM; $K_m^{G_6P} \cong 8$ μM; $K_i^{NADP} \cong 8$ μM; $V_{max} \cong 2.8$ μmol min^{-1} (mg of protein)$^{-1}$. Moreover, NAD is a potent competitive inhibitor (for NADP) of this reaction: $K_i^{NAD} \cong 0.8$ μM. Similarly, glucose-6-P is a competitive inhibitor of the NAD–glucose reaction, suggesting that glucose-6-P and NAD form a dead-end complex with the enzyme.

20. Interaction of Brewers' Yeast Pyruvate Decarboxylase with the Mechanism-Based Inactivator Conjugated α-Keto Acids. *Frank Jordan*, Zbigniew H. Kudzin, Joe Adams, and Bijan Farzami. Department of Chemistry, Rutgers University, Newark, NJ 07102.

It was demonstrated before that the conjugated α-keto acid (*E*)-4-(4-chlorophenyl)-2-oxo-3-butenoate is a mechanism-based inactivator of brewers' yeast pyruvate decarboxylase (EC 4.1.1.1) that enables direct observation of a key enzyme–thiamin diphosphate bound enamine intermediate [Kuo, D. J., & Jordan, F. (1983) *Biochemistry 22*, 3735; Kuo, D. J., & Jordan, F. (1983) *J. Biol. Chem. 258*, 13415]. A variety of conjugated substrate analogues were synthesized with the general structure *n*-X—C_6H_4—CH=CHCOCO$_2$H with different steric and electronic demands. The kinetics of formation of the enzyme-bound enamine intermediate for some substituents followed "burst"-type biphasic kinetics enabling determination of relative rate constant ratios and their pH dependencies on side-chain ionizations.

21. Enzyme-Generated Model for the Reductive Acetylation of Lipoyl-E2 by E1 in the Pyruvate Dehydrogenase Multienzyme Complex. *Frank Jordan*, Zbigniew H. Kudzin, and Donald J. Kuo. Department of Chemistry, Rutgers University, Newark, NJ 07102.

Thiamin diphosphate dependent pyruvate decarboxylases proceed by formation of a coenzyme-bound enamine intermediate that can be observed spectroscopically by employing a conjugated substrate analogue [Kuo, D. J., & Jordan, F. (1983) *J. Biol. Chem. 258*, 13415]. While the fate of this enamine is C-protonation followed by acetaldehyde release on pyruvate decarboxylase, its fate is oxidation and transfer to the concomitantly reduced dihydrolipoamide of the E2 protein in the pyruvate dehydrogenase multienzyme complex. The mechanism of this oxidation–reduction reaction and acetyl transfer were examined in an enzyme-generated model. When pyruvate decarboxylase was mixed with (*E*)-4-(4-chlorophenyl)-2-oxo-3-butenoate or pyruvic acid or α-ketobutyric acid, a new absorbance (375–385 nm) resulted. The source of this absorbance was demonstrated and provided evidence for a stepwise mechanism for the reductive acetylation step performed by the pyruvate dehydrogenase multienzyme complex.

22. Hydrogen Bonding and Proton Transfer in Model Schiff Bases. *Paul E. Blatz*, S. K. Al-Dilaimi, R. H. Johnson, and J. C. Aumiller. School of Basic Life Sciences, University of Missouri, Kansas City, MO 64110.

By means of a special variable low-temperature cell holder, spectra are obtained to temperatures as low as 88 K. When

temperature is lowered for a 3MeP solution containing *N*-2,4,6,8,10-dodecapentaenylidene-*n*-butylamine (**2**) and phenol, three separate and distinct species are detected. The first shows sharp fine structure and belongs to **2**. Upon lowering temperature, the old fine structure disappears as new develops at slightly longer wavelength. The new spectrum is that of the H-bonded species formed between **2** and phenol. Upon further lowering of temperature, the second spectrum disappears, and a new one, that of the proton-transferred species, develops at about 440 nm. The same phenomenon is repeated when donors *p*-nitrophenol or acetic acid are used. The $-\Delta H$ and ΔS values for the H-bonding process between phenol and **2** in 3MeP are 3900 cal mol^{-1} and 1.4 eu, respectively. Additional experiments establish H bonding with the phenolic hydroxyl group; alcohol also H bonds but does not proton transfer. These results do not support H bonding as a major contributor of shifts in λ_{max} for visual pigments.

23. Electrophilic Amination of an Active-Site Residue in D-Amino Acid Oxidase by *O*-(2,4-Dinitrophenyl)hydroxylamine. Claudius D'Silva, Charles H. Williams, Jr., and Vincent Massey. Department of Biological Chemistry and Veterans Administration Medical Center, University of Michigan, Ann Arbor, MI 48109.

Active-site-directed modifying agents have proved valuable tools in the study of the mechanism of enzymes. To date few examples of compounds capable of specific modification of active sites have been reported, in which very small residues are introduced. *O*-(2,4-Dinitrophenyl)hydroxylamine is an electrophilic compound that reacts with a variety of nucleophilic groups to achieve a minimal modification by the introduction of an amino group. In this poster we will describe the chemistry of this compound with a variety of nucleophilic groups found in proteins as well as its use as a potent active-site-directed modifying agent of the flavoprotein D-amino acid oxidase (from pig kidney).

24. Products of Metal Exchange Reactions of Metallothionein. D. G. Nettesheim, H. R. Engeseth, and *J. D. Otvos*. Department of Chemistry, University of Wisconsin—Milwaukee, Milwaukee, WI 53201.

Hepatic metallothionein (MT) from Cd-exposed animals contains Zn (2–3 mol/mol of protein) in addition to Cd (4–5 mol/mol), and these metals are distributed in a unique, nonuniform manner among the seven binding sites of the protein's metal–thiolate clusters. Different methods of preparing Cd,Zn-MT in vitro were investigated to provide insight into the driving force and mechanism of formation of the native mixed-metal clusters. ^{113}Cd NMR spectra of the products of stepwise displacement of Zn from Zn_7-MT by $^{113}Cd^{2+}$ show that Cd binding to clusters is not cooperative, one cluster is not selectively occupied before the other, and many clusters with a nonnative metal distribution are formed. In contrast, the native cluster compositions can be exactly reproduced simply by mixing together the appropriate amounts of Cd_7-MT and Zn_7-MT and allowing intermolecular metal exchange to occur. The driving force for this heretofore unknown reaction appears to be the relative thermodynamic instability of three-metal clusters containing Cd. The implications of this finding in terms of metallothionein's putative roles in Zn metabolism and Cd detoxification will be discussed.

25. Inhibition of Subtilisin by Organophosphinates. *C. A. Broomfield*, C. N. Lieske, C. Bakewell, J. H. Clark, and M. D. Green. U.S. Army Medical Research Institute of Chemical Defense, Aberdeen Proving Ground, MD 21010-5425.

We are interested in the reaction of organophosphinates with acetylcholinesterase (AChE) and other enzymes. Subtilisin is a serine esterase with a structure unrelated to chymotrypsin, trypsin, and AChE. Inhibition of subtilisin by 18 4-nitrophenyl organophosphinate esters was studied at pH 7.5, monitoring ΔA at 400 nm. The reaction rates of the chloromethyl(2-methoxyphenyl)- and chloromethyl(phenyl)phosphinates were too fast to measure with our procedure. The isopropyl(phenyl)- and dimethylphosphinates were nonreactive. The rest had half-times of inhibition ranging from 12 to 558 s. While inhibition rates of the enzymes tested are generally parallel, there are notable exceptions. The shift of the methoxy group from ortho to para in the methoxyphenyl methyl derivatives barely changes the reaction rate with AChE, but the rate increases with trypsin and decreases with subtilisin. Substitution of a single Cl for H in the methyl group of 4-nitrophenyl methyl(phenyl)phosphinate increases the activity by a factor of 5 to 6 toward eel AChE and trypsin and more than 15 times toward subtilisin. Further Cl substitution in the methyl group decreases inhibition rates. We hope to use these differences together with other inhibitor and substrate specificity data to derive a picture of the AChE active site.

26. Activation of Urocanase from *Pseudomonas putida* by Electronically Excited Triplet Species. *R. C. Venema* and D. H. Hug. Veterans Administration Medical Center, University of Iowa, Iowa City, IA 52240.

Electronically excited triplet species can be generated in vitro by the peroxidase-catalyzed aerobic oxidation of appropriate substrates, and these excited species can induce photochemical-like transformations in the absence of light [Cilento, G. (1980) *Photochem. Photobiol. Rev. 5*, 199]. Previous reports from this laboratory have shown that urocanase from *Pseudomonas putida* is activated by the direct absorption of UV light [Hug, D. H., & Roth, D. (1971) *Biochemistry 10*, 1397; Roth, D., & Hug, D. H. (1972) *Radiat. Res. 50*, 94]. In this report we describe the activation of urocanase in the dark when incubated with horseradish peroxidase and indole-3-acetic acid, a system that generates indole-3-aldehyde in the triplet state. The activation was reduced by the addition of triplet quenchers but not by traps for potential reactive oxygen intermediates. The photosensitive dye rose bengal can be excited by visible light to produce a triplet species of very different nature and origin that was also effective in activating urocanase. These results suggest a possible mechanism of urocanase regulation in vivo, not dependent on the environmental signal of light.

27. Identification of Cys-319 Labeled by 6-[(4-Bromo-2,3-dioxobutyl)thio]-6-deaminoadenosine 5′-Diphosphate in the NADH Inhibitory Site of Glutamate Dehydrogenase. *Surendra P. Batra* and Roberta F. Colman. Department of Chemistry, University of Delaware, Newark, DE 19716.

6-[(4-Bromo-2,3-dioxobutyl)thio]-6-deaminoadenosine 5′-diphosphate (BDB-TADP) has been shown to react at the NADH inhibitory site of bovine liver glutamate dehydrogenase (GDH) with incorporation of 1 mol of reagent/enzyme subunit [Batra, S. P., & Colman, R. F. (1984) *Biochemistry 23*, 4940]. The modified GDH had lost one of the six free sulfhydryl groups per enzyme subunit as detected by 5,5′-dithiobis(2-nitrobenzoate). In the unmodified enzyme digested with trypsin, six cysteine peptides labeled with [^{14}C]iodoacetic acid were detected by HPLC, whereas only five were observed in the BDB-TADP-modified enzyme. A cysteine peptide has

been isolated from modified enzyme digested with trypsin and chymotrypsin. Purification of the nucleotidyl peptide was accomplished by chromatography on phenyl boronate–agarose, followed by gel filtration on Sephadex G-25 and Bio-Gel P-4 in 50 mM ammonium bicarbonate, pH 7.9. The modified peptide was finally purified by HPLC on a C-18 column using 0.1% trifluoroacetic acid with an acetonitrile gradient. On the basis of the amino acid composition and N-terminus of the peptide, the residue in the NADH inhibitory site labeled by BDB-TADP has been identified as Cys-319.

28. Identification of Critical Tyrosyl Peptides Labeled by 5′-[*p*-(Fluorosulfonyl)benzoyl]adenosine in the Active Site of Pyruvate Kinase. *Dianne L. DeCamp* and Roberta F. Colman. Department of Chemistry, University of Delaware, Newark, DE 19716.

The nucleotide affinity label 5′-[*p*-(fluorosulfonyl)-benzoyl]adenosine (FSBA) reacts at the active site of rabbit muscle pyruvate kinase, with irreversible inactivation being attributed to modification of tyrosyl residues [Annamalai & Colman (1981) *J. Biol. Chem. 256*, 10276]. We have now purified peptides from 70% inactivated enzyme containing 0.7 mol of reagent/mol of enzyme subunit. Rabbit muscle enzyme reacted with [^{3}H]FSBA was digested with thermolysin. Nucleosidyl peptides were purified by chromatography on phenyl boronate–agarose and reverse-phase HPLC. After amino acid and N-terminus analysis, the peptides were identified by comparison with the primary sequences of chicken and cat muscle enzyme. About 75% of the reagent incorporated was distributed equally among three *O*-[(4-carboxyphenyl)sulfonyl]tyrosine-containing peptides: Leu-Asp-Tyr-Lys-Asn, Val-Tyr, and Leu-Asp-Asn-Ala-Tyr. These tyrosines are located in a 28-residue segment of the 530 amino acid sequence. Modification in the presence of MgATP or MgADP resulted in a marked decrease in labeling of these peptides concomitant with decreased inactivation. It is suggested that these three peptides are located in the region of the nucleotide site of pyruvate kinase.

29. Yeast Hexokinase: Evidence for a Lysine Residue at or near the Active Site. *R. N. Puri*, D. Bhatnagar, and R. Roskoski, Jr. Department of Biochemistry, Louisiana State University Medical Center, New Orleans, LA 70119.

Yeast hexokinase (HK) is a homodimer with a subunit molecular weight of 52 000. It is inactivated by *o*-phthalaldehyde (OPTH) by cross-linking an essential cysteine with a lysine to form a fluorescent isoindole derivative. A total of 2 mol of isoindole groups per mole of HK dimer is formed following a complete loss of phosphotransferase activity. Pyridoxal phosphate (PLP) forms Schiff base adducts with lysine residues and also inhibits HK activity in a time- and concentration-dependent fashion. The substrates MgATP and glucose protect HK from inactivation by either OPTH or PLP. 5′-[(Fluorosulfonyl)benzoyl]adenosine (FSBA) is an ATP analogue that inactivates several kinases following irreversible alkylation of lysine residues. The native, dimeric yeast HK is resistant to inactivation by FSBA. The enzyme becomes susceptible to inactivation by FSBA, which parallels the extent of dissociation of holoenzyme into monomers. Taken together, these experiments support the notion that there are 2 mol of lysines per mole of HK dimer at or near its active site.

30. Comparison of the Predicted Secondary Structure of Cholera Toxin A-Subunit and Fragment A of Diphtheria Toxin. *L. K. Duffy* and C.-Y. Lai. Harvard Medical School, Boston, MA 02115, and Hoffmann-La Roche, Nutley, NJ 07110.

Both cholera toxin and diphtheria toxin possess NAD-glycohydrolase and ADP-ribosyltransferase activities. These activities reside on a single polypeptide chain in each toxin. These polypeptides are called respectively A-subunit (in cholera toxin) and fragment A (in diphtheria toxin). Using the method of Chou and Fasman (1978), we have predicted the secondary structure of the NAD binding polypeptide chains of these two toxins and compared the regions of α-helix and β-sheet. In cholera toxin A-subunit, the majority of the β-structure consisted of six strands located on the NH_2-terminal portion of the molecule. This β-structure region was followed by a region characterized by alternating structures of β-sheet and α-helix. Diphtheria toxin showed much less β-structure than did cholera toxin. Several α-helices were located in the carboxyl-terminal half of the fragment A in a fashion homologous to the cholera toxin A-subunit. These α-helix regions may be of functional importance in the binding of NAD to the active site of these two proteins and, thus, in the expression of their biological activity.

31. Prediction of Dinucleotide Binding Domains from Amino Acid Sequences. *T. D. Corso*, K. E. Paulius, and K. W. Olsen. Department of Chemistry, Loyola University of Chicago, Chicago, IL 60626.

A computer program that detects three-dimensional homology in amino acid sequences has demonstrated the presence of a dinucleotide binding domain in a number of reductases, nucleic acid binding, ribosomal and oncogene proteins. The program detects the pattern of internal and external residues as well as the secondary structure that is characteristic of this fold. A series of residue properties were evaluated at each position in the sequence and compared to that expected for the domain. While it is possible that one property might fit the expected pattern by chance, it is unlikely that 10 different ones would all fit simultaneously if this fold was not the correct tertiary structure. The dinucleotide binding domain, or Rossmann fold, consists of a six-strand parallel β-sheet flanked by α-helices. In some cases, only a mononucleotide binding domain was detected. The proteins predicted to have the fold are the p21 ras oncogene proteins, mercuric reductase, pyrroline-5-carboxylate reductase, nopaline synthase, D-amino acid oxidase, fumarate reductase, elongation factor Ts, dna A protein, transposase, regulatory protein fnr, and ribosomal proteins S1 and S2.

32. Sequence Studies and Chemical Modification of *Salmonella typhimurium* Phosphoribosylpyrophosphate Synthetase with 5′-[*p*-(Fluorosulfonyl)benzoyl]adenosine. *Kenneth W. Harlow* and Robert L. Switzer. Department of Biochemistry, University of Illinois, Urbana, IL 61801.

5-Phosphoribosyl-α-1-pyrophosphate (PRPP) synthetase from *Salmonella typhimurium* catalyzes the transfer of pyrophosphate from ATP to ribose 5-phosphate to yield PRPP and AMP and is allosterically inhibited by ADP. Chemical modification studies have been undertaken to characterize the substrate and allosteric binding sites. 5′-[*p*-(Fluorosulfonyl)benzoyl]adenosine (FSBA) inactivates the enzyme in a time-dependent manner with a stoichiometry of about 1 mol of FSBA per mole of monomer corresponding to complete inactivation. The enzyme is protected from inactivation by ATP or ADP. Cyanogen bromide digestion of enzyme modified with [*benzoyl*-^{14}C]FSBA followed by separation of the

resultant peptides by RP-HPLC shows the majority of the radioactivity associated with a single peptide. The peptide contains one lysine residue, a probable site of reaction with FSBA. Automated Edman degradation of the peptides derived from CNBr digestion and alignment of their sequences by comparison to the homologous *Escherichia coli* PRPP synthetase have allowed most of the primary structure of *S. typhimurium* PRPP synthetase to be determined.

33. Sequence Comparisons of Cytoplasmic and Mitochondrial NAD^+-Dependent Dehydrogenases. *Ralph A. Bradshaw*, Ji-kang Fang, Ross T. Fernley, Ming Chen, James C. Warren, Jens J. Birktoft, and Leonard J. Banaszak. Department of Biological Chemistry, University of California, Irvine, CA 92717, and Departments of Biological Chemistry and Obstetrics/Gynecology, Washington University, St. Louis, MO 63110.

NAD^+-dependent dehydrogenases are widely distributed throughout eukaryotic and prokaryotic organisms, catalyzing a variety of reactions in many cellular locations. In some cases, the same catalytic activity is manifested in distinct forms, e.g., the cytoplasmic and mitochondrial forms of malate dehydrogenase (MDH). Both are homodimers of similar molecular weights, but comparison of the porcine heart sequences shows only $\simeq$20% identities. Nonetheless, the two proteins have highly similar main chain conformations. Interestingly, the amino terminus of *Escherichia coli* MDH shows nearly 70% identity with the mitochondrial enzyme but is equally dissimilar to the cytoplasmic form. All of the MDHs show homology to the several cytoplasmic lactate dehydrogenases but are not significantly related to β-hydroxyacyl-CoA dehydrogenase (βHADH) or 17β-estradiol dehydrogenase (17βE_2DH). βHADH is solely mitochondrial while 17βE_2DH is considered to be cytoplasmic. However, the presence of an unblocked N-terminal alanine suggests processing of a precursor consistent with an intraorganelle location.

34. Common Evolutionary Origin of Mammalian, Yeast, *Escherichia coli*, and Chloroplast Fructose-1,6-bisphosphatase. *Frank Marcus*, Judith Rittenhouse, Brigitte Gontero, and Peter B. Harrsch. Department of Biological Chemistry and Structure, The Chicago Medical School, North Chicago, IL 60064.

Fructose-1,6-bisphosphatase (FbPase) catalyzes the hydrolysis of fructose 1,6-bisphosphate, an essential step in gluconeogenesis. The amino acid sequence of the enzymes from pig kidney cortex (Marcus et al., 1982) and sheep liver (Fisher and Thompson, 1983) reveals 90% of sequence identity. We have now obtained preliminary structural data for other FbPases that have distinctive properties different from those of the mammalian enzyme. The enzymes include the phosphorylatable yeast (*Saccharomyces cerevisiae*) FbPase, the *Escherichia coli* enzyme, whose inhibition by AMP can be relieved by phosphoenolpyruvate, and the chloroplast FbPase, which is activated by a light-dependent mechanism but is not inhibited by AMP. Each of the above three enzymes were purified to homogeneity, S-carboxymethylated, and cleaved with trypsin. The resulting peptides were fractionated by reversed-phase HPLC and selected peptides were subjected to automated Edman degradation. Most sequenced peptides have been aligned within the amino acid sequence of the mammalian enzyme, suggesting a common evolutionary origin for all fructose-1,6-bisphosphatases.

35. Apparent and Standard-State Denaturation Free Energy Changes of Proteins. *M. M. Santoro*, J. F. Miller, and D. W. Bolen. Department of Chemistry and Biochemistry, Southern Illinois University, Carbondale, IL 62901.

It is known that protein denaturation in the acid region is usually accompanied by uptake of protons ($\Delta\bar{V}$). This effect can be taken into account by formally including the changes of proton concentration in the equilibrium expression for denaturation, which leads to the following expression interrelating the apparent (ΔG_D^{app}) and standard-state ($\Delta G°_D$) denaturation free energy values: $\Delta G°_D = \Delta G_D^{app} - 2.303\Delta V(RT)(pH)$. Provided that the titration curves of native and denatured forms of the proteins are known or estimable, calculation of $\Delta G°_D$ at one pH from the $\Delta G°_D$ observed at another pH is accomplished by using the following formula where $pH_1 > pH_2$: $\Delta G°_{D,pH_2} = \Delta G°_{D,pH_1} + 2.303RT(\Delta\bar{V}_{pH_2})(pH_2) + 2.303RT\int_{pH_1}^{pH_2}\Delta\bar{V}\, d(pH)$. [(Phenylmethyl)sulfonyl]-α-chymotrypsin titration and guanidine hydrochloride denaturation data were used to test the validity of this approach. Currently, we are using this methodology to evaluate the stability of a proteolytic enzyme (α-chymotrypsin) at neutral pH, which is not accessible to direct experimental evaluation in the neutral pH range due to the rapid autolysis of the denatured form of the protein.

36. Effect of Cross-Linking on the Thermal Stability of Hemoglobin. *F. L. White*, J. J. Gashkoff, T. Yang, and K. W. Olsen. Department of Chemistry, Loyola University of Chicago, Chicago, IL 60626.

Two different methods of cross-linking have been tested for their ability to stabilize hemoglobin. The first method uses a double-headed aspirin, bis(3,5-dibromosalicyl) fumarate, known to selectively cross-link hemoglobin A between Lys-82 β1 and Lys-82 β2. The thermal denaturation was done in 0.9 M guanidine and 0.01 M MOPS, pH 7. The hemoglobin was first oxidized to methemoglobin by $K_3Fe(CN)_6$. Changes in absorbance between 190 and 650 nm were monitored on a diode array spectrophotometer, using a heating rate of 0.3 °C/min between 25 and 70 °C. As expected, the apparent single transition for hemoglobin A was very broad, due to the multistate nature of this denaturation. This transition for un-cross-linked hemoglobin had a midpoint temperature of 41 °C. The cross-linked hemoglobin A showed at least two distinct transition temperatures at 42 and 60 °C. These results seem to indicate that this cross-link stabilizes some portions of the protein but not others. The second method, using dimethyl suberimidate to make random cross-links between lysine residues, gave similar results when the transition was followed at 280 nm, but only the low-temperature transition was observed when the Soret band was used.

37. Calorimetric Studies of the Thermal Denaturation of F_1ATPase. *G. C. Kresheck*, A. B. Adade, and G. Vanderkooi. Department of Chemistry, Northern Illinois University, De Kalb, IL 60115.

The thermal denaturation of F_1ATPase prepared from beef heart mitochondria has been studied by differential scanning calorimetry. A very sharp (half-height peak width of 2.0 ± 0.2°) and highly endothermic (19 ± 2 cal g^{-1}) irreversible transition centered at 80.5 ± ±° was observed [Kresheck et al. (1985) *Biochemistry* (in press)]. These values are quite similar to those previously reported for the equally unusual thermal denaturation of collagen [Privalov (1982) *Adv. Protein Chem. 35*, 1]. Another striking similarity between the ther-

modynamics of collagen melting and F_1 is the magnitude of the effective or van't Hoff enthalpy change, which is 300–400 kcal mol^{-1} for collagen and 470 ± 100 kcal mol^{-1} for F_1ATPase, as deduced from the sharpness of the transition at the midpoint in the thermal denaturation curve. Also like collagen, the stability of F_1 is sensitive to the presence of neutral salts that follow the Hofmeister series. These facts, in addition to the low-temperature lability and sensitivity of the thermal denaturation to submillimolar concentrations of local anesthetics (which are a recently discovered special class of F_1ATPase enzyme inhibitors), suggest an intimate participation of water in maintaining the F_1 structure, to an extent not present in typical globular proteins.

38. NMR Studies of Phenylalanine Analogue Interactions with Normal and Sickle Hemoglobin. *Y.-H. Lee*, B. A. Bates, B. L. Currie, and M. E. Johnson. Department of Medicinal Chemistry, University of Illinois at Chicago, Chicago, IL 60680.

^1H and ^{19}F NMR techniques were used to monitor the interaction of a nitroxide spin-label phenylalanine analogue with the Hb molecule by using Hb labeled at the Cys β93 position with a fluoroiodoacetamide derivative (IA-F_3) and by monitoring the relaxation rates of the C2 and C4 histidine protons. It has been shown that SL-Phe exhibits specific binding to Hb and an antigelling activity greater than that of Phe. T_2 relaxation measurements of the CF_3 resonances in IA-F_3-labeled COHb and deoxy-Hb exhibit substantial paramagnetically induced relaxation enhancement in the presence of SL-Phe, indicating that the fluorine nuclei strongly influenced by the presence of SL-Phe are located within a few angstroms of the SL-Phe binding site. ^1H NMR relaxation measurements of the C2 and C4 proton resonances from the β2, β143, and β146 histidines also show significant effects from the binding of SL-Phe to Hb, indicating that the SL-Phe binding site must be close to these three residues. The strong antigelation activity of SL-Phe suggests that this binding site may be one of the intermolecular contact sites of importance to the deoxy-HbS aggregation process.

39. NMR Assignments of Acetyl Groups in Acetylated Glycosides via Proton–Carbon Long-Range Couplings. *M. L. Appleton*, C. E. Cottrell, and E. J. Behrman. Department of Biochemistry, The Ohio State University, Columbus, OH 43210.

Previous methods for the assignment of acetyl groups in carbohydrates required synthesis of specifically deuterated derivatives. We report the use of a two-dimensional NMR technique which utilizes proton–carbon long-range couplings [Kessler et al. (1984) *J. Magn. Reson. 57*, 331] to assign both the protons and carbonyl carbons of the acetyl groups of methyl 2,3,4,6-tetra-*O*-acetyl-α-D-glucopyranoside (**1**). The technique utilizes coupling of a ring proton to its respective carbonyl carbon and correlates this with coupling of the carbonyl carbon to the acetyl protons, thus allowing assignment of the carbonyl carbons and acetyl protons. We have confirmed previous assignments of the solvent-dependent acetyl protons of **1** in benzene-d_6, pyridine-d_5, and chloroform-*d* and also assigned the carbonyl carbons. The methyl carbon assignments should be obtainable from ^1H–^{13}C correlations. We intend to apply the technique to various acetylated glycosides, nucleosides, and sugar nucleotides.

40. Electron Self-Exchange in Cytochrome *c*. Michael Barbush, *Dabney White Dixon*, and Francis S. Millett. Department of Chemistry, Washington University, St. Louis, MO 63130, and Department of Chemistry, University of Arkansas, Fayetteville, AR 72701.

Electron self-exchange rate constants have been measured for a number of eukaryotic cytochromes *c* by NMR line broadening techniques. These systems are in the slow exchange limit; the rate constants can be measured by line broadening of either the Fe(II) or Fe(III) resonances. The rate constants are in the range (1–2) × 10^4 M^{-1} s^{-1}. cyt a^{3+} + cyt b^{2+} ⇌ cyt a^{2+} + cyt b^{3+}. Electron self-exchange in fully trifluoroacetylated cytochrome *c* (19 lysine $COCF_3$ groups) has been probed by both ^1H and ^{19}F NMR. The rate constant in this derivatized protein is about 10 times that in the native protein.

41. Temperature-Induced Conformational Changes in Spectrin. *H.-Z. Lu*, M. E. Johnson, Rex Hjelm, and L. W.-M. Fung. Department of Chemistry, Loyola University of Chicago, Chicago, IL 60626, and Department of Medicinal Chemistry and Pharmacognosy, University of Illinois at Chicago, Chicago, IL 60680.

^1H NMR at 200 MHz was used to study spectrin, extracted from human erythrocyte membranes by low ionic strength buffer at 37 °C and then purified by gel filtration at 4 °C, as a function of temperature, ionic strength, and spectrin concentration (4–8 mg/mL). Several relatively sharp resonances (25–35 Hz) were observed in the spectra of spectrin samples that contained both dimers (M_r 460 000) and tetramers. The intensities of these relatively sharp resonances appear to be temperature and ionic strength dependent. We interpret the changes in intensity as being due to conformational changes that introduce local flexibility in the spectrin molecule. We have further studied this temperature-induced conformational change of spectrin by spin-label EPR and by CD at 4 mg/mL concentration. The EPR data show a transition temperature around 50 °C. The CD data show decreased α-helical content at high temperature. We have correlated our NMR, EPR, and CD data in order to understand these local/segmental motions in the spectrin molecule at relatively high concentrations.

42. Selenium-77 NMR Investigation of a Protein–Selenoligand Complex. *G. P. Mullen*, R. B. Dunlap, and J. D. Odom. Department of Chemistry, University of South Carolina, Columbia, SC 29208.

The first application of selenium-77 NMR spectroscopy to a protein–selenoligand complex has been demonstrated by this laboratory. The natural abundance selenium-77 NMR investigation of the binding of the inhibitor phenylselenyl acetate to α-chymotrypsin will be presented. Rapid exchange on the NMR time scale has been observed for the enzyme–inhibitor complex. On the basis of a model that allows for equal binding of the inhibitor to monomeric and polymeric α-chymotrypsin, a −39.8 ppm chemical shift between the free and enzyme-bound states has been determined. This chemical shift is notably larger than any multinuclear chemical shifts previously observed in such an equilibrium. The equilibrium inhibition constant calculated with this model is 19.7 mM. A lower limit of 6.7 × 10^3 s^{-1} is assigned to the enzyme–inhibitor dissociation rate constant.

43. High-Resolution NMR Spectroscopy of Lactoperoxidase. *Diane C. Ales*, Enrique Gonzalez-Vergara, and Harold M. Goff. Department of Chemistry, University of Iowa, Iowa City, IA 52242.

Lactoperoxidase isolated from cow's milk has been examined by high-field NMR spectroscopy in its native high-spin iron(III) form and as the low-spin cyanide complex. The isolation procedure has been refined and simplified. The proton NMR spectrum of native lactoperoxidase reveals broad, overlapping heme methyl resonances in the far downfield 65 ppm region. Addition of cyanide ion serves to convert the ferrihemoprotein to the low-spin cyano complex. Several relatively sharp resonances are apparent well outside the usual diamagnetic region. Unlike other low-spin ferrihemoproteins that exhibit heme proton resonances in the downfield 10–30 ppm region, signals for cyanolactoperoxidase are seen as far downfield as 66.5 ppm and as far upfield as −26 ppm. Extreme asymmetry in the unpaired spin distribution is thus realized. Coordination of neither azide ion nor imidazole was detected by NMR spectroscopy, possibly indicating a highly hindered heme pocket.

44. Structures of the Oligosaccharides Isolated from an Ovarian Cyst Mucin Having Blood Group "A" Activity. Virendra K. Dua, B. N. Narasinga Rao, Shing-Shing Wu, and *C. Allen Bush*. Department of Chemistry, Illinois Institute of Chemistry, Chicago, IL 60616.

Fourteen oligosaccharide alditols ranging in size from 2 to 10 monosaccharide residues were isolated by HPLC of the products of alkaline borohydride degradation of an A active ovarian cyst mucin. Their complete covalent structures were determined from the fully assigned proton NMR spectra, from nuclear Overhauser effect (NOE), and from enzymatic degradation. For most of the glycosidic linkages, the major NOE on irradiation of the anomeric proton was observed at the proton attached to the aglyconic carbon atom. However, on irradiation of the anomeric proton resonance of nonreducing terminal α-GalNAc, the major NOE was observed at H4 rather than at H3 of the galactose to which it is linked in spite of the $\alpha 1 \rightarrow 3$ linkage. This effect results from a conformation for the GalNAc($\alpha 1 \rightarrow 3$)Gal linkage in which the anomeric proton is closer to galactose H4 than it is to H3. This result indicates that some caution must be exercised in the use of NOE to directly infer the position on glycosidic linkage in complex carbohydrates. A total of 75% of the carbohydrate was isolated from the glycoprotein in the form of oligosaccharide chains having either or both type 1 and type 2 core units linked to galactosaminitol. The remaining 25% of the carbohydrate was isolated as a polysaccharide whose molecular weight was indicated by gel filtration chromatography to be at least 6000. The simple NMR spectrum of the polysaccharide implies that it has a simple repeating subunit with a backbone of β-linked sugars and a type 1 side chain with the GalNAc($\alpha 1 \rightarrow 3$) and Fuc($\alpha 1 \rightarrow 2$) substitution of the β-galactose.

45. Biophysical Properties of Chiral Thiophospholipids. *R.-T. Jiang*, D. A. Wisner, K. Bruzik, and M.-D. Tsai. Department of Chemistry, The Ohio State University, Columbus, OH 43210.

The prochiral phosphorus center of phospholipids could in principle exist in four possible states in the liquid-crystalline phase: (I) achiral, $^{\delta-}O\text{-}P\text{-}O^{\delta-}$; (II) chiral, O═P—O$^-$; (III) chiral, $^-$O—P═O; (IV) racemic, as a mixture of II and III. Using (R_P)-, (S_P)-, and ($R_P + S_P$)-DPPsC (1,2-dipalmitoyl-*sn*-glycero-3-thiophosphocholine) as models for states II, III, and IV, respectively, we found that they formed lipid bilayers which gave ^{31}P NMR line shapes and ^{14}N NMR quadrupolar splittings ($\Delta\nu_Q$) characteristic of natural membranes. In addition, they gave different magnitudes of $\Delta\nu_Q$ and of ^{31}P chemical shift anisotropy ($\Delta\sigma$). Most surprisingly, (R_P)-DPPsC showed abnormal thermotropic properties (a broad transition at 45.6 °C). Addition of 15% S_P isomer to the R_P isomer converts the abnormal DSC curve to the "normal shape", with a pretransition at 42.8 °C and a main transition at 44.7 °C. Further time-dependent DSC study indicated that (R_P)-DPPsC assumes a lower energy gel phase. The results suggest that the configuration at the phosphate of phospholipids is important in the structure of multilamellar membranes.

46. EPR and ENDOR Investigation of CO Binding to the "Bidirectional" and "Uptake" Hydrogenases from *Clostridium pasteurianum W5*. *M. J. Benecky*, M. W. W. Adams, L. E. Mortenson, and B. M. Hoffman. Department of Chemistry, Northwestern University, Evanston, IL 60201, and Exxon Research & Engineering Company, Clinton, NJ 08801.

The observation of sizable ^{13}C hyperfine couplings by EPR and ENDOR provides unambiguous evidence for covalent bonding of the competitive inhibitor CO to the "bidirectional" and "uptake" hydrogenases from *C. pasteurianum*. The binding site appears to be the novel Fe-S center, which gives rise to the characteristic EPR signal of the oxidized enzyme. EPR and ENDOR show that a single CO is bound and the strength of the interaction is nearly 5 times stronger in "uptake" hydrogenase (A^C = 34 MHz) compared to the "bidirectional" enzyme (A^C = 7 MHz). The CO binding site in "uptake" hydrogenase is unique with respect to the presence of ENDOR-detectable exchangeable protons. These protons are probably from a coordinated water molecule.

47. ENDOR Studies of Reduced Beef Heart Aconitase: Evidence for Water and Substrate Binding. *Joshua Telser*, Brian M. Hoffman, Mark H. Emptage, and Helmut Beinert. Department of Chemistry, Northwestern University, Evanston, IL 60201, and Institute for Enzyme Research, Department of Biochemistry, University of Wisconsin, Madison, WI 53705.

Aconitase has been studied by EPR and Mössbauer spectroscopy and contains an Fe_4-S_4 cluster. Reduced aconitase is an EPR-active species that has been studied by EPR and ENDOR spectroscopy. In the presence of known substrates and inhibitors, line broadening of the EPR signal in $H_2{}^{17}O$ solution is observed. ENDOR spectroscopy definitively showed a well-resolved signal assignable to ^{17}O from $H_2{}^{17}O$. Similar ^{17}O signals are observed for aconitase in the presence of citrate, nitroisocitrate, and *trans*-aconitate. Hyperfine coupling constants of ~9 MHz and quadrupole coupling constants of ~1 MHz are observed in these samples. This is indicative of strong covalent binding of water to the Fe_4-S_4 cluster. In addition, aconitase in the presence of nitroisocitrate with a ^{17}O-labeled hydroxyl functionality in $H_2{}^{16}O$ solution also shows a ^{17}O signal, although relatively weak in intensity. This suggests direct binding of the substrate to the cluster.

48. Fast Atom Bombardment Analysis of Disulfide-Containing Peptides. *R. Yazdanparast*, P. D. Andrews, D. L. Smith, and J. E. Dixon. Department of Medicinal Chemistry and Pharmacognosy, Purdue University, West Lafayette, IN 47907.

Fast atom bombardment (FAB) mass spectrometry of peptides has recently received a considerable amount of attention. Although the role of FAB mass spectrometry in

obtaining complete structural information has not yet been explored, our work indicates that this technique is well suited for the characterization of disulfide bonds in peptides. We have investigated the general behavior of some intra- and interchain disulfide-containing peptides. The method of characterization has been based on the simultaneous identification of the protonated molecular ion of the oxidized samples, and some of their significant fragment ions form as a result of the sample reduction by xenon atom beam. The potential of this technique for establishing the disulfide bond connectivities in proteins containing several disulfide bond linkages will be discussed.

49. Determination of Fluorescence Energy Transfer between Aromatic Residues of Enzymes by Computer Simulation of the Excitation Spectrum. *Warren V. Sherman*, Mark S. Boyd, and Patricia L. Palmer. Department of Physical Sciences, Chicago State University, Chicago, IL 60628.

Spectrofluorometry of the emission from intrinsic tyrosyl (Tyr) and tryptophanyl (Trp) residues of proteins is a widely used technique for studying both polypeptide conformation and protein-receptor interactions. The observation of Tyr → Trp energy transfer may be used to determine distances between these two residues by using the Förster equation for transfer between donor–acceptor pairs possessing overlapping emission and absorption bands. To determine the efficiency of this transfer, a laborious calculation must be carried out in which Trp emission quantum yields are determined at incremental wavelengths throughout the peptide absorption band. Tyr → Trp transfer efficiency is then calculated by the extent to which light absorbed by Tyr is converted to Trp emission. In the present method, the absorption spectra of monomeric Tyr and Trp, acquired separately on a digital spectrophotometer, are red-shifted to simulate peptide residues and added proportionately until a best fit to the experimental protein excitation spectrum is obtained. With this method, interresidue energy transfer ranging from 0 to 70% has been measured for a number of enzymes and other bioactive proteins.

50. Effect of pH on the Distance between Met-25 and Cys-98 of Troponin C. C. K. Wang and *H. C. Cheung*. Department of Biochemistry, University of Alabama at Birmingham, Birmingham, AL 35294.

We have studied the effect of pH on the transfer efficiency (E) of resonance energy from dansylaziridine attached to troponin C (TnC) at Met-25 to iodoacetamidoeosin linked to Cys-98. Our previous results showed the distance (R) between the two sites to be 39 Å at pH 7.5 based on $\kappa^2 = {}^2/_3$ [Cheung et al. (1982) *Biochemistry 21*, 5135]. When the pH was lowered from 7.5 to ca. 4.5, the donor quantum yield increased by a factor of 2. E decreased from 0.65 to <0.1 when measured in the presence of EGTA or Mg^{2+} and from 0.80 to <0.1 in Ca^{2+}. The pH profile of transfer efficiency was sigmoidal, and the pH at which $E = 0.5$ was 6.2–6.3. At pH 5, E was reduced to 0.1 or less regardless of whether cations were present or absent, suggesting a large increasse in the donor–acceptor separation at low pH and corresponding to R larger than 66 Å. This result is compatible with the recent crystallographic information derived from crystals grown at pH 4.9 and 5 that TnC is elongated with an axial ratio of about 3 [Sundaralingan et al. (1985) *Science* (*Washington, D.C.*) *227*, 945; Herzberg & James (1985) *Nature* (*London*) *313*, 653].

51. Evidence for Structural Organization in Bovine Myelin Basic Protein. *C. S. Randall* and R. Zand. Macromolecular Research Center, Biophysics Research Division, and Department of Biological Chemistry, The University of Michigan, Ann Arbor, MI 48109.

Previous studies from this laboratory on the solution conformation of bovine myelin basic protein (MBP) have been expanded due to our recent findings of an intrinsic esterase activity exhibited by MBP. Such enzymatic capability is inconsistent with the unfolded character often ascribed to MBP. The structural organization in MBP has been studied with TNS, a fluorescent probe for hydrophobic regions of proteins. The binding of MBP to TNS results in an appreciable increase in the fluorescence intensity of TNS, along with a characteristic blue shift in the emission maximum; the intensity is significantly diminished in 8 M urea. These results are interpreted as demonstrating that hydrophobic interactions can occur in MBP as a consequence of protein folding and are abolished in the presence of denaturing agents. The effects of chemical denaturants and temperature on organized structure in MBP have also been examined with calorimetric methods; these results indicate that, in acidic aqueous media, MBP can be unfolded in a manner analogous to many globular proteins. The studies presented here provide compelling evidence for a folded structure of MBP in aqueous solution.

52. Physicochemical Effects of Phenolic Preservatives on Human Insulin. *James Q. Oeswein* and Zoe Ann Bergstedt. Department MC-741, Lilly Research Laboratories, Indianapolis, IN 46285.

The presence of *m*-cresol or phenol in solutions of human zinc insulin at pH 7.4 results in significant changes in the circular dichroic (CD) spectrum of insulin. Increases in molar ellipticity were observed throughout the 200–282-nm region. Other changes included a 5-nm blue shift in the 276-nm transition maximum and the disappearance of ellipticity above 295 nm. No preservative-induced changes were observed in the CD spectra of sodium insulin at pH 7.4 or of zinc insulin at pH 3.0, conditions under which monomer and dimer species predominate. Additionally, analytical ultracentrifugation results suggest that *m*-cresol favors the formation of zinc insulin hexamers at pH 7.4 at lower insulin concentrations. The interpretation of these results with respect to the differential binding of *m*-cresol and phenol to insulin hexamers as opposed to monomers and dimers will be discussed.

53. Dynamic Cis–Trans Isomerization of Retinal in Dark-Adapted Bacteriorhodopsin. *Stanley Seltzer* and Ron Zuckermann. Chemistry Department, Brookhaven National Laboratory, Upton, NY 11973.

The dark reaction (eq 1) wherein light-adapted bacteriorhodopsin (bR^{LA}) reverts to resting, dark-adapted bacteriorhodopsin (bR^{DA}) has been investigated. The high percentage

$$bR^{LA}\ (100\%\ \text{all-trans}) \underset{\text{light}}{\overset{\text{dark}}{\rightleftharpoons}} bR^{DA}\ (1{:}1\ \text{13-cis/all-trans}) \quad (1)$$

of 13-*cis*-retinal in bR^{DA} (50%) compared to that in equilibrated retinal solutions (20–25%) in various solvents and the reported non-first-order process of dark adaptation have suggested that a 1:1 mixture of 13-*cis*- and *all-trans*-retinals might be a stabilizing factor for the trimer structure of bR^{DA}. The possibility that there may be present an equal number of relatively fixed complementary binding sites for specific isomers in bR^{DA} has been examined. Apomembrane was converted directly into bR^{DA} by reconstitution with a 1:1 mixture

of 13-*cis*-retinal and radiolabeled *all-trans*-retinal. Analysis of the isomeric and isotopic content of retinal with time indicates that equilibration of label and cis–trans isomerization, however, *continues in resting* bR^{DA} *in the dark.*

54. Binding of Daunomycin to Tubulin. *Larry Ward* and Serge N. Timasheff. Graduate Department of Biochemistry, Brandeis University, Waltham, MA 02254.

The interaction of daunomycin with calf brain tubulin in 10 mM phosphate and 0.1 mM GTP, pH 7.0, was investigated by using a batch gel equilibration method, Bio-Gel P100 being used as the gel matrix. The Scatchard plot describing the interaction is concave downward, indicating positive cooperativity in the binding response. A complex nature of the binding phenomenon is also indicated by the failure to observe an isosbestic point in the visible difference spectrum that results from the perturbation of the daunomycin chromophore on binding to tubulin. Concentration difference spectra generated by measuring the spectra of a 10-fold greater concentration of daunomycin in a 1-mm cell relative to daunomycin in a 1-cm cell indicate that daunomycin self-associates in the region of interest, the shape of the difference spectra being similar to the tubulin–daunomycin spectrum. The positive cooperative response is investigated in terms of preferential binding of the polymeric forms of daunomycin to tubulin relative to the monomeric form.

55. Binding of CTP to the Allosteric Effector Domain of Aspartate Carbamoyltransferase. *Richard Honzatko*, Heng-Ming Ke, and William N. Lipscomb. Department of Biochemistry and Biophysics, Iowa State University, Ames, IA 50011, and Department of Chemistry, Harvard University, Cambridge, MA 02138.

We present a model for the binding of the allosteric inhibitor CTP to aspartate carbamoyltransferase of *Escherichia coli*. The model represents the first clear interpretation of the interaction of CTP with the allosteric effector domain of the enzyme. The results derive from the refinement of a molecular model against data to 2.6-Å resolution collected from the crystalline complex of CTP with aspartate carbamoyltransferase. Density for a CTP molecule is significant only for one of two allosteric sites of the regulatory dimer. Lysines-60 and -94 of the same regulatory chain bind to the γ- and β-phosphates of CTP. Asparagine-63 binds to the 3′-hydroxyl of the ribose, and the 4-amino group of the pyrimidine base binds to carbonyl 6 of the regulatory chain. Thus, the CTP molecule noncovalently links the first half dozen residues of a regulatory chain to residues of the third and fifth β-strands of the allosteric effector domain. We attribute the difference in occupancy of CTP at the two allosteric sites of a regulatory dimer to specific differences in the packing environments of the two regulatory chains in the crystal lattice.

56. Inhibition of Methylenetetrahydrofolate Reductase by *S*-Adenosylmethionine. *David A. Jencks* and Rowena G. Matthews. Biophysics Research Division and Department of Biological Chemistry, The University of Michigan, Ann Arbor, MI 48109.

Methylenetetrahydrofolate reductase catalyzes the NADPH-linked reduction of methylenetetrahydrofolate to methyltetrahydrofolate, a reaction that commits tetrahydrofolate-bound one-carbon units to use in the regeneration of methionine from homocysteine. The pig liver enzyme is a dimer of 77-kDa subunits, each containing noncovalently bound FAD. The flavin is alternately reduced by NADPH and reoxidized by methylenetetrahydrofolate or by the artificial electron acceptor menadione. The reductive half-reaction is inhibited by adenosylmethionine (AdoMet). Inhibition and reactivation of the enzyme are first-order processes with rate constants slow enough that the kinetics of transitions between active and inactive enzymes are readily measurable. Both the equilibrium activity and the rate constant for approach to equilibrium show dependence on inhibitor (AdoMet) and substrate (NADPH) concentrations consistent with a mechanism involving the slow interconversion of active (E) and inactive (E*) forms of the enzyme, with substrate binding only to E and AdoMet binding only to E*.

57. Interaction of Polyglutamyl Derivatives of Methotrexate (MTX), 10-Deazaaminopterin (10-DAM), and Dihydrofolate (DHF) with Sheep Liver Dihydrofolate Reductase (DHFR). *P. Kumar*, Y. Gaumont, R. L. Kisliuk, M. G. Nair, C. M. Baugh, and B. T. Kaufman. Tufts University, Boston, MA 02111, University of Southern Alabama, Mobile, AL 36688, and National Institutes of Health, Bethesda, MD 20205.

We determined the effect of polyglutamylation on the inhibitory activity of folate analogues for DHFR as well as the ability of polyglutamyl derivatives of DHF to antagonize this inhibition. IC_{50} values were determined at pH 7.2, 30 °C, with enzyme (>90% pure) to start the reaction. With MTX, stepwise polyglutamylation causes small decreases in IC_{50} values with each additional Glu until 2,4-$(NH_2)_2$-10-$CH_3PteGlu_6$ has an IC_{50} value one-third that of MTX. With 10-DAM the pattern is more complex. The IC_{50} values *increase* with addition of Glu residues until a maximum is reached with 2,4-$(NH_2)_2$-10-deaza-$PteGlu_3$, which has a value twice that of 10-DAM. The Glu_4 and Glu_5 forms have progressively lower IC_{50} values, the Glu_5 form being equipotent with 10-DAM. If $H_2PteGlu_5$ is used as a substrate in place of DHF, IC_{50} is increased 2–5-fold. Similar results were found with DHFR from chicken liver and beef liver. Thus the Glu chain length of inhibitor and substrate could be important in determining DHFR inhibition in vivo.

58. Inhibition of Phosphotransferase and cGMP-Binding Activities of cGMP-Dependent Protein Kinase with *o*-Phthalaldehyde. *R. N. Puri*, D. Bhatnagar, D. B. Glass, and R. Roskoski, Jr. Department of Biochemistry, Louisiana State University Medical Center, New Orleans, LA 70119, and Department of Pharmacology, Emory University School of Medicine, Atlanta, GA 30322.

The loss of phosphotransferase activity of cGMP-dependent protein kinase (cGK) following treatment with *o*-phthalaldehyde (OPTH) follows pseudo-first-order reaction with a second-order rate constant of 35 M^{-1} s^{-1}. The fluorescence and emission spectra of the cGK–OPTH adduct are consistent with the formation of an isoindole derivative. At a given concentration of OPTH, when there is a complete loss of phosphotransferase activity, there is only 50% loss of cGMP binding activity of cGK in the same time period. The results obtained from binding studies in the presence and absence of cGMP combined with those from chemical modification followed by OPTH reaction show that there are 2 mol of OPTH bond per mole of enzyme both at catalytic and at regulatory sites of cGK. These results and those from molar transition energy measurements of the cGK–OPTH adduct show that SH and ϵ-NH_2 functions of cysteine and lysine residues participating in the isoindole derivative are located 3 Å apart in the hydrophobic environment of the enzyme.

59. Binding of the Transition-State Analogue 2′-Deoxycoformycin to Calf Adenosine Deaminase. *L. Frick*, R. Wolfenden, D. Baker, and E. Smal. Department of Biochemistry, University of North Carolina, Chapel Hill, NC 27514, and Department of Chemistry, University of Alabama, Tuscaloosa, AL 35486.

2′-Deoxycoformycin (2′dCF) binding to adenosine deaminase was investigated by using isotopic incorporation studies and the effect of pH on association and dissociation of the E·I complex. Incubation of 2′dCF and adenosine deaminase in $H_2{}^{18}O$ for 383 h, followed by isolation and by GC–MS of the 2′dCF, indicated that 2′dCF is bound intact by adenosine deaminase, confirming that the enzyme operates via direct water attack. Attempts to demonstrate a stable, covalent E·I complex using tritium-labeled 2′dCF and SDS denaturation were unsuccessful. Formation of the E·I complex showed pK_a's at pH 5.8, corresponding to the pK_a of 2′dCF and to an inflection in V_{max}, and at pH 9.3, corresponding to an inflection in the K_m for adenosine. Dissociation was relatively unaffected by pH.

60. Application of Transition-State Analogue Peptidyl Aldehyde Proteinase Inhibitors to the Study of Cancer Cell Metastasis. *R. M. Schultz*, L. E. Ostrowski, P. Pagast, A. Ahsan, B. P. Suthar, and K. A. Kozlowski. Department of Biochemistry, Loyola University Stritch School of Medicine, Maywood, IL 60153.

Peptidyl argininal (arginine aldehyde) transition-state analogue inhibitors have been synthesized as selective proteinase inhibitors. Selectivity of inhibition varies by orders of magnitude toward the different lysosomal and plasma proteinases implicated in the mechanism of metastasis. For example, D-Phe-Pro-argininal shows a K_i of 3×10^{-8} M to thrombin, Ac-Leu-Leu-argininal (leupeptin) a K_i of 4×10^{-9} M to melanoma cell cathepsin B, and Glu-Gly-argininal a K_i of 2×10^{-5} M against plasminogen activators. For each inhibitor above, inhibition constants for other proteinases implicated in metastasis were orders of magnitude poorer. Ep453, an epoxide inhibitor of cathepsins B and L, was also used in these studies. In a mouse model, leupeptin inhibits metastasis of B16 melanoma cells to the lung, while Ep453 and D-Phe-Pro-argininal have no effect. On the basis of the specificity of the transition-state analogue inhibitors, the roles of particular proteinases in tumor cell migration and invasion may be elucidated.

61. Evidence for Inverted Substrate Binding at the Catalytic Site of Estradiol 17β-Dehydrogenase. *F. Sweet*, J. C. Warren, and G. L. Murdock. Department of Obstetrics and Gynecology, Washington University, St. Louis, MO 63110.

New bromoacetate derivatives of estradiol were synthesized to further study protein–ligand binding in human estradiol 17β-dehydrogenase (hE17DH). Estradiol 17-bromoacetate (17β-BAE), estradiol 3-acetate 17-bromoacetate (17β-MAE), and 1,3,5(10)-estratriene-3,17α-diol 17-bromoacetate (17α-BAE) were synthesized with ^{14}C in the bromoacetate group. The bromoacetate group at the C-17 position prevented the steroids from acting as substrates for hE17DE. These analogues are competitive inhibitors with K_i values of 90 μM (17α-BAE), 134 μM (17β-BAE), and 115 μM (17β-MAE). Incubations of 10 μM of each analogue with hE17DH produced first-order inactivation kinetics with $t_{1/2}$ values of 38 (17α-BAE), 80 (17β-BAE), and 190 min (17β-MAE). 17α-BAE and 17β-BAE each produced over 90% of 3-[^{14}C]-carboxymethylhistidine (3-CMHis) in hE17DH. The ^{14}C-labeled enzyme was digested with trypsin, ^{14}C-labeled peptide fragments were isolated by HPLC, and the peptides were sequenced to give F-Y-Q-Y-L-A-CMH-S-K; the same peptide was labeled earlier with estrone 3-bromoacetate. The results suggest that 17β-BAE and 17α-BAE react with a His at the catalytic site of hE17DH in an inverted binding orientation relative to the catalytic binding of substrates.

62. Tryptophan Synthase and Tryptophanase Exhibit Opposite Stereospecificities for the Two Diastereoisomers of 2,3-Dihydro-L-tryptophan, a Reaction Intermediate Analogue and Inhibitor. Robert S. Phillips, *Edith Wilson Miles*, and Louis A. Cohen. National Institute of Arthritis, Diabetes, and Digestive and Kidney Diseases, National Institutes of Health, Bethesda, MD 20205.

Tryptophan synthase and tryptophanase are both strongly inhibited by 2,3-dihydro-L-tryptophan, an analogue of the indolenine tautomer of L-tryptophan, a proposed reaction intermediate. Since the proposed intermediate and 2,3-dihydro-L-tryptophan both have a tetrahedral carbon at C-3 of the heterocyclic ring, they have an asymmetric center at C-3. Thus 2,3-dihydro-L-tryptophan exists in two diastereoisomeric forms. Using preparative reverse-phase HPLC, we have separated the two diastereoisomers A and B of 2,3-dihydro-L-tryptophan. Whereas diastereoisomer B is a potent competitive inhibitor of tryptophan synthase (K_I = 6 μM) and forms a quinonoid intermediate with tryptophan synthase (λ_{max} = 494 nm), it is a very poor inhibitor of tryptophanase (K_i > 1600 μM). In contrast, diastereoisomer A is a very weak inhibitor of tryptophan synthase ($K_I \geq$ 940 μM), but a potent inhibitor of tryptophanase (K_I = 2 μM). The specific inhibition of these two enzymes by different diastereoisomers of the reaction intermediate analogue suggests that these enzymes catalyze their reactions via *enantiomeric* indolenine intermediates.

63. Interaction of Horse Liver Alcohol Dehydrogenase with F-Actin. *Jacqueline M. Taylor* and Lai-Man Chan. Department of Chemistry, Jackson State University, Jackson, MS 39217.

The interaction of horse liver alcohol dehydrogenase with F-actin was studied by separating the free and bound enzymes by ultracentrifugation and assaying the supernatant for free enzyme. When increasing amounts of F-actin were added to 0.1 mg of alcohol dehydrogenase, 50% of the enzyme became bound to F-actin at saturation; there was 0.5 mol of bound enzyme per turn of actin double helix. KCl (18 mM) decreases the binding of alcohol dehydrogenase to F-actin 35%, while 17 mM ATP increases the binding 3.6-fold. ADP, AMP, NAD^+, NADH, ethanol, or acetaldehyde has no effect on the binding. The bound enzyme has a higher K_m and is much less active than the free enzyme. The reversible interaction of alcohol dehydrogenase with F-actin could be a control mechanism of enzymatic activity in the liver cells.

64. Inactivation of Human Serum Transferrin by Oxidizing Agents. Michael H. Penner, David T. Osuga, Claude F. Meares, and *Robert E. Feeney*. Department of Food Science and Technology and Department of Chemistry, University of California, Davis, CA 95616.

Periodate was reported by Azari and Phillips [(1970) *Arch. Biochem. Biophys. 138*, 32–38] to inactivate chicken ovotransferrin with losses of tyrosine and tryptophan. We recently

reported that inactivation of human serum transferrin (HST) and human lactotransferrin also occurs with concomitant oxidation of essential tyrosines and unessential methionines [Geoghegan et al. (1980) *J. Biol. Chem. 255*, 11429–11434; Penner et al. (1983) *Arch. Biochem. Biophys. 225*, 740–747]. We now report that both periodate and permanganate at pH ~8 inactivate HST. A ratio of 1:1 for periodate and permanganate to metal-binding sites gave 52% and 35% inactivations, respectively; a ratio of 3:1 gave 74% and 67% inactivations, respectively. Since part of the oxidizing agent is consumed by the oxidation of methionines, the actual ratio is even much lower. In contrast, a ratio of 4:1 for hypochlorite gave no inactivation, while much higher levels of hypochlorite caused extensive inactivation, with a general destruction of several other amino acids. High concentrations of periodate did not cause this general destruction. Periodate and permanganate appear to resemble affinity reagents, binding in the anion-binding sites for the essential synergistic anion bicarbonate.

65. Purification and Characterization of Aminoacetone Synthetase. *B. Fubara* and L. Davis. Department of Chemistry, University of Iowa, Iowa City, IA 52242.

Aminoacetone synthetase (EC 2.3.1.29) from beef liver mitochondria has been purified to homogeneity by a five-step procedure. Aminoacetone synthetase isolated by this procedure was found to be homogeneous by sodium dodecyl sulfate (SDS) and neutral discontinuous gel electrophoresis. The purified enzyme had a turnover number of 896 (moles of substrate transformed per minute per mole of enzyme). A molecular weight of 56 000 was calculated by gel filtration and 28 000 by SDS gel electrophoresis. Thus the enzyme appears to be a dimer of identical subunits. The aminoacetone synthetase has been shown to be a pyridoxal phosphate requiring enzyme, with absorption maxima at 278 and 430 nm. Reduction of the enzyme with sodium cyanoborohydride inactivated the enzyme and shifted the 430-nm peak to 335 nm. Cysteine has been used to inactivate the enzyme and resolve it of its pyridoxal phosphate. Results with cysteine have demonstrated 2 mol of pyridoxal phosphate per mole of enzyme. Thus beef liver mitochondrial aminoacetone synthetase has been shown to be an anionic, dimeric enzyme containing one pyridoxal phosphate per subunit, with an isoelectric pH of 5.2 and a pH optimum of 7.6–7.8.

66. Mechanistic Studies of Bovine Aminoacetone Synthase. *F. M. Eckenrode* and L. Davis. Department of Chemistry, University of Iowa, Iowa City, IA 52242.

Aminoacetone synthase (EC 2.3.1.29) isolated from bovine liver mitochondria has been shown to catalyze the condensation of glycine and acetyl-CoA to produce CO_2, CoA, and the stable product aminoacetone. This reaction likely proceeds by one of two possible mechanisms: through the formation and release of an unstable oxoaminobutyrate that undergoes spontaneous decarboxylation or through an enzymatic decarboxylation resulting in direct aminoacetone formation. Product inhibition studies with $NaHCO_3$ and aminoacetone are utilized to determine if aminoacetone is a true enzymatic product. Initial velocity kinetic studies suggest a sequential mechanism for glycine and acetyl-CoA addition and product release. Enzymatic $^{14}CO_2$ release from (1-^{14}C)glycine in the absence of acetyl-CoA is approximately 10% of that released in the presence of acetyl-CoA. Aminoacetone synthase has also been shown to catalyze the conversion of aminomalonate to glycine and aminoacetone, further demonstrating a decarboxylative ability of this enzyme.

67. Coupling of Two Mammalian Liver Mitochondrial Enzymes, L-Threonine Dehydrogenase and Aminoacetone Synthetase. *T. J. Tressel* and L. Davis. Department of Chemistry, University of Iowa, Iowa City, IA 52242.

L-Threonine dehydrogenase (EC 1.1.1.103) and aminoacetone synthetase (EC 2.3.1.29) have been purified to homogeneity from mammalian liver mitochondria. These two enzymes can be coupled to produce glycine and acetyl-CoA from L-threonine. This coupled reaction requires NAD and CoA as cofactors. The oxidative cleavage of L-threonine is not a tightly coupled reaction in that production of aminoacetone always accompanies production of glycine and acetyl-CoA. Several models have been examined to explore the mechanism by which L-threonine dehydrogenase and aminoacetone synthetase couple since 2-amino-3-oxobutyrate, the product of the dehydrogenase, is unstable and undergoes a spontaneous decarboxylation. Evidence will be presented to distinguish between a random diffusion model, in which 2-amino-3-oxobutyrate dissociates from the dehydrogenase, and a direct transfer model, which involves the formation of an enzyme–2-amino-3-oxobutyrate–enzyme complex. Kinetic studies, size exclusion chromatography, and fluorescence spectroscopy have been used to provide evidence of protein–protein interaction and transfer of the 2-amino-3-oxobutyrate between the two enzymes.

68. Conversion of Phytol to Phytanic Acid in Vitro in Rat Liver: Enzyme Characterization. *V. B. Muralidharan* and Florentina N. Muralidharan. John F. Kennedy Institute and Department of Neurology, The Johns Hopkins University School of Medicine, Baltimore, MD 21205.

Phytol and phytanic acid are minor constituents of the human diet. In vivo studies have indicated that phytol is rapidly converted to phytanic acid. We recently studied phytol–phytanate conversion in vitro in rat liver using [U-^{14}C]phytol as the substrate and showed that phytenic acid is formed as an intermediate in this conversion, consistent with earlier in vivo observations (*Biochim. Biophys. Acta*, in press). We now report the synthesis of a new substrate, [1-^{3}H]phytol, and characterization of the enzyme system that converts phytol to phytanic acid in rat liver. The assay procedure involves measurement of tritium released in the aqueous medium when [1-^{3}H]phytol is oxidized. The phytol to phytanate-converting enzyme activity appears to be present mainly in mitochondrial and microsomal fractions. In the mitochondrial fraction, the activity required NAD^+, did not require molecular oxygen, and was stimulated by albumin. The amount of water-soluble radioactivity increased with time up to 7 min. The activity was linear with mitochondrial protein up to 200 μg. Further details on this enzymatic conversion will be presented.

69. Measurement of the Stability of Asymmetrical Hybrid Hemoglobins by Anaerobic High-Performance Ion-Exchange Liquid Chromatography. *C. Yu Ip*, M. Anbari, and T. Asakura. Departments of Pediatrics and Biochemistry and Biophysics, The Children's Hospital of Philadelphia, University of Pennsylvania, Philadelphia, PA 19104.

Asymmetrical hybrid hemoglobins formed from mixtures of oxyhemoglobins S and F, A and S, York (β146 His → Pro) and A, and York and S were separated by high-performance ion-exchange liquid chromatography (HPLC) under anaerobic conditions. The resulting HPLC chromatograms showed three

peaks, with the middle peak representing the hybrid hemoglobin. The areas of these three peaks were quantified. The amount of hybrids formed was less than that predicted theoretically. We found that the deviation was due to instability of the hybrid hemoglobins. We determined the rate of dissociation for deoxy-AS and deoxy-FS hybrid hemoglobins by the recycle HPLC method. The rates of dissociation of deoxy-AY and deoxy-SY were also estimated. Hybrid hemoglobins AY and SY dissociated into dimers at a considerably higher rate than did AS and FS hybrid hemoglobins. The mutation at the β146 (His → Pro) in hybrid hemoglobins containing $\alpha\beta^Y$ dimers hinders the formation of the salt bridges that normally stabilize the "T" quaternary conformation; therefore their rate of dissociation into dimers is expected to increase.

70. Amphibian Adenosine Deaminases. *Pang Fai Ma.* Center for Medical Education, Ball State University, Muncie, IN 47306.

Multiple forms of adenosine deaminase have been found in a wide variety of organisms, including amphibian. These molecular forms differ in molecular sizes and can be separated by gel filtration chromatography. The molecular form distribution pattern varies among different tissues of the same organism. One form of the enzyme may be predominating in one tissue but not in other. An attempt has been made to isolate these enzyme forms. Some characteristic features, such as molecular weight and catalytic properties, of the amphibian hepatic adenosine deaminases will be discussed.

71. A Fatal Variant of Human Ornithine Carbamoyltransferase Can Be Stimulated by Mg^{2+}. *Beulah M. Woodfin.* Department of Biochemistry, University of New Mexico, Albuquerque, NM 87131.

Ornithine carbamoyltransferase (OCTase) activity was determined to be 2% of normal in the post-mortem liver of a severely mentally retarded female who died at the age of 2 years and 3 months. Assay of the activity in the presence of added Mg^{2+} (0.05 M) had no effect in normal liver homogenates but resulted in stimulation to 13% of normal in the subject liver homogenate. (OCTase activity above 5% of normal has been reported to be consistent with normal development.) There was no apparent change in K_M for either substrate or in pH optimum in the mutant enzyme. Kinetic studies using the transition-state analogue δ-*N*-(phosphonoacetyl)-L-ornithine yield data consistent with the proposed ordered bi-bi mechanism for both normal and mutant enzymes, although the apparent K_I's for the mutant enzyme are smaller than those for the normal enzyme. In the presence of this inhibitor, Mg^{2+} exhibits a more pronounced effect when ornithine (the second substrate in the ordered bi-bi mechanism) is the varied substrate than when carbamoyl phosphate is the varied substrate.

72. Carbonic Anhydrase in *Musca autumnalis*. *E. T. Burt*, M. V. Darlington, G. Graf, and H. J. Meyer. Departments of Biochemistry and Entomology, North Dakota State University, Fargo, ND 58105.

In a recent study we localized, purified, and partially characterized a carbonic anhydrase (carbonate hydro-lyase; EC 4.2.1.1) in the face fly *Musca autumnalis* (DeGeer) (Diptera: Muscidae). Here we report a procedure that yields sufficiently large amounts of pure carbonic anhydrase isozymes (CA-I and CA-II) to perform structural and kinetic studies. Use of the preparative PAGE technique allowed us to obtain 6- and 0.6-mg quantities of CA-I and CA-II, respectively, in 50% yield and with a high degree of purity. The molecular characteristics of these proteins showed many similarities to well-characterized mammalian, bacterial, and plant carbonic anhydrases. These similarities suggest the great evolutionary antiquity of this enzyme.

73. Alterations in Characteristics of Progestin Receptors (PR) by Sodium Molybdate. *W. B. Mujaji*, L. A. van der Walt, and J. L. Wittliff. Hormone Receptor Laboratory, James Graham Brown Cancer Center, University of Louisville, Louisville, KY 40292.

Sodium molybdate appears to exert a stabilizing effect on the labile PR either by inhibition of protease activity or through control of phosphorylation. Specific binding capacities and affinities of PR were determined in cytosol from human breast tumors and uteri by using [^{3}H]R5020 and [^{3}H]-ORG2058 as ligands to titrate PR binding sites. Measurements of molecular properties were assessed with vertical tube sucrose density gradient centrifugation, gel filtration, and HPLC. The specific binding capacity of most biopsies showed an elevation of 100–150% as a function of increasing [molybdate] reaching a maximum at 5–10 mM. Sucrose density gradient analysis showed molybdate greatly reduced the extent of nonspecific ligand association. In addition, the quantity of PR sedimenting as 8S isoforms increased significantly and only a single specific component was observed. HPLC with size exclusion columns resolved extensive size heterogeneity. Analyses of PR in 10 mM molybdate by HPLC in either ion exchange or chromatofocusing modes showed several isoforms. Sodium molybdate appeared to retain high molecular weight, acidic PR species. These data suggest that molybdate should be used in stabilizing PR either in clinical or in research samples during analysis.

74. Glycolytic Enzymes of the Fetal Middle Ear Fluid. *Leon L. Gershbein.* Northwest Institute for Medical Research, Chicago, IL 60634.

The guinea pig cochlear fluid has been investigated in the fetus and adult as such and under high-intensity sound presentation, and differences in glycolytic enzymes such as LDH, aldolase (ALD), and phosphohexose isomerase (PHI) have been noted [Gershbein et al. (1974) *Environ. Health Perspect. 8*, 157; Manshio & Gershbein (1977) *Acta Oto-Laryngol. 84*, 233]. The fetus also possesses a middle ear fluid of rather unique glycolytic enzyme makeup differing from those of maternal blood and perilymph of the scalae tympani and vestibuli of either the fetus or adult. As it was thought that this fluid might be derived from the amniotic fluid, the latter of which can be swallowed by the fetus and flow from the oral cavity by way of the nasopharynx and Eustachian tubes, several enzymes in both fluids were compared. For the fetal (10 pools or samples) and individual amniotic fluids (n = 95), the mean levels (U/L ± SE) were 352 ± 29 and 232 ± 18 for LDH, 6.7 ± 0.6 and 8.9 ± 0.6 for ALD, and 74 ± 13 and 181 ± 12 for PHI, in the order stated. The LDH isoenzyme patterns were not too delineative. Although some similarity might be construed, possibly, the middle ear fluid arises from a derived ultrafiltrate.

75. Antibodies Directed against Plant Polysaccharides. *John H. Pazur* and Sherry A. Kelly-Delcourt. Paul M. Althouse Laboratory, The Pennsylvania State University, University Park, PA 16802.

Little information is available on the immunological properties of plant polysaccharides in contrast to that available for microbial polysaccharides. The latter were shown many years ago to be capable of stimulating the immune system to produce anti-carbohydrate antibodies. It has now been found that anti-carbohydrate antibodies are also induced in animals immunized with vaccines of the gum arabic in Freund's complete adjuvant. Gum arabic is composed of rhamnose, arabinose, galactose, and glucuronic acid. Periodate oxidation of gum arabic destroyed a high percentage of the rhamnose, arabinose, and glucuronic acid residues but not galactose residues. The periodate-oxidized gum arabic no longer yielded a precipitin reaction with anti-gum arabic antibodies. Such antibodies have been isolated by affinity chromatography on a gum arabic–Sepharose adsorbent. The antibodies were bound to the adsorbent from buffer solution and eluted with ammonium thiocyanate. The antibody fractions were collected, the thiocyanate was removed by dialysis, and the solution was analyzed for antibody activity. Antibodies directed against gum arabic were detected by agar diffusion and enzyme-linked immunoassays.

76. Deglycosylation of Human Serum Orosomucoid. *J. R. Wermeling* and H. Brian Halsall. Department of Chemistry, University of Cincinnati, Cincinnati, OH 45221-0172.

The roles of the glycan chains in glycoproteins appear to be various and poorly understood. Little attention has been given to the effect of deglycosylation on those properties of the polypeptide core intrinsic to it; i.e., do coupling phenomena exist between the glycan and protein components of the molecule? Human serum orosomucoid (OMD) is a physically and chemically well-described glycoprotein and was the model system chosen for the study. Deglycosylation by trifluoromethanesulfonic acid yielded a molecule (dGOMD) of M_r ~24 000 as expected, chemically and physically homogeneous. dGOMD gave lines of immunochemical identity with OMD and essentially identical PMR spectra at 360 MHz. Compared to OMD, intrinsic Trp fluorescence was red-shifted 5 nm and the fraction quenched by I^-, Cs^+, and chlorpromazine increased. These data, combined with comparative K_Q values, indicate that although the essential integrity of OMD has been retained, Trp(s) in the drug binding domain has (have) moved to a more polar environment.

77. Influence of Sialic Acid on the Interactions of Human Orosomucoid. *Mark L. Friedman* and H. Brian Halsall. Department of Chemistry, University of Cincinnati, Cincinnati, OH 45221-0172.

Sialic acids (SA) are universal components of glycoproteins. Their detailed physiological function(s) is (are) unknown. It can be surmised that in some glycoproteins a functional relationship exists between SA and the polypeptide backbone. To examine this question, orosomucoid (α_1-acid glycoprotein; OMD) was chosen as a model system. The effects of sequential removal of the SA were examined by using the intrinsic fluorescence of the protein and by monitoring the binding of drugs as extrinsic probes. All three tryptophans are located in the binding domain [(1985) *Biophys. J. 47*, 409a] and may provide a sensitive measure of domain integrity. Desialylation did not change the quenching parameters of these Trps by diverse quenchers, suggesting a lack of change in the Trps' environment. However, of the three drugs monitored, only the interaction of chlorpromazine decreased significantly and monotonically with decreasing SA content. Data will be presented to show that the depression in CPZ binding is due to either a loss of an electrostatic interaction with SA or a (−) charge on the surface of the protein.

TUESDAY MORNING—ELI LILLY AWARD SYMPOSIUM IN HONOR OF GERALD RUBIN—N. COZZARELLI, SYMPOSIUM CHAIRMAN

78. Determination of the Mechanisms of Genetic Recombination by New Topological Methods. Howard W. Benjamin, James B. Bliska, *Nicholas R. Cozzarelli*, Jan M. Dungan, Stephen P. Gerrard, Sylvia J. Spengler, and Steven A. Wasserman. Department of Molecular Biology, University of California, Berkeley, CA 94720.

The two stages in site-specific recombination are bringing the target DNA sites together on the recombinase surface (synapsis) and DNA breakage and crossed reunion at each site. Using topological methods, we determined important features of the mechanism of synapsis and strand exchange for the resolvase encoded transposon Tn3 and the phage λ site-specific recombination system. Irrespective of substrate supertwist density, the resolvase synaptic mechanism ensures that there are three (−) supercoils between the resolvase sites. Two are metamorphosed into the links of the singly linked catenane product whereas the third is cancelled by the single (+) supercoil introduced by strand exchange. In contrast, synapsis in the λ system is essentially by random collision, giving a variety of product knots and catenanes both in vivo and in vitro. The topological methods are rapid and simple and can be used to study a wide range of other problems including the cellular level and structure of supercoils, the mechanism of strand passage by topoisomerases, the properties of paranemic recombination joints, and the untangling of daughter chromosomes at termination.

79. Amplification and Expression of *Drosophila* Chorion Genes. Terry Orr-Weaver, Diane deCicco, Laura Kalfayan, Richard Kelley, Joseph Levine, Suki Parks, Barbara Wakimoto, and *Allan Spradling*. Department of Embryology, Carnegie Institution of Washington, Baltimore, MD 21210.

P element mediated gene transfer was used to study cis-acting regulatory elements within the two major chorion gene clusters of *D. melanogaster*. Both clusters contain a single region that could induce developmentally normal gene amplification at its site of insertion into the genome. In vitro mutagenesis of these "amplification control elements" (*ACE*), which show little or no sequence homology, has been carried out. Sequences necessary for *ACE3* function were mapped 200–600 bp upstream from the s18-1 gene within a region also required for s18-1 transcription. Individual chorion genes were expressed with normal temporal and tissue specificity following transformation. Detailed study of the s38-1 gene delimited the requisite control sequences to a region of, at most, 550 bp 5′ to the transcribed sequences. This has allowed the construction of several potentially useful fusion genes. These studies reveal that the tandemly clustered chorion genes share a single amplification control element but have gene-specific sequences regulating their expression.

80. Regulation and Products of the *Ubx* Domain of the Bithorax Complex of *Drosophila*. *David S. Hogness*. Department of Biochemistry, Stanford University, Stanford, CA 94305.

The functions of the *Ubx* domain of the bithorax complex (BX-C) act as transducers of positional information for the specification of the compartment identities of T2p, T3a, T3p,

and A1a (where T2, T3, and A1 refer to the second and third thoracic segments and the first abdominal segment, respectively, and a and p refer to the anterior and posterior compartments of these segments). This domain contains two adjacent long transcription units of identical orientation: the 75-kb *Ubx* unit and the 25-kb *bxd* unit, which are coextensive with the sites of *Ubx* and *bxd* mutations, respectively. *Ubx* mutations cis-inactivate all known functions of the domain, which we designate as ABX (required for T2p identity), BX (T3a identity), PBX (T3p identity), and BXD (A1a identity) according to a model based on the phenotypes of four mutational classes that, in the model, inactivate subsets of these functions. The *abx* and *bx* classes, which occupy distinct regions within the *Ubx* unit, inactivate respectively ABX + BX and BX, while the *bxd* and *pbx* classes of the *bxd* unit inactivate respectively BXD + PBX and PBX.

81. P Transposable Elements and Their Use as Genetic Tools in *Drosophila*. *G. M. Rubin*. Department of Biochemistry, University of California, Berkeley, CA 94720.

Transposable elements are segments of DNA that move as discrete units from place to place in the genome. P transposable elements are of particular interest because their mobility has been shown to be under genetic control and can be manipulated experimentally. Work in our laboratory on the structure(s) of P elements and their gene products will be discussed. P element transposition appears to be limited to the germ line. A model for the mechanisms of this restriction, based on the results of in vitro mutagenesis experiments, will be presented. P elements have proven to be useful to *Drosophila* molecular geneticists as tools for "transposon tagging" and DNA-mediated gene transfer. These two methods will be described.

TUESDAY AFTERNOON—PFIZER AWARD SYMPOSIUM IN HONOR OF THOMAS CECH—PERRY FREY, SYMPOSIUM CHAIRMAN

82. Synthesis of Nucleotides with Chiral Phosphorus. Application to Stereochemical Analysis of Phosphotransferase Action. *Perry A. Frey*. Institute for Enzyme Research and Department of Biochemistry, University of Wisconsin, Madison, WI 53705.

Recently developed methods make possible the practical syntheses of nucleotide analogues having any desired stereochemically specific pattern of sulfur and ^{18}O or/and ^{17}O substitution for ^{16}O in the phosphate, diphosphate, or triphosphate moieties. These are very often substrates for phosphotransferases and nucleotidyltransferases and are important in the stereochemical analysis of the reaction mechanisms. When suitably protected with a removable alkyl or aryl group at terminal phosphoryl groups, the nucleoside 1-thio- or 2-thiodi- and triphosphates are also excellent precursors for nucleotides having heavy isotopes of oxygen stereospecifically placed at the α-, β-, or γ-phosphorus. As examples, the syntheses of (R_P)-[α-^{17}O]ADP and (S_P)-[α-^{17}O]ADP and also (R_P)-[β-^{17}O]ATP and (S_P)-[β-^{17}O]ATP will be described. These compounds are used for determining the absolute configurations of Mn(II) nucleotides at P_α and P_β when bound at the active sites of enzymes. Representative data will be presented.

83. Studies on the Mechanism of Action of DNA Polymerase I. Valerie Mizrahi, Paul Darke, Patricia Benkovic, and *Stephen J. Benkovic*. Department of Chemistry, The Pennsylvania State University, University Park, PA 16802.

Experiments will be discussed that focus on relating the structure and function of DNA polymerase I. Pulse-chase, stop-flow, and double-labeling experiments have been designed to elucidate the minimal kinetic sequence for the enzyme, the possible locus of rate-limiting steps, and the integration of the polymerase and 3′–5′-exonuclease activities. In addition, nucleoside triphosphates that bear fluorescent labels have been employed as nucleoside triphosphate analogues and incorporated into the 3′-hydroxyl ends of template-primers to furnish evidence for both rate processes and acceptors/donors for fluorescence energy transfer experiments. The Klenow fragment has been labeled at its single sulfhydryl by a complementary fluorescent probe, and distance measurements to fluorescent labels were recorded. Finally, the effect of active site mutations on the individual steps within the kinetic sequence has been investigated to further define the relationship between protein structure and function.

84. New Chemical Methods for Synthesizing DNA and RNA. *M. H. Caruthers*. Department of Chemistry, University of Colorado, Boulder, CO 80309.

Current DNA synthesis methodologies utilize silica gel and protected deoxynucleoside 3′-phosphoramidites as synthons. Synthetic DNAs containing at least 100 mononucleotides have been successfully prepared. For the synthesis of large DNAs (50–100 monomers), one troublesome problem has been depurination of deoxyadenosine during synthesis. Recent research, which will be discussed, has focused on developing a new series of amidine protecting groups that render deoxyadenosine 20 times more stable toward depurination. With these synthetic methods, base and phosphorus analogues have been introduced into promoters and operators. Biochemical studies involving these analogue sequences will be reported. Because of recent developments in RNA molecular biology, rapid methods for synthesizing RNA have been developed and will be presented. One approach utilizing ribonucleotide 3′-phosphoramidite synthons and nucleosides attached to silica is analogous to current DNA methods. Biochemically reactive heptadecanucleotides have been prepared (2 days) by this approach. A second methodology whereby ribonucleosides are attached covalently to silica through the 5′-hydroxyl has also been developed. 3′-Phosphoramidites are first formed on the support, then condensed with a 2′-tetrahydropyranylnucleoside, and finally oxidized to phosphate (one cycle, 1.5 h).

85. Self-Splicing RNA. *Thomas R. Cech*. Department of Chemistry, University of Colorado, Boulder, CO 80309.

Splicing of the ribosomal RNA precursor of the ciliated protozoan *Tetrahymena* occurs in vitro in the absence of any protein. The folded structure of the intervening sequence (IVS) portion of the RNA is responsible for lowering the activation energy for highly specific phosphodiester bond cleavage–ligation reactions. The reactions occur many orders of magnitude faster than known rates of chemical cleavage of RNA. In essence, the splicing reaction is self-catalyzed. Recent results have given an indication of how the *Tetrahymena* RNA mediates its own splicing. Binding of guanosine to a specific site on the RNA molecule promotes the rate and specificity of the first transesterification reaction involved in splicing. Such substrate binding is a mechanism of catalysis that is familiar from classical enzymology. In addition, the folding of the RNA molecule somehow enhances the electrophilicity of the phosphates at the splice sites, priming them for nucleophilic attack. The IVS RNA molecule can also act as a true regenerated catalyst in vitro, catalyzing cleavage and

ligation of added oligonucleotide substrates. Thus, the IVS RNA is an enzyme.

WEDNESDAY MORNING—SYMPOSIUM ON ONCOGENES, TYROSINE KINASES, AND RECEPTORS—J. A. SHAFER, SYMPOSIUM CHAIRMAN

86. c-*fms* Protooncogene Product. *Charles J. Sherr*, Martine F. Roussel, and Carl W. Rettenmier. Department of Tumor Cell Biology, St. Jude Children's Research Hospital, Memphis, TN 38105.

The retroviral oncogene v-*fms* encodes an integral transmembrane glycoprotein of M_r 140 000 whose expression at the cell surface is required for transformation. The biochemical and topological properties of the transforming glycoprotein closely resemble those of cell surface receptors for growth factors and include the presence of an associated tyrosine-specific protein kinase activity. The c-*fms* protooncogene encodes a 4.0-kilobase mRNA, which is expressed at relatively high levels in placental trophoblasts and in spleen cells. Glycoproteins encoded by c-*fms* were identified in spleen cells with an immune complex kinase assay performed with antibodies to v-*fms*-coded epitopes. The major form of the c-*fms*-coded glycoprotein has an apparent M_r of 170 000 and like the product of the viral transforming gene, serves as a substrate for an associated tyrosine-specific protein kinase activity in vitro. The results suggest that the transforming glycoprotein specified by v-*fms* is a truncated form of a c-*fms*-coded receptor. We speculate that the receptor plays a physiological role in normal hematopoietic cells.

87. Platelet-Derived Growth Factor: Role in Growth of Normal and Simian Sarcoma Virus Transformed Cells. *Thomas F. Deuel* and Benton Tong. Division of Hematology/Oncology, Jewish Hospital at Washington University, St. Louis, MO 63110.

The human platelet derived growth factor (PDGF) is both a potent mitogen and chemoattractant protein for cells involved in inflammation and in repair. The amino acid sequence of human PDGF showed striking homology with $p28^{v\text{-}sis}$, the putative transforming protein of the simian sarcoma virus (SSV), and essential identity with the predicted sequence of the c-sis gene product. A protein identical with PDGF in mitogenic and immunological reactivity has been identified in cell lysates and conditioned media from SSV-transformed cells. This PDGF-like protein competes with purified human ^{125}I-PDGF for receptor binding. Anti-PDGF antiserum added to growth medium blocks thymidine incorporation into $p28^{v\text{-}sis}$-secreting SSV-transformed cells, suggesting that the PDGF-like mitogen stimulates cell growth by autocrine feedback regulation. Transformation, as opposed to autocrine stimulation of cell growth, may be mediated through an intracellular receptor for $p28^{v\text{-}sis}$ because not all SSV-transformed cells secrete detectable growth-promoting activity nor are inhibited in [^{3}H]thymidine uptake by anti-PDGF antisera.

88. Human Insulin Receptor. *O. M. Rosen.* Department of Molecular Biology and Virology, Sloan-Kettering Institute, New York, NY 10021.

The human placental insulin receptor, a glycoprotein tetramer (M_r 350 000) composed of two A and two B subunits linked to each other by disulfide bonds, was purified to homogeneity and shown to contain two functionally discrete activities: insulin binding and insulin-dependent tyrosine protein kinase. The specificity of the protein kinase moiety is similar to that of the v-src gene product with acidic amino acids N-terminal to the tyrosine residue enhancing the affinity of the enzyme for the model peptide substrate. The insulin receptor is synthesized as a single polypeptide precursor containing domains that will ultimately be segregated into the individual subunits found in the processed plasma membrane receptor. N-Terminal amino acid sequences of the purified subunits of the processed receptor were used to construct oligonucleotide probes to screen a human placental cDNA library [Ullrich et al. (1985) *Nature* (*London*) *313*, 756–761]. An insert that encoded the entire insulin receptor precursor was isolated and sequenced. The principal features of the deduced amino acid sequence and implications for the mechanism of insulin action will be discussed.

89. Purification and Characterization of Insulin Receptor Kinase with Phosphotyrosyl-Binding Antibodies. D. T. Pang, B. R. Sharma, L. Argetsinger, and *J. A. Shafer.* Department of Biological Chemistry, The University of Michigan, Ann Arbor, MI 48109.

Studies of insulin-promoted autophosphorylation of partially purified insulin receptor from human placenta demonstrated that only the intact form of insulin receptor ($\alpha_2\beta_2$) undergoes autophosphorylation on tyrosyl residues. The insulin-binding nicked forms of insulin receptor [$\alpha_2\beta\beta_1$ and $\alpha_2(\beta_1)_2$] do not undergo this autophosphorylation reaction. The competence of the phosphorylated receptors to bind insulin was demonstrated by cross-linking the phosphorylated receptor with $N^{\epsilon B29}$-biotinylinsulin. Purification of the phosphorylated form of insulin receptor was achieved by adsorption on and elution (with a hapten) from a column of *O*-phosphotyrosyl-binding antibody immobilized on protein A–Sepharose. This procedure effected a 500-fold purification of the insulin receptor to yield a preparation containing >80% intact catalytically active insulin receptor kinase. The tyrosyl kinase activity of the autophosphorylated form of insulin receptor toward polypeptide substrates was shown to be inhibited by Zn^{2+} and was further characterized with phosphotyrosyl-binding antibody.

WEDNESDAY AFTERNOON—SYMPOSIUM ON ARACHIDONIC ACID METABOLISM—L. MARNETT, SYMPOSIUM CHAIRMAN (PRESENTED WITH SUPPORT FROM UPJOHN AND WARNER-LAMBERT/PARKE-DAVIS; COSPONSORED BY THE DIVISION OF MEDICINAL CHEMISTRY)

90. Recent Studies on Lipoxygenase Chemistry. *E. J. Corey.* Department of Chemistry, Harvard University, Cambridge, MA 02138.

No abstract available.

91. Arachidonic Acid Epoxygenase, a New Member of the "Arachidonate Cascade". *J. Capdevila* and J. R. Falck. Departments of Biochemistry and Molecular Genetics, University of Texas Health Science Center at Dallas, Dallas, TX 75235.

Microsomal cytochrome P-450 catalyzes the NADPH-dependent metabolism of arachidonic acid to a variety of oxygenated products including four regioisomeric *cis*-epoxyeicosatrienoic acids (EETs). The EETs are substrates for further metabolism by cytosolic epoxide hydratase and glutathione-*S*-transferases and for further NADPH-dependent oxidation to diepoxy and epoxy alcohol derivatives. The EETs are potent in vitro mediators for the release of several peptide hormones such as somatostatin from the median eminence, anterior and posterior pituitary hormones, and the pancreatic

hormones insulin and glucagon. The stimulatory effect of the EETs for the release of luteinizing hormone from rat anterior pituitary cells is linked to changes in cell Ca^{2+} homeostasis and to further metabolism of the EETs. Utilizing a combination of gas chromatography and mass spectral analysis, we have demonstrated the in vivo presence of the EETs. These results suggest a role for the epoxygenase reaction in the in vivo metabolism of arachidonic acid.

92. Peroxide Synthesis and Metabolism by Prostaglandin H Synthase. *Lawrence J. Marnett*, Paul Weller, Christine Markey, Abdo Alward, and Thomas Dix. Department of Chemistry, Wayne State University, Detroit, MI 48202.

Prostaglandin H (PGH) synthase possesses cyclooxygenase and peroxidase activities and catalyzes the oxidation of arachidonic acid and peroxidase reducing substrates by using a single heme prosthetic group. Studies of the metabolism of peroxidase reducing substrates that are also competitive inhibitors of arachidonate oxygenation indicate separate active sites exist for cyclooxygenase and peroxidase action. Quantitation of the effects of reducing substrates on cyclooxygenase activity reveals dramatic protection from hydroperoxide- and arachidonate-induced irreversible inactivation. The data strongly suggest that the primary function of the peroxidase component of PGH synthase is to protect the cyclooxygenase capacity of the protein. The hydroperoxide intermediate PGG_2 triggers xenobiotic oxidations by classical peroxidase mechanisms or by reacting with nanomolar concentrations of heme to generate free radicals. These reactions trigger metabolic activation of precarcinogens to ultimate carcinogens. Studies indicate that the hydroperoxide-generated oxidizing agents are peroxyl radicals, that peroxyl radical-dependent epoxidation is widespread in biochemical systems, and that such epoxidations occur in intact tissue.

93. Enzymic Prostacyclin and Thromboxane A_2 Formation Requires Heme Thiolate Catalysis. Hermann Graf, Michael Haurand, and *Volker Ullrich*. Faculty of Biology, University of Konstanz, D-7750 Konstanz, Federal Republic of Germany.

Both enzymes that catalyze the formation of prostacyclin (PGI_2) and thromboxane (TxA_2) from 9,11-epidioxy-15-hydroxy-5,13-eicosadienoic acid (PGH_2) have been isolated as homogeneous proteins with molecular weights of 53 000 (porcine) and 58 800 (human), respectively. Both contain 1 mol of hemin bonded to a thiolate group as indicated by optical and EPR spectra typical for cytochrome P-450 proteins. PGI_2 synthase selectively forms PGI_2, but TxA_2 synthase yields TxA_2 and L-12-hydroxy-5,8,10-heptadecatrienoic acid (plus malondialdehyde) in a 1:1.2 ratio. Pyridine- and imidazole-based inhibitors are affecting only TxA_2 synthase by coordinating to the hemin, whereas substrate analogues spectrally interact similarly with both isomerases. From such studies it can be concluded that the endoperoxide oxygen at the 9-position binds to the iron, leading to a transition state with a covalently linked –S–Fe–O–C(9) entity.

THURSDAY MORNING—SYMPOSIUM ON RADICAL MECHANISMS IN BIOCHEMISTRY—J. STUBBE, SYMPOSIUM CHAIRMAN

94. A Radical Mechanism for Monoamine Oxidase. *Richard B. Silverman*, Paul A. Zieske, and Gregory M. Banik. Departments of Chemistry and of Biochemistry, Molecular Biology, and Cell Biology, Northwestern University, Evanston, IL 60201.

Mitochondrial monoamine oxidase (MAO) contains a covalently bound flavin (FAD) coenzyme and catalyzes the oxidation of biogenic amines. The mechanism of this enzyme has not been elucidated. Our approach to the investigation of this mechanism has involved studies of the mechanism of inactivation of MAO by various substituted amines that should be activated via enzyme-catalyzed radical reactions. The identification of the structures of inactivated enzyme adducts and of enzyme-generated metabolites allows mechanistic rationalizations to be made that are consistent with the results. The mechanisms of several different mechanism-based inactivators will be discussed and a unified picture for a radical mechanism of action of MAO will be presented.

95. Radical Mechanisms in Cytochrome P-450 Oxygenase Reactions. *F. P. Guengerich*, J. P. Shea, R. J. Willard, W. H. Schaefer, T. L. Macdonald, L. E. Richards, and L. T. Burka. Department of Biochemistry, Vanderbilt University, Nashville, TN 37232, Department of Chemistry, University of Virginia, Charlottesville, VA 22901, and National Institute of Environmental and Health Sciences, Research Triangle Park, NC 27709.

Several lines of evidence suggest the involvement of radicals in cytochrome P-450 (P-450) mediated oxidations. Olefin oxidation is rationalized by the formation of an Fe–O– substrate intermediate having radical character. The oxidation of heteroatom-substituted cyclopropyls is also rationalized with an electron abstraction mechanism, as carbon-based radicals appear to inactivate the porphyrin and are sites for oxygen rebound. Examination of the rates of demethylation of para-substituted *N*,*N*-dimethylaniline showed an inverse correlation with σ-para, consonant with a positively charged intermediate, which we suggest is the aminium radical. Further studies with these compounds and some substituted anisoles suggest a Marcus free-energy relationship, and a formal potential for the active $(FeO)^{3+}$ can be estimated. Pro-prochiral [1-^{2}H,1-^{3}H]octane is 1-hydroxylated with a large isotope effect and extensive but not complete racemization, indicative of rehybridization of a methylene radical intermediate. The degradation of the heme porphyrin by H_2O_2 produced by P-450 oxidation can also be rationalized by radical mechanisms involving similar intermediates. Thus, all of the P-450 reactions can be viewed in mechanisms involving radical species generated with a formal $(FeO)^{3+}$ complex with a high oxidation potential and collapse of the intermediates.

96. Recent Advances and Simplifications in the Mechanistic Metallobiochemistry of Coenzyme B_{12}: Bound Radical Mechanism. *R. G. Finke*, B. P. Hay, D. A. Schiraldi, B. L. Smith, and B. J. Mayer. Department of Chemistry, University of Oregon, Eugene, OR 97403.

Following a brief introduction summarizing current knowledge of the B_{12}-dependent enzymes and their mechanism of action, the three key remaining questions addressed by this work will be discussed. First, our successful studies of the Co–C5′ bond thermolysis of coenzyme B_{12} will be presented, studies that provide the first Co–C5′ BDE for B_{12} of 31.5 ± 1.3 kcal/mol and the key finding that the enzyme diol dehydratase must further weaken the Co–C5′ bond by >14.7 kcal/mol for a rate enhancement of $\gtrsim 10^{10}$ [Finke, R. G., & Hay, B. P. (1984) *Inorg. Chem. 23*, 3041]. Second, our model studies probing the participation or nonparticipation of cobalt in the rearrangement step will be presented, work that provides the first good evidence for the simplifying picture of cobalt nonparticipation in diol dehydratase [Finke, R. G., & Schi-

raldi, D. A. (1983) *J. Am. Chem. Soc. 105*, 7605]. Third, a unifying mechanism of action for B_{12}-dependent reactions will be presented, the bound radical mechanism [Finke, R. G., Schiraldi, D. A., & Mayer, B. J. (1984) *Coord. Chem. Rev. 54*, 1–22], and the probable relevance of this picture to other systems, such as the B_{12}- or Fe_2-dependent ribonucleotide reductases, will be presented.

97. Evidence for Radical Formation Catalyzed by *Escherichia coli* Ribonucleotide Reductase. *JoAnne Stubbe*, Mark Ator, Scott Salowe, David Ballou, Jack Peisach, and John McCracken. University of Wisconsin, Madison, WI 53706, University of Michigan, Ann Arbor, MI, and Albert Einstein Medical College, Bronx, NY.

2-Azido-2′-deoxyuridine 5′-diphosphate (N_3UDP) irreversibly inactivates *Escherichia coli* ribonucleotide reductase (RDPR) in one turnover. Inactivation is accompanied by loss of the tyrosyl radical on the B_2 subunit concomitant with formation of a new radical located on the azide moiety of N_3UDP. Electron spin resonance spectroscopy and electron spin–echo spectroscopy have been utilized with [1′-, 2′-, 3′-, or 4′-^{2}H]N_3UDP to better define the structure of this new radical. Incubation of [3′-^{2}H]N_3UDP with RDPR results in an isotope effect of 2.2 on tyrosyl radical loss as well as on the inactivation. Incubation of [β-^{32}P]N_3UDP with RDPR results in production of $\approx$1 equiv of [^{32}P]PP_i after protein denaturation. Results of interaction of [^{15}N]N_3UDP with RDPR using isotope ratio mass spectrometry to look for N_2 release will be reported. No N_3^- is released. A working hypothesis will be presented to account for the reported facts consistent with a 3′-nucleotide radical intermediate.

THURSDAY AFTERNOON—SYMPOSIUM ON SITE-DIRECTED MUTAGENESIS OF PROTEINS—J. GERLT, SYMPOSIUM CHAIRMAN

98. Staphylococcal Nuclease: Probes of Mechanism and Structure. *John A. Gerlt*, David W. Hibler, Mark A. Reynolds, Neal J. Stolowich, and Philip H. Bolton. Department of Chemistry, University of Maryland, College Park, MD 20742, and Department of Chemistry, Wesleyan University, Middletown, CT 06457.

Primer-directed mutagenesis is being used to generate mutations in the functional groups present in the active site of staphylococcal nuclease A so that the roles of these groups in both catalysis and substrate binding can be better defined. For example, we have generated mutants of the nuclease in which the glutamate at position 43 has been replaced with aspartate, glutamine, and asparagine; these enzymes have significant reduced catalytic activity, with the simplest explanation being that the glutamate carboxylate group is essential for catalysis. We are also investigating the use of NMR spectroscopy as a facile probe for comparing the solution conformations of mutant and wild-type enzymes since proper interpretation of the catalytic properties of mutant enzymes demands information about active site structure; our approach involves isotopic labeling of selected amino acids with carbon-13 and the use of a zero quantum filter to permit the specific observation of the one- and two-dimensional NMR spectral properties of only those protons directly bonded to the carbon-13 nuclei.

99. Enzyme Redesign via Recombinant DNA Techniques. *E. T. Kaiser*, S. C. Bock, S. Ghosh, D. Kendall, and S. Rokita. The Rockefeller University, New York, NY 10021.

We are using site-specific mutagenesis procedures to alter rationally the active site and signal peptide region of the *Escherichia coli* periplasmic enzyme alkaline phosphatase (BAP). The active site nucleophile of BAP has been changed from a hydroxyl to a sulfhydryl by replacing the codon for Ser-102 with a Cys-encoding triplet. The resultant gene product thiol alkaline phosphatase (TAP) has been purified, and activity levels that are comparable to wild type have been demonstrated for phosphate monoester substrates with good leaving groups. Additional active site mutations are currently being examined. A series of mutations in the hydrophobic core region of the BAP signal peptide have also been generated, and the kinetics of BAP secretion have been studied in these strains. These studies have as their goal the determination of the structural features of the hydrophobic core element necessary for signal peptide function.

100. Catalytic and Substrate Specificity Studies of Trypsin and Carboxypeptidase A via Site-Specific Mutagenesis. *C. S. Craik*, S. Gardell, S. Roczniak, R. Fletterick, and W. J. Rutter. Hormone Research Institute, University of California, San Francisco, CA 94143.

Codon replacements have been made by oligonucleotide-directed site-specific mutagenesis of cloned trypsin and carboxypeptidase A (CPA) genes and the resultant genes expressed in mammalian cells and yeast, respectively. The heterologously expressed wild-type and mutant enzymes have been purified to homogeneity and their properties studied. Tyr-248, a putative general acid in the active site of CPA, has been replaced with a Phe. CPA(Tyr^{248} $\rightarrow$ Phe) shows no change in k_{cat} and increased K_m (3-fold) on peptide substrates. Asp-102, a proposed member of the catalytic triad of trypsin, has been replaced with an Asn. Trypsin(Asp^{102} $\rightarrow$ Asn) has 0.1% (pH 7)–15% (pH 9) k_{cat} with small changes in K_m on peptide and ester substrates compared to the wild-type enzyme. Substrate binding pocket mutants in trypsin show altered substrate specificities (k_{cat}/K_m): Gly^{216} $\rightarrow$ Ala (Arg $\gg$ Lys), Gly^{226} $\rightarrow$ Ala (Lys $\gg$ Arg), and Gly^{216,226} $\rightarrow$ Ala (Arg > Lys). Mutant trypsins with Ala at position 226 exhibit substrate-induced conformational changes. Other substrate specificity modifications are presently being characterized: trypsin(Asp^{189} $\rightarrow$ Lys) and -(Asp^{189} $\rightarrow$ Glu) and CPA(Ile^{255} $\rightarrow$ Asp).

101. Site-Directed Mutagenesis of Yeast Triosephosphate Isomerase. Robert C. Davenport, Jr., and *Gregory A. Petsko*. Department of Chemistry, Massachusetts Institute of Technology, Cambridge, MA 02139.

Oligonucleotide primer-directed mutagenesis has been used to alter the amino acid sequence of yeast triosephosphate isomerase. Determination of the three-dimensional structure of the enzyme–substrate complex by X-ray crystallography has suggested that two active-site residues, His-95 and Lys-13, function as electrophiles to polarize the carbonyl oxygens of the substrates and to stabilize the ene-diolate-like transition state. This hypothesis has been tested by changing the histidine to glutamine. The mutant enzyme has been expressed (in *Escherichia coli*), purified, characterized, and crystallized. The k_{cat} of the mutant is 1% that of the wild-type enzyme, while K_m is unchanged, suggesting a role for the histidine in transition-state stabilization. Lys-13 has also been changed to Gln; the mutant protein is being purified. The double mutant (His-95 and Lys-13 to Gln) has been made and appears devoid of catalytic activity. The talk will also discuss the structures of the mutants and the role of other active-site residues.

102. Mutagenesis Studies on Dihydrofolate Reductase and Cytochrome *c* Peroxidase. *Joseph Kraut.* Department of Chemistry, University of California/San Diego, and The Agouron Institute, La Jolla, CA 92093.

Our laboratory has in recent years published high-resolution, refined X-ray crystal structure for *Escherichia coli* DHFR (and other DHFRS) and yeast CCP. We believe oligonucleotide-directed, site-specific mutagenesis techniques can be used to help solve some of the structure/function riddles that immediately emerge upon examining these molecular models, especially if the structural and enzyme-kinetic effects of mutation are carefully documented. I plan to give several examples of the kinds of information that can be obtained by such experiments.

THURSDAY AFTERNOON—POSTER SESSION—R. G. MATTHEWS, CHAIRMAN

103. Thermodynamic Analysis of T4 Lysozyme Variants Containing an Engineered Disulfide Bond. *R. Wetzel*, L. J. Perry, W. J. Becktel, and W. Baase. Genentech, Inc., South San Francisco, CA 94080, and Institute of Molecular Biology, University of Oregon, Eugene, OR 97403.

Recently we reported the introduction of a disulfide bond, using rDNA/protein engineering methods, into the normally disulfide-free lysozyme from coliphage T4. The cross-linked product was enzymatically active, and its activity was significantly more stable to incubation at elevated temperatures when compared to the wild-type enzyme [Perry, L. J., & Wetzel, R. (1984) *Science (Washington, D.C.) 226*, 555]. The mechanism(s) by which the disulfide stabilize(s) lysozyme, both in reversible melting experiments and toward irreversible thermal inactivation, is (are) of considerable interest. We have prepared a series of multiple variants, containing a disulfide in addition to other mutations, to address the relationship between thermodynamic stability and irreversible inactivation. Inactivation rates and thermodynamic parameters, derived from van't Hoff analysis of CD melting profiles, for this series of variants will be presented and discussed.

104. Site-Directed Mutagenesis of the Active-Site of Ribulosebisphosphate Carboxylase. Frank W. Larimer, Richard Machanoff, Robert S. Foote, Sankar Mitra, Thomas S. Soper, Robert K. Fujimura, and *Fred C. Hartman.* Biology Division, Oak Ridge National Laboratory, Oak Ridge, TN 37831.

Two different lysyl residues (Lys-166 and Lys-329) have been implicated at the active site of ribulosebisphosphate carboxylase from *Rhodospirillum rubrum* by affinity labeling studies [Hartman et al. (1984) *Arch. Biochem. Biophys. 232*, 280]. Although the previously cloned carboxylase gene has a high expression level in *Escherichia coli*, the gene product is a fusion protein with an NH_2-terminal appendage derived from β-galactosidase [Nargang et al. (1984) *Mol. Gen. Genet. 193*, 220]. To avoid complications in interpreting results based on introduction of point mutations into a structurally altered enzyme, a new plasmid has been constructed that encodes authentic wild-type enzyme. Oligodeoxynucleotide-directed mutagenesis with bacteriophage vector M13 as template has been used to replace Lys-166 of the carboxylase with Arg. The mutant protein is devoid of enzymic activity, consistent with a catalytic role for Lys-166. Like the wild-type enzyme, the mutant is expressed in *E. coli* as a dimer that is immunologically cross-reactive with antibody raised against pure *R. rubrum* carboxylase. The substrate-binding properties of the mutant protein are being explored.

105. Effects of Genetic Substitution of a Ca^{2+}-Liganding Amino Acid in Staphylococcal Nuclease (SN). *Engin H. Serpersu*, David R. Shortle, and Albert S. Mildvan. Department of Biological Chemistry, Johns Hopkins Medical School, Baltimore, MD 21205.

The X-ray structure of SN suggests coordination of the essential Ca^{2+} by Asp-21, Asp-40, and Thr-41 [Cotton et al. (1979) *Proc. Natl. Acad. Sci. U.S.A. 76*, 2551]. Mutation of the Asp-40 codon to Gly (D40G) results in a (5 ± 2)-fold weaker binding of Ca^{2+} to the enzyme as found by kinetics (K_A^{Ca} = 0.46 mM → 3.4 mM) and by Ca^{2+}-binding studies (K_D^{Ca} = 0.51 mM → 1.7 mM) in competition with Mn^{2+}, a linear competitive inhibitor. Similarly, as found by EPR, Mn^{2+} binds to D40G with a 3-fold greater K_D (1.25 mM) than to wild type (0.42 mM). These differences in K_D are increased by saturation of SN with the DNA substrate such that K_M^{Ca} is 12-fold greater and K_I^{Mn} is 15-fold greater for D40G than for wild type, although K_M^{DNA} is only 1.5-fold greater. 5′-TMP and 3′,5′-pdTp raise the affinities of both enzymes for Mn^{2+} by similar factors of ~8- and ~40-fold, respectively. Structural differences in ternary metal complexes of D40G are revealed by a 30-fold slowing of V_{max} with Ca^{2+} and a 1.6-fold decrease in $1/T_{1p}$ of water protons with Mn^{2+}. The frequency dependence of $1/T_{1p}$ suggests greater asymmetry of the ligands of Mn^{2+} in D40G.

106. Studies on the Function of Invariant Amino Acids of Cytochrome *c* by Site-Directed Mutagenesis. *D. D. Miller*, M. S. Swanson, S. M. Zieminn, and E. Margoliash. Department of Biochemistry and Molecular Biology, Northwestern University, Evanston, IL 60201.

The primary structure of cytochrome *c*, the only water-soluble protein component of the eukaryotic electron transport chain, has been highly conserved throughout evolution at particular amino acid positions. The reason for the conservation of a few of these amino acids is obvious, such as those that are required for covalent binding of the heme; however, it is not known why the majority of these invariant positions are conserved. Cytochrome *c* is coded for by the nuclear genome and follows a complex life cycle, including (1) translation of the mRNA on free polysomes and specific binding of the nascent apoprotein to the outer mitochondrial membrane, (2) translocation of this bound apoprotein into the intermediate space, and (3) addition of the heme by a cytochrome *c* synthetase and subsequent modification of the tertiary structure that results in the holocytochrome. To dissect which invariant residues are important for the various functions of both the apo- and holoproteins, we are performing site-directed mutagenesis of the cloned cytochrome *c* genes from *Saccharomyces cerevisiae* and *Drosophila melanogaster.* Production of the apoproteins is performed in *Escherichia coli*, while function of the holoprotein is investigated in a cytochrome *c* deficient yeast strain (GM-3c-2).

107. Messenger RNAs from *Aspergillus niger. Kim H. Tan*, Kuo-Mei Chang, and Yaulanda M. Lowe. Department of Biology, Winston-Salem State University, Winston-Salem, NC 27110.

Procedures were developed for the isolation of poly(A+) RNAs from the fungus *A. niger.* The poly(A+) RNAs were the source for further purification of specific messenger RNAs such as those of glucoamylase, glucose oxidase, etc. Fresh cells were frozen quickly in liquid nitrogen, ground into fine powder, and then homogenized in extraction buffer. The supernatant

was obtained by differential centrifugation and was the source of total RNA. Deproteinization of RNA was effected by a series of extractions with a phenol/chloroform/isoamyl alcohol mixture. Total RNA was collected by precipitation with 95% alcohol at −20 °C. The poly(A+) RNAs separated from the total RNA on an oligo(dT)–cellulose column. The in vitro translation assays were used to identify the mRNA fractions. Amyloglucosidase mRNA was purified from the pooled mRNAs and was used to study its translation product.

108. Kinetic Studies of the Transfer of recA Protein between Polynucleotides. *Joseph P. Menetski* and Stephen C. Kowalczykowski. Department of Molecular Biology, Northwestern University Medical School, Chicago, IL 60611.

The rate of transfer of recA protein from one polynucleotide to another has been studied by using fluorescently modified M13 DNA, etheno-M13, and poly(dT) as a high-affinity competitor. The time course of this reaction shows either single or double exponential behavior depending on conditions. The rate has been found to depend on a variety of parameters such as poly(dT), NaCl, magnesium, ADP, and ATP concentration. The rate is increased by increasing NaCl concentration and in the presence of ADP, as expected from equilibrium results [Menetski, J. P., & Kowalczykowski, S. C. (1985) *J. Mol. Biol. 181*, 281–295]. The effect of ATP concentration is 2-fold: below 100 μM, ATP increases the rate while above 100 μM, ATP decreases the transfer rate. The poly(dT) concentration dependence data are consistent with a two-step mechanism. The recA protein–etheno-M13 complex first interacts with poly(dT) to form a ternary complex that then proceeds through an isomeric exchange of poly(dT) for etheno-M13. In strand assimilation, recA protein is required to interact with two different polynucleotides. The result that the transfer reaction is bimolecular suggests it has implications in the recA-promoted strand assimilation reaction. The effects of ATP, ADP, and magnesium in this mechanism will also be discussed.

109. Highly Efficient Strand Assimilation Catalyzed by the recA Protein of *Escherichia coli*. *Linda J. Roman* and Stephen C. Kowalczykowski. Department of Molecular Biology, Northwestern University Medical School, Chicago, IL 60611.

The strand assimilation reaction catalyzed by the *E. coli* recA protein is generally performed in a buffer containing chloride ions. Because it was found that recA protein binds much more tightly to single-stranded DNA in the presence of acetate, rather than chloride, ions [Menetski, J. P., & Kowalczykowski, S. C. (1985) *J. Mol. Biol. 181*, 281–295], strand assimilation was assayed in an acetate-based buffer with the expectation that the rate and/or yield of the reaction would increase. We found that, in the buffer containing acetate ions, both the initial rate and the final yield of the reaction increased 2-fold as compared to those in chloride buffer under the same conditions. Aggregation of recA protein is shown to be necessary but not sufficient for strand assimilation to occur. Both duplex DNA binding and ATPase activity on duplex DNA are increased in acetate buffers and were found to be less sensitive to ionic strength in acetate rather than chloride buffer. The role of the enhanced duplex DNA binding and ATPase activity will be discussed with regard to the strand assimilation reaction.

110. Properties of the Duplex DNA-Stimulaed ATPase Activity of *Escherichia coli* recA Protein. *Stephen C. Kowalczykowski*. Department of Molecular Biology, Northwestern University Medical School, Chicago, IL 60611.

The DNA-dependent ATPase activity of recA protein is greatly stimulated by single-stranded (ss) DNA but is stimulated by double-stranded (ds) DNA only under limited conditions. The enzymatic properties of the ds DNA stimulated activity have been investigated as a function of DNA, protein, magnesium, NaCl, and ATP concentrations, as well as temperature and DNA composition. The time course of the ds DNA stimulated reaction differs from the ss DNA stimulated reaction in that a pronounced lag in ATPase activity is observed when ds DNA is used as a substrate. This lag time has the property that factors that contribute to the stability of the ds DNA structure increase the duration of the lag; i.e., increased magnesium and NaCl concentration, decreased temperature, and increased GC content of the DNA increase the length of lag. These results suggest that the ds DNA stimulated ATPase activity occurs via a transient ss DNA intermediate that is formed upon binding of the ATP–recA protein complex and that both the ss and ds DNA stimulated reactions are, in fact, identical activities. The significance of these results, as well as those from DNA and ATP binding studies carried out in the laboratory, to the mechanism of the recA protein catalyzed strand assimilation reaction will be discussed.

111. Construction of a Vector for the Overproduction of a Human β-Globin Fusion Protein in *Escherichia coli*. J. K. O'Donnell, J. F. Young, and *W. S. Brinigar*. Department of Chemistry, Temple University, Philadelphia, PA 19122, and Molecular Genetics Division, Smith Kline and French Laboratories, Philadelphia, PA 19101.

A plasmid has been constructed that overproduces a fusion protein containing the complete human β-globin sequence. This plasmid, pJK05, is a pAS1 derivative coding for the first 81 amino acid residues of NS1, an influenza A protein, followed by a synthetic DNA segment coding for a recognition sequence of blood coagulation factor Xa (-Ile-Glu-Gly-Arg-), and a cDNA copy of the β-globin gene from which the initiation codon ATG was removed. The β-globin gene was excised from pB6-6, kindly provided by Dr. B. G. Forget, Yale University. pJK05 is similar to the plasmid reported by Nagai and Thogerson [(1984) *Nature (London) 309*, 810]. Upon temperature induction, pJK05 in *E. coli* strain N5151 produces 10–15 mg of the fusion protein per liter of medium. Treatment of the fusion protein with factor Xa yields two proteins, one of which was indistinguishable from authentic human β-globin on sodium dodecyl sulfate–polyacrylamide gel electrophoresis. This plasmid holds promise as a system by which site-specific hemoglobin variants can be produced in amounts sufficient for biochemical studies.

112. Influence of *Escherichia coli* Single-Stranded DNA Binding Protein on DNA Synthesis by T7 DNA Polymerase. *Thomas W. Myers* and Louis J. Romano. Department of Chemistry, Wayne State University, Detroit, MI 48202.

DNA synthesis by the purified T7 replication system is stimulated 7–10-fold by the addition of *E. coli* single-stranded DNA binding protein (SSB). In an attempt to understand the mechanism by which this stimulation occurs, we have studied the effect of SSB on in vitro DNA synthesis by the T7 DNA polymerase using polyacrylamide gel electrophoresis and DNA sequencing analysis. Using a primed single-stranded M13 mp8 DNA template as a model for T7 lagging-strand synthesis, we have compared the effect of SSB specifically on

both the elongation and priming reactions. Acrylamide gel analysis of the product DNA synthesized in the absence of SSB revealed that elongation was interrupted in numerous locations, resulting in few full-length product molecules and a characteristic banding pattern. Sequence analysis indicated that the major pause sites occurred at potential stable hairpin structures in the M13 template DNA. Presumably, these structures are destabilized by SSB since, in its presence, DNA synthesis is markedly stimulated, resulting in product DNA that is mostly full length. SSB was also shown to increase the rate of DNA synthesis by the T7 DNA polymerase by specifically stimulating the ability of the polymerase to initiate DNA synthesis from a primer on a single-stranded template. Using a uniquely primed single-stranded DNA molecule and carrying out the synthesis in the presence of any dTTP, we find that SSB stimulates approximately 4-fold the addition to the primer of a single [^{32}P]dTTP.

113. Preparation and Characterization of a DNA Molecule Containing a Site-Specific 2-Aminofluorene Adduct: A New Probe for Mutagenesis by Carcinogens. *Dana Lee Johnson*, Thomas M. Reid, Charles M. King, and Louis J. Romano. Department of Chemistry, Wayne State University, Detroit, MI 48202, and Department of Chemical Carcinogenesis, Michigan Cancer Foundation, Detroit, MI 48203.

The synthetic oligonucleotide heptamer 5′ATCCGTC3′ was reacted in vitro with *N*-acetoxy-*N*-(trifluoroacetyl)-2-aminofluorene and the product resolved by reverse-phase high-performance liquid chromatography (HPLC). The resulting product, a heptamer containing a single *N*-(deoxyguan-8-yl)-2-aminofluorene adduct, was used to situate a putatively mutagenic lesion at a specific site in the genome of M13 mp9. This was accomplished by ligating the adduct containing heptamer into a single-stranded region complementary to the heptamer within the duplex M13 mp9 DNA molecule. The adduct was so positioned to be within the *Hin*cII restriction endonuclease recognition site, and the enzyme was shown to be inhibited by the presence of the adduct. This result, in view of other supportive data, demonstrates the incorporation of the adduct with high efficiency into the *Hin*cII recognition site. This system would prove useful, in vivo, for the study of mutagenesis by chemical carcinogens and, in vitro, to study the interaction of purified DNA metabolizing proteins on a template containing a site-specific lesion.

114. Contrasting Effects of *Escherichia coli* Single-Stranded DNA Binding Protein on Synthesis by T7 DNA Polymerase and *Escherichia coli* DNA Polymerase I: Proof That Polymerase I Can Bypass Aminofluorene Adducts in DNA. *Mark L. Michaels*, Mei-Sie Lee, and Louis J. Romano. Department of Chemistry, Wayne State University, Detroit, MI 48202.

Aminofluorene lesions in DNA are mutagenic and have been implicated in the initiation step of the carcinogenic process. The effect of *E. coli* single-stranded DNA binding protein (SSB) on DNA synthesis using native and aminofluorene-modified M13 templates by T7 DNA polymerase and the *E. coli* DNA polymerase I large fragment was evaluated by in vitro DNA synthesis assays and acrylamide gel electrophoresis. T7 DNA polymerase, a replication enzyme, was stimulated by the addition of SSB whether native or modified templates were used while *E. coli* DNA polymerase I, a DNA repair enzyme, was slightly stimulated by the addition of SSB to the native template but substantially inhibited on modified templates. This suggested polymerase I might normally bypass these lesions but that this process was prevented in the presence of SSB. Acrylamide gels further support this inference since SSB causes a substantial increase in the accumulation of short DNA products induced by AF blockage. Finally, we have obtained conclusive proof that DNA polymerase I and T7 DNA polymerase can normally bypass AF adducts in DNA by carrying out synthesis on a single-stranded template containing an AF lesion located at a unique location.

115. Effect of a Rare Leucine Codon on Regulation of the *ilv* Operon in *Serratia marcescens*. *Etti Harms*, Jung-Hsin Hsu, and H. E. Umbarger. Department of Biological Sciences, Purdue University, West Lafayette, IN 47907.

Control of expression of the *ilvGEGA* operon of *Escherichia coli* and *Serratia marcescens* by all three branched-chain amino acids, isoleucine, leucine, and valine, is thought to occur by attenuation of transcription at the end of a leader. Tandem or consecutive codons in the leader transcript play a crucial role in this model, as they serve to stall the ribosome when regulatory amino acids are in limiting supply. This stalling leads to the formation of one of two mutually exclusive structures of the leader, namely, the one that allows transcription into the structural genes. The leader of *S. marcescens*, however, differs from that of *E. coli* in having only a single leucine codon that could be involved in perturbing secondary structure of the leader. Comparison of the two leaders reveals that, in *S. marcescens*, attenuation is due to ribosome stalling at the single leucine codon, which, interestingly, is the rarely used CUA. To evaluate the role of this rare codon, a variety of codon changes have been introduced into the leader region. It is concluded that the rare codon enhances attenuation control but is not essential for it.

116. Oligomerization of 3′-Amino-3′-deoxynucleotides in Aqueous Solution. *W. S. Zielinski* and L. E. Orgel. The Salk Institute, San Diego, CA 92138.

3′-Amino-3′-deoxynucleoside-5′-phosphorimidazolidates prepared from corresponding 3′-azido-3′-deoxynucleosides condense in aqueous solutions to give oligomers containing 3′–5′-linked phosphoramidate bonds up to at least the pentamer. In the presence of oligonucleotide templates they give higher yields and longer oligomers. Oligomerization of 3′-amino-3′-deoxyguanosine-5′-phosphorimidazolidate on poly(C) or poly(dC) templates, for example, gave high yields of oligo(G)phosphoramidates up to 12 long. Short templates are also effective. The template oligomer CCGCC, for example, facilitated the synthesis of the complementary phosphoramidate-linked strand GGCGG when the 3′-amino-3′-deoxycytidine and the 3′-amino-3′-deoxyguanosine derivatives were present in the reaction mixture. In an extension of these studies several additional activated mono- and dinucleoside-phosphoramidates have been synthesized and used for oligomerization in template-directed or template-free systems. Some chemical, structural, and biological properties of analogues are discussed.

117. Alkyl Substitution Effects on the Intercalation of Carcinogenic Hydrocarbon and Hydrocarbon Metabolites into DNA. *P. R. LeBreton*. Department of Chemistry, University of Illinois at Chicago, Chicago, IL 60680.

A large number of carcinogenic hydrocarbons and hydrocarbon metabolites intercalate into DNA with binding constants in terms of PO_4^- concentration that lie in the range 10^3–10^4 M^{-1}. These binding constants are similar to those

associated with base stacking and hydrogen bonding interactions that occur naturally in DNA. Previous studies show that different metabolites derived from the same parent hydrocarbon exhibit different binding properties. In recent studies we have examined the effects of alkyl substitution on hydrocarbon binding to calf thymus DNA. Such groups can enhance or inhibit carcinogenic activity. Studies of 1-alkylbenzo[*a*]pyrene derivatives and of their 7,8-dihydrodiols indicate that the alkyl groups ethyl, isopropyl, and *tert*-butyl inhibit intercalation. Methyl groups can either inhibit or enhance intercalation into DNA. The binding constants of 7,12-dimethylbenz[*a*]anthracene (DMBA) and benz[*a*]-anthracene are nearly the same. However, 9,10-dimethylanthracene, which is a π-electron model compound of the bay region diol epoxide of DMBA, binds 6.7 times better than anthracene. Similarly, highly carcinogenic 5-methylchrysene binds to DNA 3.9 times better than chrysene.

118. Cloning and Overproduction of the B2 Subunit of *Escherichia coli* Ribonucleotide Reductase. *S. P. Salowe* and J. Stubbe. Department of Biochemistry, College of Agricultural and Life Sciences, University of Wisconsin—Madison, Madison, WI 53706.

Ribonucleotide reductase catalyzes the conversion of the four common ribonucleotides to the corresponding 2′-deoxyribonucleotides essential for DNA synthesis. The enzyme is composed of two nonidentical subunits that are products of *nrd* genes. Subunit B2 contains a binuclear iron center and a unique tyrosyl radical that has been implicated in the catalytic mechanism. To further our biophysical studies on this protein, we have cloned the *nrdB* gene that encodes the B2 polypeptide into a multicopy plasmid containing the P_L promoter of bacteriophage λ and the tetracycline resistance gene of pBR322. The vector is maintained in a lysogenic host that synthesizes a temperature-sensitive λ repressor protein. After heat induction, B2 constitutes approximately 25% of the soluble protein, an amplification over the level in wild type of several hundred fold. Preliminary results on the purified protein will be presented.

119. Stereospecific Proton Removal from Formylglycinamidine Ribonucleotide Catalyzed by 5-Aminoimidazole Ribonucleotide Synthetase. *Fred Schendel*, Jeffrey L. Schrimsher, and JoAnne Stubbe. Department of Biochemistry, College of Agricultural and Life Sciences, University of Wisconsin—Madison, Madison, WI 53706.

The de novo purine biosynthetic enzyme 5-aminoimidazole ribonucleotide (AIR) synthetase catalyzes the conversion of formylglycinamidine ribonucleotide (FGAM) to AIR. Stereospecifically labeled FGAM has been synthesized from (2*R*)- and (2*S*)-[2-^{3}H]glycine, and the stereospecificity of proton removal has been investigated. AIR synthetase was found to specifically remove the *pro-R* hydrogen from FGAM during the reaction. In addition to these studies, the riboside of AIR has been characterized and its properties have been investigated.

120. Purification and Characterization of 5-Aminoimidazole Ribonucleotide Synthetase. *Jeffrey L. Schrimsher*, Fred Schendel, and JoAnne Stubbe. Department of Biochemistry, College of Agricultural and Life Sciences, University of Wisconsin—Madison, Madison, WI 53706.

The purification, physical properties, and kinetic mechanism of 5-aminoimidazole ribonucleotide (AIR) synthetase (EC 6.3.3.1) from chicken are described. Through gel filtration and sodium dodecyl sulfate gel electrophoresis, the enzyme was found to have a native molecular weight of about 400 000 and a subunit weight of 100 000. The steady-state kinetic mechanism of AIR synthetase was investigated through the use of substrate studies and product inhibition and by analyzing the role of K^+ and Mg^{2+} in catalysis. In addition, the fate of the amide oxygen from the substrate formylglycinamidine ribonucleotide (FGAM) as a result of catalysis was examined through the use of [*formyl*-^{18}O]FGAM.

121. Inactivation of Coenzyme B12 Dependent Ribonucleotide Reductase by 2′-Azidonucleotides. *Gary W. Ashley* and JoAnne Stubbe. Department of Biochemistry, University of Wisconsin, Madison, WI 53706.

The ribonucleotide reductase from *Lactobacillus leichmanii* is rapidly inactivated by 2′-azido-2′-deoxyarabinofuranosyladenine 5′-triphosphate (2′-N_3-araATP). Use of specifically radiolabeled inactivator shows that both the PPP_i and adenine portions of 2′-N_3-araATP remain tightly bound to the enzyme after inactivation and no significant amounts of free PPP_i or adenine are produced. This contrasts with the behavior of 2′-chloronucleotides with this enzyme, where inactivation results in formation of free PPP_i and heterocycle and only the ribosyl residue remains protein bound. During inactivation by 2′-N_3-araATP, 1 equiv of cofactor is irreversibly converted to cob(II)alamin and 5′-deoxyadenosine. It is proposed that 2′-N_3-araATP is acting as a trap for some radical species generated during the normal catalytic process of this enzyme.

122. Cobamide Biosynthesis by Extracts from *Clostridium tetanomorphum*. *S. H. Ford*, A. Nichols, and D. Walton. Department of Physical Sciences, Chicago State University, Chicago, IL 60628.

The biosynthesis of the cobamides (e.g., vitamin B_{12}) is as yet not completely understood. The cobamides are synthesized de novo only by certain bacterial producers such as the anaerobe *Clostridium tetanomorphum*. This organism was thus utilized as an enzyme source to begin study of two of the poorly understood steps in cobamide biosynthesis: amidation of and (*R*)-1-amino-2-propanol addition to the corrin ring. Cobinic acid pentaamide and cobyric acid for use as enzyme substrates were prepared by chemical degradation of commercially available vitamin B_{12}. Enzyme extracts of *C. tetanomorphum* cells were prepared either by resuspension in buffer of actone powders from freshly harvested bacteria or by sonication in buffer of freshly harvested bacteria. Nucleic acids were removed by precipitation with $MnCl_2$, and following exhaustive dialysis against fresh buffer, the extract was the subjected to DEAE (OH^- form) column chromatography. Enzyme assays were performed by incubating bacterial extract, energy source, and corrinoid substrate, separating neutral product from acidic substrate on small ion-exchange columns, and determining product concentration by spectrophotometry. Substrate conversion to product varied from 0.1% up to 28%, depending on the origin and age of enzyme source.

123. Mechanism of Superoxide Dismutases: The Copper, Zinc Containing Protein. James A. Fee and Christopher Bull. Los Alamos National Laborary, Los Alamos, NM 87545, and Washington Research Center, W. R. Grace & Company, Columbia, MD 21044.

Our work at the Biophysics Research Division of the University of Michigan has shown for the iron-containing superoxide dismutase (FeSD) that the rate-limiting step when saturated with superoxide is abstraction of a proton from water. We have now found that the Cu,ZnSD can also be saturated with superoxide ($K_m \sim 5$ mM). The limiting turnover number (TN) for one cycle (two superoxide molecules) is 5 000 000/s, one of the fastest known. Observation of a substantial deuterium isotope effect [TN(H)/TN(D) ~ 2.5] suggests that proton abstraction is again the rate-limiting step. The imidazolate bridge between Cu and Zn in oxidized enzyme is broken on reduction and has been proposed to be involved in proton transfer. This was tested directly by using the Zn-free enzyme wherein this group should have a much lower pK_a. The catalytic properties of the Zn-free enzyme were nearly identical with the holoenzyme, so the bridging imidazolate does not appear to be involved in the rate-limiting proton abstraction step.

124. Mechanism of Superoxide Dismutases: The Manganese-Containing Protein. Christopher Bull and James A. Fee. The BioProducts Department, Washington Research Center, W. R. Grace & Company, Columbia, MD 21044, and Los Alamos National Laboratory, Los Alamos, NM 87545.

The catalytic behavior of the manganese-containing superoxide dismutase (MnSC) from *Escherichia coli* has been reported to be complex, consisting of a fast and a slow catalytic cycle. Our work at the Biophysics Research Division of the University of Michigan establishes a simpler mechanism for similar behavior in MnSD from *Thermus thermophilus*. The only catalytic cycle involves cyclic reduction and reoxidation of the metal center by superoxide. The maximum turnover number shows a deuterium isotope effect of 2.5, suggesting that the abstraction of a proton from water is the rate-limiting step, as we have also found in FeSD and Cu,ZnSD. The presence of an additional dead-end complex, which is in equilibrium with one of the catalytic intermediates, can explain the time-dependent (hysteretic) behavior found in the MnSD enzymes. We have measured the visible absorption spectrum of this dead-end complex and have shown that it forms during the oxidative half-reaction.

125. Induction of Manganese Superoxide Dismutase Activity in Heart Tissue of Rats. *A. A. Mylroie*, C. Umbles, F. Ariyo, A. Boseman, and J. Kyle. Department of Physical Sciences, Chicago State University, Chicago, IL 60628.

In previous experiments, we have reported a decrease in Cu and a corresponding decrease in superoxide dismutase activity (SOD) in some tissue of lead-exposed rats. In the present experiment, Cu deficiency was induced for a 1–13 week experimental period as a result of two treatments: diet and Pb. Controls and Pb-treated rats (500 ppm of Pb in drinking water) were fed a nutritionally adequate purified diet (6 ppm of Cu); the dietary Cu-deficient group was fed the purified diet at a reduced level of Cu (1 ppm). Total SOD, Cu-dependent SOD (CuSOD), and Mn-dependent SOD (MnSOD) were assayed. Total SOD and CuSOD increased from week 1 to week 13 in heart tissue of controls. In dietary Cu-deficient rats, total SOD also increased with time; however, this increase was primarily the result of an increase in MnSOD. In Pb-exposed rats, CuSOD activity decreased from week 1 to week 5 and then returned to values obtained in controls by week 13. MnSOD increased in response to the decrease in CuSOD. This induction in MnSOD activity in response to a decrease in CuSOD activity lends additional support to the view that SOD has a protective function in mammalian tissue.

126. Effects of Reversible Freezing Inactivation on the Redox Properties of L-Amino Acid Oxidase. Brian G. Fox, *Marian T. Stankovich*, and Sean Soltysik. Department of Chemistry, University of Minnesota, Minneapolis, MN 55455.

The redox properties of the freezing inactivated enzyme L-amino acid oxidase (EC 1.4.3.2) differ greatly from those of the active enzyme. The inactive enzyme is reduced by two electrons with $E_m = -0.192$ V at pH 7.0. The inactive enzyme also exhibits the expected potential pH behavior for a two-electron, one-proton reduction. No stabilization of the anion radical species is seen upon reduction of the inactive enzyme. Therefore, reversible freezing inactivation has likely destroyed crucial hydrogen-bonding interactions at the flavin N(1)—C(2)═O position. E_a of reactivation for the reduced inactive enzyme is 19–22 kcal/mol, representing a decrease in the E_a value of 23–26 kcal/mol compared to reactivation of the oxidized inactive enzyme. The lowering of E_a for the reduced inactive enzyme suggests reduction causes a realignment due to tighter binding of the reduced FAD. The tighter binding allows hydrogen bonding near the flavin N(1)—C(2)═O position to be re-formed.

127. Purification, Characterization, and Crystallization of a Phthalate Oxygenase System. Christopher J. Batie, Edward LaHaie, Carl C. Correll, Martha L. Ludwig, and David P. Ballou. Department of Biological Chemistry, University of Michigan, Ann Arbor, MI 48109.

A two-protein system has been purified that catalyzes dioxygenation of phthalate at the expense of NADH. Oxygenase activity was associated with a 217-kDa protein, while a 34-kDa protein transfers electrons from NADH to the oxygenase (PO). PO consists of four 48-kDa subunits, each containing a Rieske-type [2Fe-2S] center and a dissociable Fe^{2+} required for activity. Phthalate oxygenase reductase (POR) has one FMN and one plant-type Fd [2Fe-2S] center per 34-kDa peptide. POR crystallizes at pH 6.7 from poly(ethylene glycol) 6000 in space group $R3$ with $a = b = 113.4$ Å and $c = 77.7$ Å. At 4 °C V_{max} for the oxygenase is 90 min^{-1}. K_m's are 2 μM for POR, 300–500 μM for phthalate, and 125 μM for O_2. Details and rapid kinetic studies will be described.

128. Ligand Binding to the Iron of Fe(II)-Containing Dioxygenases. *J. D. Lipscomb*, D. M. Arciero, A. M. Orville, and M. R. Harpel. Department of Biochemistry, University of Minnesota, Minneapolis, MN 55455.

Extradiol catechol and protocatechuate (PCA) dioxygenases as well as gentisate dioxygenase employ an essential Fe^{2+} for O_2 activation, cleavage, and insertion. Previous work has failed to reveal whether O_2 and/or substrates bind at or near the Fe. Nitric oxide (NO) binds to the Fe^{2+} to form an EPR-active, $S = {}^3/_2$ type complex. NO also binds to the Fe in the substrate complex, but the resulting $S = {}^3/_2$ EPR spectrum is altered, suggesting that the environment of the Fe is changed. Moreover, the affinity of each enzyme for NO increases by 100-fold when substrate binds, showing that the substrate and NO binding are coupled. The EPR spectra of the NO complex of the native enzymes in $^{17}OH_2$ are broadened by hyperfine interactions, showing that water is also bound to the Fe in the NO complex; thus at least two of the Fe ligands can be exogenous. Substrates eliminate the broadening, suggesting that they exclude the H_2O from the Fe ligation. Broadening in EPR spectra of the NO adducts of extradiol dioxygenases

complexed with PCA labeled with ^{17}O in either of the two OH groups shows that both OH groups bind to the Fe. If NO functions as an O_2 analogue for these enzymes, the results suggest that both O_2 and substrates bind directly to the Fe at an early stage of the reaction cycle.

129. Anthranilate Hydroxylase from *Trichosporon cutaneum*. J. Powlowski, D. P. Ballou, and V. Massey. Department of Biological Chemistry, University of Michigan, Ann Arbor, MI 48109.

This enzyme catalyzes the conversion of anthranilate (2-aminobenzoate) to 2,3-dihydroxybenzoate and ammonia using NADPH. It is a simple flavoprotein that inserts one atom of oxygen from O_2 and one from H_2O into the substrate. Steady-state and stopped-flow studies show the enzyme to be similar to previously studied flavoprotein monooxygenases in many respects. Thus, the rate of enzyme reduction is greatly enhanced by binding of the aromatic substrate, and C-4aOOH and C-4aOH flavin adducts are observed during the oxidative half-reaction. However, a lag lasting several turnovers is observed in steady-state assays. The basis for this lag appears to be very slow binding of the aromatic substrate to the resting enzyme, accompanied by a slow conformational change prior to reduction by NADPH. After the oxidative half-reaction completes the first turnover, the enzyme is in a form which binds anthranilate much more quickly than resting enzyme.

130. Kinetic Mechanism of Dopamine β-Hydroxylase: Study by the Use of Reversible Inhibitors. *Walter E. DeWolf, Jr.*, and Lawrence I. Kruse. Department of Medicinal Chemistry, Smith Kline & French Laboratories, Philadelphia, PA 19101.

A potent "multisubstrate" inhibitor, SK&F 101368 (see following abstract), and certain related substructural inhibitors have been used to probe changes in the kinetic mechanism of dopamine β-hydroxylase (DBH) as a function of pH and fumarate activation. Consistent with a recent study of microscopic rate constants [Ahn & Klinman (1983) *Biochemistry 22*, 3096–3106] by kinetic isotope effects, pH- and fumarate-dependent changes in kinetic order are observed. Our results suggest that at pH 4.5 the kinetic mechanism is ordered with tyramine binding first, whereas at pH 6.6 in the absence of furmarate, the order of binding of tyramine and oxygen is random. Consistent with the results of Ahn and Klinman, fumarate prevents the conversion to a random mechanism at high pH. A double inhibition study using two of the substructures of SK&F 101368, *p*-cresol and 1-methylimidazole-2-thiol, indicated mutually exclusive binding of these two compounds. This suggests that the binding of an oxygen mimic significantly larger than diatomic oxygen occludes the phenethylamine binding site and provides additional evidence for a very close proximity between that site and the copper atom(s).

131. Kinetic Characterization of a Novel Class of "Multisubstrate" Inhibitors of Dopamine β-Hydroxylase. *Walter E. DeWolf, Jr.*, and Lawrence I. Kruse. Department of Medicinal Chemistry, Smith Kline & French Laboratories, Philadelphia, PA 19101.

Potent (K_i = 3–50 nM), reversible inhibitors of dopamine β-hydroxylase (DBH) are reported. The rational design of these new inhibitors was based on an active site model wherein the binding site for phenethylamine substrate is in close proximity to the active site copper atom(s). SK&F 101368 [1-(4-hydroxybenzyl)imidazole-2-thiol; K_i = 50 nM], a prototypical inhibitor that incorporates structural features of both the phenethylamine substrate and the soft bidentate imidazole-2-thiol ligand, an "oxygen mimic", appears to satisfy the structural and kinetic criteria for a "multisubstrate" type of inhibitor. SK&F 102048 (K_i = 5 nM), the 3′,5′-difluoro analogue of SK&F 101368, binds DBH approximately 10^6-fold more tightly than tyramine substrate. Under conditions of apparent rapid equilibrium random substrate binding (pH 6.6 in the absence of fumarate), SK&F 101368 is a competitive inhibitor with respect to both oxygen and tyramine. Additional kinetic evidence is presented to support the conclusion that these inhibitors bind directly to the phenethylamine binding site, rather than by acting at a remote, allosterically linked site.

132. Catalytically Active Oligomeric Species of Phenylalanine Hydroxylase. *M. A. Parniak* and S. Kaufman. Lady Davis Institute for Medical Research, Montreal, Quebec H3T 1E2, Canada, and Laboratory of Neurochemistry, NIMH, Bethesda, MD 20205.

Purified rat liver phenylalanine hydroxylase exists as a mixture of two oligomeric forms—a tetramer of M_r 200 000 (which accounts for 75–80% of the hydroxylase protein at 25 °C) and a dimer of M_r 100 000. Both species are catalytically active and show identical specific activities when assayed with the synthetic cofactor 6-methyltetrahydropterin. In contrast, the specific activity of the tetramer is 5 times that of the dimer when assayed with the natural cofactor tetrahydrobiopterin. Preincubation of the hydroxylase with phenylalanine results in the formation of tetramer from dimer, whereas low temperatures promote the formation of the dimeric species. The tetramer shows a high degree of cooperativity (n_H = 2) to variations in phenylalanine concentration in the presence of tetrahydrobiopterin; the response of the dimer is noncooperative (n_H = 1). A model is presented in which regulatory or activator sites for phenylalanine are absent in the dimeric enzyme. These sites are formed or become functional upon interaction of two dimers to form a tetramer. This latter species is thus subject to cooperative control by the substrate phenylalanine.

133. Effect of pH on Cofactor-Dependent Activity of Phenylalanine Hydroxylase. *M. A. Parniak* and S. Kaufman. Lady Davis Institute of Medical Research, Montreal, Quebec H3T 1E2, Canada, and Laboratory of Neurochemistry, NIMH, Bethesda, MD 20205.

The variation in the maximum velocity of rat liver phenylalanine hydroxylase with pH is dependent on the structure of the cofactor employed and on the state of activation of the enzyme. The tetrahydrobiopterin-dependent activity of native phenylalanine hydroxylase has a pH optimum of about 8.5. In contrast, after the enzyme has been activated by preincubation with phenylalanine or by limited proteolysis, the activity has a pH optimum of 7.0. The maximum velocity of the 6,7-dimethyltetrahydropterin-dependent activity of both the native and the activated species of phenylalanine hydroxylase is optimal at pH 7.0. Phenylalanine hydroxylase, which has been preincubated at an alkaline pH in the absence of phenylalanine and subsequently assayed at pH 7.0, shows an increased tetrahydrobiopterin-dependent activity similar to that exhibited by the enzyme, which has been activated by preincubation with phenylalanine at neutral pH. The hydroxylase at alkaline pH appears to be in an altered conformation that is essentially identical with that of the enzyme activated by preincubation with phenylalanine.

134. Characterization of the Reductive Activation of Phenylalanine Hydroxylase. *Leslie M. Bloom* and Stephen J. Benkovic. Department of Chemistry, The Pennsylvania State University, University Park, PA 16802.

The reductive activation of phenylalanine hydroxylase is required to generate enzyme capable of hydroxylation. The quantity of reducing agent consumed during hydroxylase reduction is dependent on the assay conditions. We demonstrate that a relationship exists between the stoichiometry of reduction and oxygen consumption in the system. Oxygen consumption is observed when phenylalanine hydroxylase is reduced by 1 equiv of 6-methyltetrahydropterin. However, reduction of phenylalanine-activated phenylalanine hydroxylase with half an equivalent of 6-methyltetrahydropterin occurs without oxygen consumption. The differences in oxygen consumption are related to activity recovery after reduction; recovery is significantly enhanced by reduction without oxygen consumption or reduction in the presence of catalase.

135. Hemoglobin as a Monooxygenase: Mechanistic Studies. *Michael A. Marletta*, Hugh A. Barton, and Brian H. Magee. Department of Applied Biological Sciences, Massachusetts Institute of Technology, Cambridge, MA 02139.

Hemoglobin has been reported to exhibit monooxygenase activity. Some basic mechanistic questions concerning this activity have been investigated in this study. Aniline in the presence of methemoglobin (or oxyhemoglobin), oxygen, and ascorbic acid is hydroxylated to *o*- and *p*-aminophenol. The oxygen in the products is derived from molecular oxygen. No NIH shift was detectable in this reaction with *p*-deuterioaniline as a substrate. Hemoglobin also catalyzes the S-oxidation of the phenothiazine chlorpromazine in the presence of reducing equivalents. The flavoprotein methemoglobin reductase and the hemoprotein cytochrome b_5 were isolated from human erythrocytes and when reconstituted with NADH and oxy- or methemoglobin were found to support this S-oxidation. Ascorbic acid is also capable of providing reducing equivalents for this reaction. Further mechanistic studies are under way to compare the described hydroxylation reactions to those catalyzed by cytochrome P-450 and horseradish peroxidase.

136. Intramolecular Nitrogen Atom Transfer Catalyzed by Cytochrome P-450. *E. Svastits*, J. H. Dawson, R. Breslow, and S. H. Gellman. Department of Chemistry, University of South Carolina, Columbia, SC 29208, and Department of Chemistry, Columbia University, New York, NY 10027.

Phenobarbital-induced rabbit liver cytochrome P-450 has been found to catalyze the intramolecular amidation of **1**, yielding a cyclic product, **2**, containing a new carbon–nitrogen bond. This reaction has previously been demonstrated with

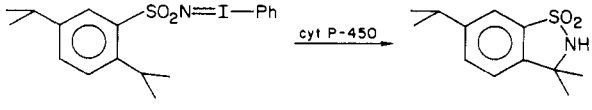

1 2

metalloporphyrin catalysts, but this is the first time P-450 has been successfully used as the catalyst. P-450 showed multiple turnovers and had an activity of 1.0 nmol of product (nmol of P-450)$^{-1}$ min^{-1}, a minimum value since enzyme saturation was not achieved due to the low solubility of **1**. P-450 activity was also isozyme dependent; the LM2 isozyme was only minimally active relative to a mixture of the LM3 and LM4 isozymes.

137. Resonance Raman Investigation of Glutathione Reductase Intermediates. *Chris R. Lively*, Camilo J. Rojas, and James T. McFarland. Department of Chemistry, University of Wisconsin—Milwaukee, Milwaukee, WI 53201.

Glutathione reductase (EC 1.6.4.2) is a flavin-containing enzyme that catalyzes the reduction of oxidized glutathione by NADPH; the X-ray structure of the oxidized flavoprotein has been determined. Addition of NADPH to the oxidized enzyme results in two reduction products, the so-called EH_2 and EH_4 intermediates. Both of these intermediates show long-wavelength absorbance bands that have been ascribed to charge-transfer complexation. Chemical studies and the electronic spectra of these intermediates suggest that EH_2 consists of oxidized flavin and reduced disulfide at the active site while the EH_4 intermediate consists of a charge-transfer complex of reduced flavin and oxidized nicotinamide with the disulfide in the reduced state. We have determined the resonance Raman spectra of these intermediates and our experiments show that, indeed, EH_2 clearly contains oxidized flavin in a different hydrogen bonding environment from native oxidized glutathione reductase. We currently are trying to assign any RR bands due to the charge-transfer donors especially between the thiolate anion of cysteine and flavin. The resonance Raman spectrum of EH_4 includes the RR bands of reduced flavin and oxidized nicotinamide.

138. *retro*-Glutathione: Synthesis and Biochemistry of the End Group Modified Retro-Inverso Isomer of Glutathione. *R. N. Armstrong*, D. Y. Lee, and W.-J. Chen. Department of Chemistry, University of Maryland, College Park, MD 20742.

The tripeptide glutathione (GSH) is an extremely important cofactor involved in amino acid transport, maintenance of thiol–disulfide equilibria, and metabolism of electrophiles. In an attempt to design GSH analogues that can participate in the biochemistry of the sulfhydryl group but are refractory to processing of the peptide bonds, the end group modified retro-inverso isomer of GSH (*retro*-GSH) has been synthesized. The analogue in which the direction of the peptide bonds has been reversed with inversion of stereochemistry at the α-carbon of the Cys residue has essentially the same molecular topology as GSH. *retro*-GSH was synthesized by condensation of N^{α}-Cbz-L-2,4-diaminobutyrate with *N*-*t*-Boc-*S*-benzyl-D-cysteine, followed by removal of the *t*-Boc group, condensation of the dipeptide with monobenzyl malonate, and global deprotection with trifluoromethanesulfonic acid and thioanisole. *retro*-GSH is a substrate for glutathione *S*-transferase, suggesting it will be a novel tool for the study of enzyme mechanisms and metabolism involving GSH.

139. Protection by Heat-Treated Microsomes against Dilution Inactivation of Cytochrome P-450 Activities in Untreated Microsomal Fractions. *J. Rabovsky* and D. Judy. National Institute for Occupational Safety and Health, Morgantown, WV 26505.

Two cytochrome P-450 activities were studied as a function of enzyme concentration in isolated, *intact* microsomes. Ethoxycoumarin deethylase (ECase) and ethoxyresorufin deethylase (ERase) activities were measured in microsomes obtained from mouse liver (MLi) and β-naphthaflavone-treated rat liver (BNF-RLi). Representative specific activities (nanomoles per minute per milligram of protein) were as follows: BNF-RLi-ECase, 2.5; BNF-RLi-ERase, 2.2; MLi-ERase, 0.25. Decreased specific activities were observed at

low microsomal protein concentrations (<15 μg/mL in the assay), but they were recovered if microsomes heated at 60 °C for 20 min (Δ60) were also present. No ECase or ERase activity was detected after heat treatment. The recovery of ERase was dependent on the concentration of Δ60 microsomes. Substrate dependence measurements showed the assays were carried out at saturating concentrations (0.5 mM ethoxycoumarin; 2 μM ethoxyresorufin). In the case of BNF-RLi-ERase V_{max} for low enzyme < low enzyme + 5-fold Δ60 ≤ high enzyme = 2.6 nmol min^{-1} (mg of protein)$^{-1}$. K_m's were estimated as low enzyme < low enzyme + 5-fold Δ60 < high enzyme = 0.20 μM. The data suggest microsomal membranes protected the two P-450 activities against the adverse effects of high dilution of intact microsomes.

140. Reductive Metabolism of Nitrated Polycyclic Aromatic Hydrocarbons to DNA Binding Derivatives. *Kim K. Colvert* and Peter P. Fu. National Center for Toxicological Research, Jefferson, AR 72079.

Nitrated polycyclic aromatic hydrocarbons (PAHs) are genotoxic pollutants that are formed from atmospheric reactions of PAHs with NO_x and from incomplete combustion processes. We have investigated whether or not the reductive metabolism of 1- and 3-nitrobenzo[*a*]pyrene, 7-nitrobenz-[*a*]anthracene, 9-nitroanthracene, and their eight *trans*-dihydrodiol metabolites to DNA binding derivatives correlates with the observed bacterial mutagenicity for these compounds. In vitro incubations were conducted with the ^{3}H-nitrated PAHs, the model mammalian nitroreductase xanthine oxidase, and calf thymus DNA. 1- and 3-nitrobenzo[*a*]pyrene-*trans*-9,10-dihydrodiols gave the greatest binding, 1- and 3-nitrobenzo[*a*]pyrene showed medium binding levels, and 9-nitroanthracene, 7-nitrobenz[*a*]anthracene, and their dihydrodiols exhibited lower binding levels. High in vitro DNA binding generally correlated with bacterial mutagenicity as measured in *Salmonella typhimurium* TA98 while exceptions may indicate differences in substrate specificity between the mammalian and bacterial nitroreductases or subsequent activation by transacetylation in the mutagenesis assay.

141. Metabolism of 2-Aminoanthracene by Rat Liver Microsomes. *David A. Haugen.* Division of Biological and Medical Research, Argonne National Laboratory, Argonne, IL 60439.

As determined by high-performance liquid chromatography (HPLC), numerous enzyme-dependent products of 2-aminoanthracene (NH_2An) were formed in reaction mixtures containing rat liver microsomes and NADPH. The principal mutagenic metabolite was 2-nitrosoanthracene (NOan). Although NOAn probably arises from oxidation of the initial enzymatic product *N*-hydroxy-2-aminoanthracene [NH(OH)An], rigorous attempts to detect NH(OH)An in metabolic reaction mixtures have generally been unsuccessful. Synthetic NH(OH)An is readily oxidized by ferric cytochromes, yielding further products of N-oxidation, including NOAn. Mixtures of NOAn and NH(OH)An readily yield two products, which appear in enzymatic reaction mixtures and are being characterized. N-Oxidation of NH_2An is enhanced 10- to 20-fold by pretreatment of rats with 3-methylcholanthrene or Aroclor 1254, but not with phenobarbital, as determined by HPLC and by measurements of mutagenesis in the microsome/*Salmonella* assay. All inducers increased the formation of polar metabolites, including products of ring hydroxylation.

142. Mechanism of the Irreversible Transport of L-Ascorbic Acid into Human Erythrocytes. *Eugene S. Wagner*, Lisa Shaffer, and Karen Bennett. Center for Medical Education, Ball State University, Muncie, IN 47306.

L-Ascorbic acid-*1*-^{14}C was incubated with human blood. Our studies indicated that L-ascorbic acid did not bind irreversibly to any of the protein components of plasma but did migrate irreversibly into erythrocytes. Isolation and characterization via IR of the moiety trapped within the cell established its identity as chemically unchanged L-ascorbic acid. Evidence will be presented to differentiate between two mechanisms of transport into the cells: (1) L-dehydroascorbic acid transport into the cell followed by reduction to L-ascorbic acid and (2) the involvement of anion recognition sites on the surface of the cell in the transport of L-ascorbic acid into the cells.

143. Utilization of 7,10,13,16-Docosatetraenoate by Ovine and Porcine Seminal Vesicle Cyclooxygenase. *Aldo Ferretti* and Vincent P. Flanagan. Lipid Nutrition Laboratory, Beltsville Human Nutrition Research Center, ARS, USDA, Beltsville, MD 20705.

We have studied the comparative utilization of exogenous 7,10,13,16-docosatetraenoate (22:4w6, adrenic acid) by ovine and porcine seminal vesicle cyclooxygenase in vitro. Ram vesicular microsomes readily converted 22:4w6 into C_{22}-prostaglandins (PGs) in good yields. Conversely, swine microsomes, prepared under identical conditions, were unable to produce cyclooxygenase products. Positive results were obtained, however, when the porcine vesicles were homogenized in the presence of the substrate, but incubation after homogenization brought about only a minor yield improvement. If one assumes that the specific activities of ovine and porcine vesicular cyclooxygenases are identical—an assumption justified by data in the literature—then the aggregate of our experimental data suggests that the swine vesicles contain very little enzyme. Furthermore, we observed an apparent age effect on the PGE/PGF production ratio in the ram. Conclusive mass spectrometric evidence for the formation of 1a,1b-dihomo-PGE_2 and 1a,1b-dihomo-$PGF_{2\alpha}$ will be presented and discussed.

144. PGH Synthase: A Case of Enzymic Symbiosis. R. J. Kulmacz, J. F. Miller, and *W. E. M. Lands.* Department of Biological Chemistry, University of Illinois at Chicago, Chicago, IL 60680.

The oxygenation reaction catalyzed by PGH synthase requires hydroperoxide for initiation. The reaction has an autoaccelerative nature, as the reaction product prostaglandin G is a hydroperoxide that produces further initiation. Several observations indicate that the presence of peroxidase activity in the same protein acts symbiotically to provide more effective initiation of catalysis. Cosubstrates for peroxidase action stimulated the cyclooxygenase activity, and blocking the peroxidase action cut this stimulation of cyclooxygenase activity. Lipid hydroperoxides were several hundred fold better than HOOH as substrates for peroxidase activity and were also several hundred fold better initiators of cyclooxygenase activity. The peroxidase activity of aspirin-treated PGH synthase did not stimulate the cyclooxygenase activity of native PGH synthase, but rather it inhibited activity by removal of hydroperoxide activator. Peroxidase intermediates thus appear to provide an intramolecular mechanism for rapid initiation of the cyclooxygenase reaction by product hydroperoxides in

a manner that rapidly amplifies small initial amounts of hydroperoxide activator and enhances prostaglandin biosynthesis.

145. Effects of L-Lysine Oligomers and Polymers on Normal and on Aspirinized Human Platelets. *B. H. Ragatz*, G. Modrak, M. Engle, S. Lee, and L. Ostergren. Fort Wayne Center for Medical Education, Biology Department, and Parkview Memorial Hospital, Fort Wayne, IN 46805.

It is well known that aspirinized (A) platelets lack the enzymatic ability to produce various proaggregatory metabolites from arachidonic acid, which is released by various platelet-activating stimuli. Accordingly, we have examined the direct effects of L-lysine oligomers and polymers on normal (N) and on A platelets and the interactions of these compounds with other aggregators. We have found no direct interaction of lysyllysine (dilysine, DL), pentalysine, or poly(L-lysines) (PLs) in the M_r 4000–14000 range with N or A platelets. PLs in the M_r 55000–240000 range aggregate N or A platelets. PLs of M_r <14000 have no effect on ADP- or epinephrine-induced aggregation of N or A platelets. M_r 4000 or 14000 PL inhibits the onset of collagen-induced aggregation in A platelets, and M_r 4000 PL is effective in inhibiting ristocetin aggregation in A platelets. These minor differences between A and N platelets suggest that PL interaction is not an arachidonic acid pathway dependent phenomenon. Transmission electron microscopy reveals N or A platelet clumping and degranulation following exposure to 1 mg/mL solutions of M_r 240000 PL.

146. Arachidonic Acid Release by a Phospholipase Is the Mechanism of the Initial Injury in Cell Killing by Elevated Intracellular Calcium. *W. T. Shier* and D. J. DuBourdieu. College of Pharmacy, University of Minnesota, Minneapolis, MN 55455.

Cell killing in ischemic diseases (e.g., myocardial infarction, stroke) appears to involve altered intracellular Ca^{2+}. We are studying the mechanism of cell killing by altered intracellular Ca^{2+} using as a model system the killing of cultured 3T3 mouse fibroblasts by ionophore A23187 plus Ca^{2+}. Cell killing in this system involves two Ca^{2+}-dependent injury steps followed by a Na^+-dependent step. A23187 plus Ca^{2+} also stimulates release of arachidonic acid from biosynthetically labeled phospholipids in cells, indicating activation of a phospholipase. We have obtained five lines of evidence that the arachidonic acid release reaction either mediates the first injury step or is very closely linked to it: (i) the two processes exhibit the same time course; (ii) they exhibit the same Ca^{2+} dependency (0–200 μM Ca^{2+}); (iii) they exhibit the same inhibitor specificity with Mn^{2+} and Ni^{2+}; (iv) they are both stimulated by Hg^{2+}, apparently acting as an analogue of Ca^{2+}; (v) clonal variation in Mn^{2+}-inhibitable arachidonic acid release stimulated by A23187 correlates well with the extent of cell killing. Possibly overactivation or prolonged activation of a normal regulatory process induces the initial injury.

147. Selective Arachidonoyl Group Transfer between Dog Heart Phospholipids. *Padala V. Reddy* and Harald H. O. Schmid. The Hormel Institute, University of Minnesota, Austin, MN 55912.

Dog heart microsomes catalyze the transfer of acyl groups from the *sn*-2 position of exogenous phosphatidylcholine to 1-acyllysophosphatidylethanolamine. Approximately equal amounts of free fatty acids are produced as well. The reaction exhibits a pH optimum of 7.5–8.5 and does not require Ca^{2+} or other divalent cations. Sulfhydryl reagents and free fatty acids are inhibitory. 1-*O*-Acyl- and 1-*O*-alkenylglycerophosphoethanolamines are equally effective as acyl acceptors. The reaction proceeds in the absence of exogenous coenzyme A, but acyl transfer is enhanced by its addition. The transacylase exhibits a strong preference (10:1) for arachidonate over linoleate, a selectivity not observed in the acylation of lysophosphatidylethanolamine by the acyl-CoA requiring acyltransferase of dog heart microsomes. Transacylation from phosphatidylcholine may thus be involved in the maintenance of the high amounts of arachidonate found in microsomal ethanolamine phospholipids.

148. Phorbol Esters Stimulate the Release of Free Arachidonic Acid from Membrane Phospholipids in U937 Cells. *Mark D. Wiederhold*, David W. Ou, and Vincent M. Papa. Rush-Presbyterian-St. Lukes Medical Center, Chicago, IL 60612.

Activation of protein kinase C by phorbol myristate acetate and other stimulants has been associated with increased action of cellular phospholipase enzymes. An important consequence of this activity is the synthesis of prostaglandins and other arachidonic acid metabolites. We are concerned with an initial event in this cascade, the action of lipases to cleave fatty acids esterified to membrane phospholipids. U397 cells, a human macrophage cell line, were analyzed for lipase activity by determining the amount of free fatty acid released into culture supernatants following stimulation by phorbol esters. Fatty acid levels were determined by gas chromatography and also by thin-layer chromatography following incorporation of [^{3}H]arachidonic acid into membrane phospholipids. Levels of arachidonic acid in culture supernatants were increased after incubation with phorbol myristate acetate, phorbol 12,13-dibutyrate, and phorbol myristate acetate 4-*O*-methyl ether for 2 h at 37 °C. Other fatty acids were also detected in supernatants by gas chromatography. The release of free fatty acids from cells following membrane perturbation may be an important biological response.

149. Isolation of Apolipoprotein A from Lipoprotein A. *G. M. Fless*, M. E. ZumMallen, and A. M. Scanu. Departments of Medicine and Biochemistry and Molecular Biology, The University of Chicago, Chicago, IL 60637.

An easy method was developed for the rapid and selective isolation of apoA from human plasma LpA. This procedure was applied to a "low-density" LpA subspecies from a single individual whose apoA was of a size smaller than apoB-100. After reduction with 0.01 M dithiothreitol, apoA was separated from the LpA particle by rate zonal centrifugation on a 7.5–30% NaBr density gradient. Two completely water-soluble products were recovered: the lipid-free apoA that remained at the bottom of the gradient and a lipid-rich floating LDL-like particle that contained apoB but not apoA and which we referred to a LpA–. The separation of these two components was also achieved by subjecting reduced LpA to electrophoresis on 2.5–16% polyacrylamide gradient gels. However, dissociation of reduced LpA could not be achieved by gel filtration in either low- or high-salt solutions. These observations indicate that apoA is linked to LpA by disulfide bonds to apoB and by noncovalent interactions to the particle surface. The former are sensitive to chemical reduction while the latter are disrupted by the action of gravitational or electrical field. This rapid method for isolating apoA should facilitate studies on its structure and function.

150. Energetics of Fatty Acid β-Oxidation. *William G. Gustafson* and James T. McFarland. Department of Chemistry, University of Wisconsin—Milwaukee, Milwaukee, WI 53201.

Mitochondrial general fatty acyl-CoA dehydrogenase (gAD) catalyzes the dehydrogenation of C4–C12 saturated fatty acyl-CoA thio esters. The electron equivalents liberated in the oxidation are transferred to the specific acceptor electron-transfer flavoprotein (ETF). We have used an anaerobic spectroelectrochemical titration method to determine general fatty acyl-CoA dehydrogenase and ETF flavin reduction potentials. In contrast to free flavin adenine dinucleotide, where two-electron reduction is thermodynamically favored, both ETF and gAD thermodynamically stabilize a significant proportion of one-electron reduced flavin. Values of the reduction potential for the substrate butyryl-CoA reported in the literature are inconsistent with the observation of substantial reduction of gAD by butyryl-CoA. We have reevaluated the reduction ptoential of substrate using the chromophore-producing substrate β-(2-furyl)propionyl-CoA (FPCoA). From these data and previous work from our laboratory we have calculated the reduction potential of butyryl-CoA. These data suggest that gAD and its substrates are essentially equipotential. We propose that the increased stability of the enzyme–product charge-transfer complex is the thermodynamic driving force for substrate oxidation.

151. New Chromophoric Substrate for the Investigation of the Enzyme Lipoprotein Lipase. *Camilo Rojas* and James T. McFarland. Department of Chemistry, University of Wisconsin—Milwaukee, Milwaukee, WI 53201.

We have synthesized a new substrate, 1,2-dipalmitoyl-3-(β-2-furylacryloylytriacyl)glyceride, for the resonance Raman and kinetic investigation of the enzyme lipoprotein lipase. This substrate is soluble as a monomer in aqueous solution and can also be prepared as a mixed micelle with phosphatidylcholine. The monomer hydrolyzes in the presence of catalytic enzyme to produce β-2-furylacrylic acid; this reaction can be followed spectrally at 308 nm, permitting the continuous monitoring of the time course of the reaction. Hydrolysis of the monomeric substrate proceeds without apoC-II as an activator, and the pH profile is consistent with base catalysis. The hydrolysis of the phosphatidylcholine–substrate mixed micelle requires the addition of calf serum as an activator, indicating that apoC-II may be required as an activator of hydrolysis of micellar substrate. The activation of the enzyme-catalyzed hydrolysis of micellar substrate exhibits a lag time indicating that the interaction of activator, substrate, and enzyme is kinetically slow and that this interaction can be studied with this new substrate.

152. Dietary Fatty Acids in Tumorigenesis. *Alice S. Bennett.* Department of Biology, Ball State University, Muncie, IN 47306.

Diets containing high levels of certain polyunsaturated fatty acids (PUFA) are more effective than saturated fats in promoting the development of murine mammary gland tumors. Results of studies in our laboratory indicate that strain A/ST female mice maintained on a high fat (15%) diet rich in stearic acid developed initial spontaneous mammary adenocarcinomas at an older age than mice fed a low fat (4.5%) stock diet (STD). The percentage of 18:2, 20:3, and 20:4 was reduced in tumor tissues of mice on the SA diet. We suggested that dietary stearic acid interfered with the synthesis of arachidonic acid and, subsequently, certain prostaglandins from minimally available linoleic acid. Phospholipids of tumors of mice fed a 15% safflower oil diet (SAF) exhibited an increase in the long-chain PUFA. These mice are heavier at 5, 8, and 18 months of age than those fed either the SA or STD diets. Adipose tissues are less firm and exhibit altered fatty acid content. Fatty acids play specific roles in controlling cholesterol synthesis, fatty acid synthesis, and lipogenesis. Implications of feeding various fatty acids for control of obesity, tumorigenesis, and cardiovascular disease will be discussed.

153. Inhibition of Human Leukocyte HMG-CoA Reductase Activity by Physiological Concentrations of Ascorbic Acid. *H. James Harwood Jr.*, Yvonne J. Greene, and Peter W. Stacpoole. University of Florida College of Medicine, Gainesville, FL 32610.

High doses of ascorbic acid (AA) decrease cholesterol levels in patients with hypercholesterolemia. Dietary AA also decreases the in vivo activity of guinea pig liver HMG-CoA reductase (R), the rate-limiting enzyme in cholesterol synthesis. We asked whether AA influenced R activity by directly affecting the human enzyme. R activity in microsomes isolated from cultured human leukocytes (IM-9 cells) was markedly decreased by either AA or its oxidized derivative, dehydroascorbate (DHA). Inhibition was log linear between 0.01 and 10 mM AA (25% and 81% inhibition, respectively) and between 0.05 and 10 mM DHA (7% and 71% inhibition, respectively). Inhibition was noncompetitive with respect to HMG-CoA [K_i(AA) = 6.4 mM; K_i(DHA) = 15 mM] and competitive with respect to NADPH [K_i(AA) = 6.3 mM; K_i(DHA) = 3.1 mM]. Since AA and DHA may be interconverted through the free radical intermediate, monodehydroascorbate (MDA), we asked whether R inhibition may be mediated by MDA. The reducing agent dithiothreitol (DTT), which prevents oxidation of AA to DHA but promotes conversion of DHA to AA, abolished R inhibition by AA but promoted R inhibition by DHA. MDA may thus mediate the inhibitory action of both AA and DHA on R activity.

154. Association and Influence of Tamoxifen on Estrogen Receptors in Uterus. *Y. J. He*, N. A. Shahabi, L. Myatt, and J. L. Wittliff. Hormone Receptor Laboratory, James Graham Brown Cancer Center, University of Louisville, Louisville, KY 40292.

Our laboratory has demonstrated that estrogen receptors exhibit polymorphism based on properties of size, shape, and surface charge using high-performance liquid chromatography (HPLC) [e.g., *J. Chromatogr. 266*, 115 (1983), *297*, 313 (1984), and *307*, 39 (1984)]. Tamoxifen (TAM) is thought to exert its effect by associating with estrogen receptors. To study the origin and role of receptor heterogeneity (isoforms) in relation to antihormone treatment, TAM was administered at 0.5, 3, 6, and 30 mg/kg body weight for 5 days to female rabbits. Estrogen receptors measured by titration with 17β-[^{3}H]estradiol were decreased 10-fold compared to control levels while progestin receptors were increased 2-fold, indicating the mechanism was intact. HPLC profiles using ion-exchange columns (SynChropak AX 1000) indicated two isoforms eluting at 80–90 and 170 mM phosphate. When [^{3}H]estradiol, [^{3}H]TAM, or 4-OH-[^{3}H]TAM was directly associated with these receptors in rat uteri, three isoforms were resolved; one eluted in the void volume (10 mM) while the others eluted at 90 and 155 mM phosphate. It appears all three ligands bound to identical isoforms of activated and nonactivated estrogen receptors as identified by HPLC with

ion-exchange columns.

155. Evaluation of the B-Protein Assay as an Aid in Cancer Management. *J. C. Morrison*, W. D. Whybrew, and E. T. Bucovaz. Departments of Biochemistry, Obstetrics, and Gynecology, University of Tennessee Center for the Health Sciences, Memphis, TN 38163, and Department of Obstetrics and Gynecology, University of Mississippi Medical Center, Jackson, MS 39216.

B-Protein is a general biological serum marker that can be used to detect cancer. The standard B-protein assay is based on an interaction between the B-protein and a radiolabeled protein, named binding protein, of bakers' yeast. Human and laboratory animal data indicate that the level of serum B-protein is directly related to the course of the malignancy. Furthermore, studies conducted have shown that the assay is an effective aid to use for monitoring patients for the recurrence of cancer following surgery for the disease. Thus, it would appear that the monitoring of B-protein levels in patients may be a practical cancer management aid because the test is an inexpensive, simple, and sensitive test that can be used on a routine basis without potential harm to the patient.

156. Cancer Detection: Utilization of the B-Protein Assay Quick Test and Standard Procedure as an Approach to Cancer Control. *E. T. Bucovaz*, J. C. Morrison, J. L. Rhoades, and W. D. Whybrew. Department of Biochemistry, University of Tennessee Center for the Health Sciences, Memphis, TN 38163.

Serum of individuals with cancer contains a specific protein designated B-protein; thus, B-protein can be utilized as a general biological marker for the detection of cancer. Two assay procedures have been developed for the detection of B-protein. One is a qualitative procedure named the B-protein assay quick test, and the other is a quantitative procedure named the standard B-protein assay. The quick test is designed for cancer screening in clinicians' offices. The standard assay procedure is principally for use in clinical laboratories and is recommended for use as a cancer management aid. On the basis of studies involving both procedures, the following protocol appears appropriate. Whenever a positive result utilizing the B-protein assay quick test is observed, a sample of the patient's serum is sent to a clinical laboratory for verification by the standard B-protein assay procedure and by other tests. The standard assay is then used to monitor the patient throughout therapy. Utilization of both forms of the B-protein assay in the manner described may prove to be a practical approach to cancer control.

157. Cancer Detection: The Serum Pattern of B-Protein and Its Precursor during the Progression of Malignancies. *A. W. Schweikert*, W. D. Whybrew, and E. T. Bucovaz. Departments of Biochemistry, Obstetrics, and Gynecology, University of Tennessee Center for the Health Sciences, Memphis, TN 38163.

A protein with unique properties, present in the serum of individuals with cancer, has been designated B-protein. One method of detecting this protein is through its interaction with radiolabeled binding protein. Binding protein is a substructure of the coenzyme A synthesizing protein complex (CoA-SPC) of bakers' yeast. In the assay system, radiolabeled binding protein interacts with B-protein to form a B-protein–binding protein complex. The precursor of B-protein, which is also present in the serum of noncancerous individuals, has different properties and is not detected by the assay procedures. The amount of radiolabeled complex formed is used to determine if cancer is present in the serum donor and to follow the progression of the malignancy. During the progression of a malignancy, the precursor of B-protein appears to decrease to the same extent that B-protein increases. The increasing concentration of B-protein and/or the decreasing concentration of its precursor may have an influential role in the development of this disease.

158. Tryptophan Fluorescence Lifetimes in Proteins Measured by Multifrequency Phase Fluorometry Employing Mode-Locked Laser Excitation. *R. Alcala*, Franklyn G. Prendergast, and Enrico Gratton. Department of Physics, University of Illinois, Urbana, IL 61801, and Department of Pharmacology, Mayo Foundation, Rochester, MN 55905.

The output of a synchronously pumped and mode-locked argon ion laser was used to pump a dye laser. An acoustooptic modulator was employed to amplitude modulate the dye laser output and to introduce quasi-continuously variable harmonic content (1–416 MHz). UV excitation light was obtained by frequency doubling the acoustooptic modulated dye laser output and was used for a multifrequency phase fluorometry study of indole fluorescence lifetimes in model systems, peptides and proteins. Invariably the fluorescence decays in peptides and proteins were at least biexponential. In contrast, the fluorescence of 5-methylindole complexes in α-cyclodextrin showed a single fluorescence lifetime. Molecular graphics examination of the environs of the tryptophan side chain in these proteins seldom provided an explanation for the observed lifetime. It is unclear whether the two lifetimes observed in single tryptophan proteins represent two protein species; alternative explanations will be discussed.

159. Correlation of Protein Structure and Luminescence: Use of Molecular Electrostatic Potentials. Michael Liebman and *Franklyn G. Prendergast*. Department of Pharmacology, Mt. Sinai School of Medicine, New York, NY 10029, and Department of Pharmacology, Mayo Foundation, Rochester, MN 55905.

Molecular graphics analysis of several proteins, each of which contains a single tryptophan residue, shows that it is difficult to correlate the protein structure and fluorescence. The relative contributions of the protein matrix and solvent to the fluorescence are most often in question. To probe this issue further, we have calculated molecular electrostatic potentials for the environs of tryptophan residues in proteins. The contributions from charged moieties, dipole–dipole interactions, and supramolecular structures (helices, β-structures) were all assessed. The electrostatic potentials generated have been graphically displayed. Fluorescence spectra, quantum yields, and steady-state anisotropies were measured by usual methods. Fluorescence lifetimes were determined with picosecond resolution by multifrequency phase fluorometry. An attempt has been made to correlate the measured fluorescence properties with the electrostatic character of the environs of the tryptophan and with apparent water accessibility.

160. New Protein Sequencing Techniques: Detection and Quantitation of *N*-Formylmethionine Species of rDNA-Derived Proteins. *P. H. Lai*, C. Graham, and H. Lu. Amgen, Thousand Oaks, CA 91320.

Protein synthesis in bacteria starts with formylmethionine (fMet). The formyl group at the N-terminus of bacterial proteins is removed by a deformylase. During the synthesis of proteins expressed in genetically modified bacteria, the efficiency of hydrolysis of the formyl group can be influenced by expression levels and/or fermentation conditions. Therefore, three different species, i.e., fMet-, Met-, and des-Met-proteins, may be present in the rDNA-derived protein products. These three species of a protein often are copurified through purification steps and are extremely difficult to separate. However, it is important to quantify these species for both process control and product identification reasons. Quantitation of the fMet species by composition analysis and by direct sequencing is impossible, and quantitation by peptide mapping is tedious and inaccurate. Here we describe an effective and rapid method for detection and quantitation of *N*-fMet species of rDNA-derived protein using r-interferons and rIL-2 as examples. This method involves initial amino acid sequencing, followed by in situ chemical cleavage in sequenator and subsequent sequencing of fragments.

161. HPLC Separation of Natural Mixtures of Ovomucoid Third Domains Differing by a Single Neutral Amino Acid Substitution. *Tiao-Yin Lin*, James A. Cook, and Michael Laskowski, Jr. Department of Chemistry, Purdue University, West Lafayette, IN 47907.

To determine the sequence to reactivity algorithm for protein inhibitors of serine proteinases, we use the third domains of avian ovomucoids. We need highly sensitive separation techniques to characterize these third domains, especially in cases of polymorphism. Three ovomucoid third domains are polymorphic. They are Japanese quail, Ser and Gly at P'_{14}, plumed whistling duck, Glu and Asp at P_9, and grey junglefowl, Ala and Val at P_1. In each case the substitution does not affect the net charge on the molecule. However, we are able to separate all three pairs to the base line by HPLC on μBondapak C_{18} columns with a binary gradient involving H_2O, trifluoroacetic acid, and 2-propanol. In order to use very small amounts of material, we monitor at 214 nm. The separation can be achieved with mixture loads of 2 μg–1 mg. We can also resolve pairs of proteins differing in length of the chain by one or two (out of 56) neutral amino acids. Proteins differing by a single neutral amino acid have been occasionally resolved in the past for insulin variants by Shoelson et al. [(1983) *Proc. Natl. Acad. Sci. U.S.A. 80*, 7390] and for hemoglobin by Strahler et al. [(1983) *Science* (*Washington, D.C.*) *211*, 860].

162. Quantitation of Stable Isotopic Tracers of Metals. Xinjie Wu, *David Smith*, and Connie Weaver. Department of Medicinal Chemistry and Pharmacognosy and Department of Foods and Nutrition, Purdue University, West Lafayette, IN 47907.

While radioisotopic tracers have been used extensively, stable isotopic tracers offer several advantages, which include total elimination of radiation exposure, the possibility of long-term labeling experiments, and use of multiple tracers. In spite of these advantages, stable isotopes of metals have rarely been used as tracers because there has not been a satisfactory method of detection. Although neutron activation analysis and thermal ionization mass spectrometry have been used successfully, both techniques require extensive sample preparation and are costly. We are presently investigating high-resolution fast atom bombardment mass spectrometry as an alternative method for quantifying stable isotopic tracers of metals in biological material. This method uses nonselective atomic sputtering to produce ions and high-resolution mass spectrometry to separate and detect the ions of interest. Recent developments in methodology as well as results from tracer administration of calcium and magnesium to humans will be presented.

163. Amino Acid Sequence of an Active Site Peptide from Avian Liver HMG-CoA Synthase. *H. M. Miziorko* and C. E. Behnke. Medical College of Wisconsin, Milwaukee, WI 53226.

3-Hydroxy-3-methylglutaryl-CoA synthase is irreversibly inhibited by the active site directed inhibitor 3-chloropropionyl-CoA. Enzyme modification, which can be minimized by the substrates acetyl-CoA or acetoacetyl-CoA, involves stoichiometric alkylation of an active site cysteine sulfhydryl. DEAE-Sephadex chromatography of tryptic digests prepared from enzyme inactivated by using chloro-[^{14}C]propionyl-CoA suggested that one peptide accounts for most of the bound radioactivity. Specificity of the modification is also indicated by reversed-phase HPLC, which was used to isolate the radioactively labeled peptide in a chemically homogeneous form. Automated gas-phase Edman degradation techniques have been employed to confirm the assignment of cysteine as the inhibitor's target residue and to elucidate the sequence of amino acids that flank the ^{14}C-carboxyethylated residue: Glu-Ser-Gly-Asn-Thr-Asp-Val-Glu-Gly-Ile-Asp-Thr-Thr-Asn-Ala-[^{14}C]CECys-Tyr-Gly-Gln-Thr-Ala. These data represent the first assignment of active site structure for HMG-CoA synthase, an enzyme that catalyzes the first irreversible reaction in the ketogenic and cholesterogenic pathways.

164. Purification and Site-Directed Inactivation of Phosphoribulokinase. *T. J. Krieger* and H. M. Miziorko. Medical College of Wisconsin, Milwaukee, WI 53226.

Spinach leaf phosphoribulokinase has been purified to homogeneity by utilizing an agarose–ATP affinity column. The enzyme is stable when stored at −70 °C in the presence of ATP and glycerol. The enzyme slowly loses activity upon prolonged storage and can be reactivated by incubation with dithiothreitol (a divalent cation is required for activity). The homogeneous enzyme has a specific activity of 350 units/mg and consists of two apparently identical subunits (M_r 45 000). A reactive ATP analogue, 5′-[(fluorosulfonyl)benzoyl]adenosine (FSBA), inactivates the enzyme in a site-directed fashion (K_i = 4.9 mM). The inactivation demonstrates pseudo-first-order kinetics (k = 0.32 min^{-1}). Protection is afforded by ATP but not by ribulose 5′-phosphate or Mg^{2+}. The enzyme is not inhibited by phenylmethanesulfonyl fluoride. Treatment of the inactivated kinase with 50 mM dithiothreitol at 30 °C restores 70–80% of the initial activity within 15 min; this suggests that the modified residue is an active-site cysteine.

165. A Novel High-Speed Liquid Chromatographic System for the Analysis of Methylglyoxal Bis(guanylhydrazone) (MGBG) in Clinical Samples. *David L. Gildersleeve*, Michael C. Tobes, and Ronald B. Natale. Divisions of Nuclear Medicine and Hematology/Oncology, Department of Medicine, University of Michigan Medical Center, Ann Arbor, MI 48109.

MGBG is a potent antineoplastic agent and analogue of the polyamine spermidine. Clinical trials of MGBG in combination with α-(difluoromethyl)ornithine, the irreve le in-

hibitor of ornithine decarboxylase, the rate-limiting enzyme in polyamine biosynthesis, require the close monitoring of MGBG levels in plasma and bone marrow aspirates. A high-speed reversed-phase ion-pair HPLC assay for MGBG, which uses only a 4.6 × 45 mm guard column for the separation with detection at 283 nm, has been developed. The mobile phase consists of methanol–200 mM sodium acetate, pH 4.5, 20 mM 1-octanesulfonate, and 0.004% NaN_3 (2:3 v/v). At a flow rate of 3.0 mL/min, MGBG elutes in 1.7 min (t_0 = 7 s). The detection limit was 20 pmol/mL, and the peak height response as a function of MGBG concentration was linear over the 0.02–40 nmol/mL range (r = 0.999). Plasma and tissue specimens are deproteinated with 0.4 N perchloric acid and neutralized with KOH while urine is diluted 1:10 with water and extracted with a C-18 Sep-Pak. Recoveries were quantitative if exposure to perchloric acid were minimized. Coefficients of variation for reproducibility were <5%. The application of this method to clinical samples is demonstrated.

166. Effects of Carboxyatractyloside on Cardiac Output and Recovery from Myocardial Ischemia. *John J. Noonan*, Mary J. Schmidt, Richard E. Dugan, and Austin L. Shug. Metabolic and Lipid Research Laboratory, William S. Middleton Memorial Veterans Hospital, and Department of Neurology, University of Wisconsin, Madison, WI 53705.

Carboxyatractyloside (CA) is a specific inhibitor of the mitochondrial adenine nucleotide translator (ANT). We have studied the effect of CA, administered intravenously to rats, on cardiac output and mitochondrial respiration. Successive conditions imposed on perfused heart were nonworking (Langendorf perfusion), working, ischemic, and reestablishment of working. In controls, cardiac output did not decrease during working and recovered to 25% of the original after ischemia. In CA treated, cardiac output decreased 71% during the working period and showed no recovery after ischemia. Mitochondria collected from hearts that were CA treated and Langendorf perfused for 30 min showed an 87% decrease in state 3 respiration as compared to mitochondria from untreated, unperfused hearts. Perfusate samples taken at the end of the 30-min Langendorf perfusion indicated that CA had been effectively removed from the heart as measured by state 3 mitochondrial respiration. These studies suggest that mitochondrial ANT activity is required for cardiac output and recovery from ischemia.

167. Protein Degradation in Cultured Human Fibroblasts. *K. Thyagarajan* and A. Frankfater. Department of Biochemistry and Biophysics, Loyola University Stritch School of Medicine, Maywood, IL 60153.

We have studied the metabolism of ^{125}I-labeled bovine ribonuclease A (RNase) and human serum albumin (HSA) in cultured human fibroblasts (GM 3440) following a 1-h delivery either by endocytosis or by liposomes composed of lecithin, lysolecithin, and stearylamine. The cells were observed to show a considerable reactivity with respect to proteins internalized by endocytosis with 95% of ^{125}I-RNase and 75% of ^{125}I-HSA initially taken up by the cells being released into the medium in a fast phase with a half-life of about 10 min. Fifty percent of the label from HSA and 75% of the label from RNase were trichloroacetic acid (TCA) soluble. These results indicate a remarkable degradative capacity of cultured fibroblasts together with a very active endosome/lysosome to plasma membrane bidirectional traffic. Liposome-delivered proteins showed qualitatively similar patterns of multiphase release of TCA-soluble and insoluble label except that they occurred 10 times slower. This may mean that the degradation of liposome-delivered proteins and ingested proteins involves common steps. In the former case these would be preceded by additional slow steps(s).

168. Biochemical Events in the Rapid Regulation of Ionic Iron Absorption. *R. W. Topham*, S. A. Joslin, and J. S. Prince, Jr. Department of Chemistry, University of Richmond, Richmond, VA 23173.

It has been proposed that increases in the iron content and amount of mucosal transferrin are responsible for the increase in iron absorption when body iron stores are low and that increases in the iron content and amount of mucosal ferritin are responsible for the inhibition of iron absorption when body iron stores are large. Short-term alterations in the amount of iron in the diets of rats caused substantial differences in the distribution of a test dose of ^{59}Fe between mucosal transferrin and mucosal ferritin and also caused a change in the relative amounts of these proteins in mucosal tissue without resulting in any detectable change in body iron stores. These differences correlated with changes in the retention of ^{59}Fe by the intestinal mucosa and the transport of ^{59}Fe to the blood stream. These studies emphasize the importance of local changes in the intestinal mucosa in the regulation of dietary iron absorption.

169. Effect of Phosgene on the Pulmonary Surfactant System (PSS): Dose–Response Relationships. *M. F. Frosolono* and W. D. Currie. Department of Radiology, Duke University Medical Center, Durham, NC 27710.

Previous experiments at 240 ppm·min phosgene demonstrated significant increases in PSS constituents as pulmonary edema developed. In the present studies separate groups of rats were exposed to 30, 120, and 240 ppm·min phosgene and the concentration of PSS constituents determined prior to and daily for 3 days after exposure. Phosphatidylcholine (PC) may be considered the major compositional and functional constituent of the PSS. At the nonpulmonary edematogenic dose of 30 ppm·min phosgene, PSS–PC concentration showed no significant changes. There were significant 2- and 1.5-fold increases in PSS–PC concentrations at 2 and 3 days after exposure to 120 ppm·min phosgene; lung wet weight was significantly elevated, 1.2- and 1.2-fold. At 240 ppm·min, lung wet weight was significantly elevated (1.5-, 1.3-, 1.3-, and 1.2-fold) immediately after exposure and at postexposure days 1, 2, and 3, respectively. PSS–PC levels exhibited a different pattern of response: 1.2-, 2.3-, 4.4-, and 3.3-fold increases at the same time points. These results, therefore, suggest there is a compensatory response of the PSS, perhaps to aid in the removal of excess lung water, after pulmonary edematogenic doses of phosgene.

170. Pulmonary Damage due to Phosgene Exposures. *W. D. Currie* and M. F. Frosolono. Department of Radiology, Duke University Medical Center, Durham, NC 27710.

Pulmonary edema is the characteristic pathological feature of severe phosgene poisoning. Previous experiments demonstrated that rats developed pulmonary edema following exposure to 240 ppm·min phosgene, and the lung adenosine triphosphate (ATP) concentration was decreased. The present study was conducted to define further the relation between lung damage and ATP concentration. Separate groups of rats were exposed to 30, 60, 120, and 240 ppm·min phosgene in Rochester-type chambers and were sacrificed immediately

following exposures and on successive days. At 240 ppm·min, lung wet weight was significantly increased immediately after exposure and at postexposure days 1–3; lung ATP concentration was decreased immediately after exposure and remained decreased at days 1 and 2. Following 120 ppm·min, lung wet weight was significantly increased on days 2 and 3 postexposure; lung ATP concentration was significantly decreased immediately after exposure but returned to the control value or higher on days 1–3 postexposure. After 30 and 60 ppm·min phosgene exposures no edema was observed, but there was a significant decrease in the lung ATP concentration immediately following the exposures. The results show that a decrease in ATP concentration precedes the onset of edema due to phosgene and suggest a central role for ATP in the edematogenic process.

171. Kidney Stone Inhibitors (Glycoprotein Crystal Growth Inhibitor) Isolated from Human Calcium Oxalate Kidney Stones. *Y. Nakagawa*, S. Deganello, C. Chow, M. Ahmed, and F. L. Coe. Biochemistry and Nephrology Program, University of Chicago, Chicago, IL 60637.

Previously we characterized urinary glycoprotein calcium oxalate crystal growth inhibitors (CGIs) [(1983) *J. Biol. Chem. 258*, 12594] and more recently found that kidney stone forming patients excrete less potential GCIs from kidneys than non-stone-forming controls. We have extracted CGIs from kidney stones using fresh 0.05 M EDTA seven consecutive times. Each extract contained different amounts of GCIs we had previously purified from human urine. Scanning electron microscopy and X-ray powder diffraction analyses indicate that the residue consists mainly of calcium oxalate monohydrate that became purified during extraction of GCIs (6.57 and 4.03 Å diffraction disappeared). Amino acid composition, kinetic studies, and surface properties that were measured by using a film balance indicate that GCIs isolated from kidney stones are similar to those purified from human urine. This suggests that in vivo GCIs bind to the surface of calcium oxalate monohydrate seed crystals; however, the inhibitors isolated from stone formers do not inhibit crystal growth.

172. Structure–Activity Relationships between Carbon-11-Labeled Mono-, Bi-, and Tricyclic Amino Acids: Tissue Distribution Studies in a Rat Tumor Model. *Peter S. Conti*, Bernard Schmall, Edward Kleinert, Harry Herr, and Willet F. Whitmore, Jr. Memorial Sloan-Kettering Cancer Center, New York, NY 10021.

Carbon-11 ($T_{1/2}$ = 20.4 min) has been incorporated into a number of natural and synthetic amino acids for use as potential tumor-imaging agents. We reported tissue distribution studies in the Dunning R3327G rat prostate tumor model including comparison of the monocyclic amino acid aminocyclopentanecarboxylic acid (ACPC) and the bicyclic amino acid 2-aminobicyclo[2.2.1]heptane-2-carboxylic acid (BCH) [Conti et al. (1984) *Biochemistry 23*, 3379]. The effect of modification of chemical structure on tissue distribution was further investigated with a new C-11 tricyclic amino acid 2-amino-2-carboxyadamantane (ADM) prepared by the Bucherer–Strecker synthesis (cpm found/g of tissue divided by cpm administered/g of rat mass):

	blood	tumor	pancreas	kidney	liver	prostate
ACPC	1.09	1.47	5.29	1.84	1.23	0.92
BCH	0.89	1.24	5.41	1.48	0.99	0.85
ADM	0.61	0.75	4.69	1.49	1.33	0.31

(mean: 45-min postinjection, five rats per group). Diminished levels of ADM in tumor tissue cannot be explained solely on the basis of low blood levels since values in most normal tissues were similar for all three compounds.

173. Stroma-Free Methemoglobin Solution (SFMS): An Effective Antidote for Acute Cyanide Poisoning. *William E. Ottinger*, Arthur D. Schaerdel, and Raymond P. Ten Eyck. Clinical Research Laboratory and Department of Emergency Medicine, Keesler USAF Medical Center, Keesler AFB, MS 39534-5300.

Using a rat model and administering all solutions through a central venous catheter, we investigated several aspects of SFMS as a cyanide antidote. SFMS was more than 90% effective in resuscitating rats administered multiples of the LD_{90} (36 μmol/kg) of cyanide up to and including four times the LD_{90}. SFMS was approximately 50% effective against multiples of six and eight times the LD_{90}. With no supportive therapy the SFMS was still an effective resiscitant 60 s after respiration had ceased. These results are in marked contrast to the standard nitrite–thiosulfate regimen, which was effective against only 2 times the LD_{90} even when administered first. The concentration of the SFMS was found to have no significant influence on the efficacy of the treatment. Concentrations of SFMS as high a 33 g/dL could be used efficaciously. Administration of a large bolus of SFMS alone showed no morbidity or mortality. SFMS appears to be an alternative antidote for the treatment of acute and subacute cyanide poisoning.

174. Subtle Forms of Human Lactoferrin. *Ronald E. Wiener* and Archie L. Murdock. Departments of Diagnostic Radiology and Biochemistry, University of Kansas Medical Center, Kansas City, KS 66103.

The iron-saturated form of lactoferrin (LF) has been suggested to be an inhibitor of leukocyte colony stimulating factors in clonal cultures. Broxmeyer and co-workers [(1980) *Blood 55*, 324] found that LF was inhibitory over a concentration range of 10^{-17}–10^{-6} M whereas Bagby and Bennett [(1982) *Blood 60*, 108] reported that LF was not active above 10^{-10} M, presumably due to Ca^{2+}-induced aggregation of LF to form inactive tetramers. Our attempts to prepare the tetrameric form with two different commercial sources of LF failed; with one source, 20 mM Ca^{2+} caused retardation of LF on a Sephacryl column. Next, LF was isolated from human milk. DEAE chromatography resulted in two major and several minor peaks that contained LF. The first major peak was shown to be electrophoretically homogeneous by protein staining, iron staining, and LF antibody. When the purified material, either as an ammonium sulfate suspension or as a lyophilized powder, was exhaustively dialyzed against the elution buffer of an analytical Sephacryl S-200 column, a symmetrical 77K peak was obtained. Additional studies with the Sephacryl column showed that exposure of LF to various nondenaturing conditions could alter the elution volume, peak profiles, and percent recovery; tetramer was not observed. The ability of LF to be transformed into these subtle forms may be related to its activity.

175. Can Supplemental Vitamin A (VA) Improve Nitrosourea (NU) Tumor Therapy? *E. Seifter*, J. Weinzweig, and J. Padawer. Albert Einstein College of Medicine, Yeshiva University, Bronx, NY 10461.

Some nitrosamine derivatives, especially NU, are useful broad-spectrum cancer chemotherapeutic agents. We think

they also may yield highly organ- or tumor-specific agents as follows:

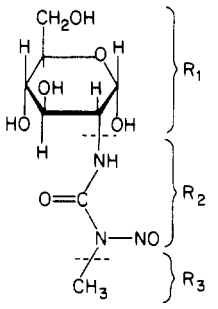

NU's have three functional groups: R_1 (2-deoxyglucose) carries the molecule (streptozotocin) to organs or tissues with glucose receptors (endocrine pancreas, islet cell tumors, other tumors consuming large amounts of glucose); R_2 destabilizes part of the molecule, causing R_3 to alkylate the R_1 receptor site. Varying R_1, appropriately, will yield agents that can alkylate hormone receptor sites, etc. NU's have two drawbacks: (a) host toxicity and (b) carcinogenicity. Whereas VA does not affect the (early) genotoxic action of alkylating agents, it markedly diminishes host toxicity and the (late) promotion stages in carcinogenesis. These properties suggest that VA will improve the antitumor action of NU and decrease its carcinogenicity.

176. Response of Chloride Electrode (CLE) Reveals Unsuspected Case(s) of Bromism. *Arvind K. N. Nandedkar* and Gordon F. Fairclough, Jr. Department of Biochemistry, College of Medicine, Howard University, Washington, DC 20059, and Laboratory of Clinical Biochemistry, New York Hospital–Cornell Medical Center, New York, NY 10021.

Using Technicon Stat-Ion, we noticed high serum chloride (Cl) values that did not match up with the expected anion gap. Cl analysis of these samples by titrimetric methods showed normal ranges (100–110 mmol/L). Quantitations by the gold chloride method indicated the presence of bromide (Br). Acknowledging the suspicion following appropriate therapy, the symptoms of bromism (BM) disappeared. The response of CLE to the subsequent serum samples returned to the expected values. In the method of additions using pool serum [representing a constant halide concentration (100 mmol/L)], 1–4 times higher apparent Cl values dependent on Br concentrations were observed. Although Br therapy has largely been outmoded, one may encounter occasional cases of Br intoxication (BM). Elevation of Cl (by any method) especially with ion-selective electrodes should be further investigated to rule out BM. The patients' medications (Rx and OTC) should be known along with clinical analysis of Br.

177. Biodegradation of Environmental Pollutants by a White Rot Fungus. *John A. Bumpus* and Steven D. Aust. Center for the Study of Active Oxygen in Biology and Medicine, Michigan State University, East Lansing, MI 48824.

Phanerochaete chrysosporium utilizes a unique hydrogen peroxide dependent enzyme system to degrade lignin, a complex, chemically resistant, nonrepeating heteropolymer. We have proposed that the lignin degrading system of this fungus may also have the ability to degrade environmentally persistent organopollutants. In this study we have shown that *P. chrysosporium* degraded ^{14}C-labeled DDT, DDE, Mirex, hexachlorobenzene, 3,4,3′,4′-tetrachlorobiphenyl, 2,4,5,2′,4′,5′-hexachlorobiphenyl, 2,3,7,8-tetrachlorodibenzo-*p*-dioxin (TCDD), Lindane, and benzo[*a*]pyrene to $^{14}CO_2$. Colateral studies indicated that the ability of *P. chrysosporium* to degrade these chemicals is dependent on the lignin degrading system of this fungus. Model studies show that both DDT and lignin degradation were induced in nitrogen-deficient cultures whereas nitrogen-sufficient cultures suppressed both degradations. Similarly, the temporal onset and disappearance of DDT and lignin degradation coincided.

178. Biological Activity of Very Low Molecular Weight Heparin Oligosaccharides. *Zohar M. Merchant*, Yeong Shik Kim, Kevin G. Rice, Dan L. Lohse, and Robert J. Linhardt. Division of Medicinal Chemistry and Natural Products, College of Pharmacy, University of Iowa, Iowa City, IA 52242.

Heparin is a highly sulfated glycosaminoglycan used clinically as an anticoagulant. Heparin is known to possess additional secondary activities that permit its use in the treatment of atherosclerosis, immune-related disorders, and solid tumors. Our approach has been to prepare very low molecular weight oligosaccharides containing defined sequences and test their activities. Heparin is depolymerized by flavobacterial heparinase (EC 4.2.2.7) into different sized components with the degree of polymerization ranging from 2 to 20 sugar residues. This mixture is separated by gel permeation, ion-exchange and affinity chromatography. The individual oligosaccharides are then screened for different biological activities. New coupled affinity chromatographic techniques have been devised by using various purified heparin binding proteins to separate oligosaccharides possessing different biological activities. This has resulted in isolation of oligosaccharides showing in vitro anticoagulant, anti-atherosclerotic, and complement inhibition activities.